Assessing the Performance and Stability of Intensified and Diversified Dryland Cropping Strategies in the Inland Pacific Northwest with the CropSyst Model

A Thesis

Presented in Partial Fulfillment of the Requirements for the

Degree of Master of Science

with a

Major in Water Resources

in the

College of Graduate Studies

University of Idaho

by

Julia Reese

Approved by:

Major Professor: Erin Brooks, Ph.D.

Committee Members: Jodi Johnson-Maynard, Ph.D.; Claudio Stöckle, Ph.D.

Department Administrator: Timothy Link, Ph.D.

August 2022

Abstract

Farmers in the Inland Pacific Northwest (IPNW) typically cultivate dryland wheat-based crop rotations, which often include spring crops and, in lower precipitation areas, fallow. As part of the Landscapes in Transition (LIT) project, the CropSyst model was employed to evaluate traditional (business-as-usual, BAU) and novel crop rotations at two locations: St. John, Washington, an annual crop-fallow transition site, and Genesee, Idaho, an annual crop site. Incremental (INC) and aspirational (ASP) crop rotations, which included winter peas and cover crops, respectively, allow farmers to intensify and diversify operations through the inclusion of winter crops and reduction in fallow. Data collected during LIT field studies, carried out during the 2018-2021 growing seasons, was used to parameterize and calibrate the CropSyst model and evaluate its ability to simulate field conditions. Subsequently, scenario testing explored the viability of the alternate crop rotations under long-term, historic climate conditions.

The developed CropSyst models appeared powerful and robust, especially given the variability and range of the observed data. CropSyst achieved good agreement between predicted yield and biomass and observed values on an overall, rotational, and yearly basis (R^2 greater than 0.5 and root mean square error, RMSE, less than the standard deviation, σ, of observations). Additionally, soil moisture simulated by Cropsyst exhibited greater accuracy than the precision available in the observed datasets. Crop nitrogen was also predicted well ($R^2>0.5$ and RMSE<σ). However, more work is necessary to improve simulated soil inorganic nitrogen.

Long-term simulations of the models, from 1980-2010, suggest opportunities exist for adoption of diversified and intensified rotations in both the annual crop and annual crop-fallow transition regions of the IPNW. In both Genesee and St. John, INC produced the greatest biomass and yield and displayed the greatest stability, based on its coefficient of variation (c_v). Baling a cover crop for forage markedly increased ASP's yield and presents an opportunity for producers to diversify. Overall, winter crops better utilized available water and reduced water loss. However, in St. John, the inclusion of fallow in the BAU rotation reduced its susceptibility to drought. Scenario testing suggested that altering management practices strategically can improve outcomes. For example, in St. John, terminating the previous cover crop earlier in the year prevented any detrimental effects on subsequent ASP winter wheat yields. Additionally, the inclusion of legume crops (winter pea, chickpea, or a nitrogen-fixing cover crop) reduced fertilization requirements.

CropSyst simulations emphasize relationships and trade-offs existing between cropping choices and production outcomes and contribute to a better overall understanding of these traditional and novel

crop rotations. However, consideration of factors not captured by CropSyst, such as weeds, disease, and pests would prove valuable. Additional model simulations could include future climate to explore longer-term implications of changing environmental conditions.

Acknowledgments

First, I would like to thank my advisor Erin Brooks for his guidance and expertise. I appreciate the knowledge and perspective he imparted. I am also grateful for my committee members, Jodi Johnson-Maynard and Claudio Stöckle, for their time and feedback.

Thank you to the members of the Landscapes in Transition (LIT) project who directly and indirectly contributed to my work, including Saugat Baskota, who shared detailed field trial management information with me, and Zachary Smith, who assisted with field and laboratory efforts. I am especially grateful for Kendall Kahl. She provided me with an immense amount of data, representing years of effort, which proved instrumental to the development of this project. Also, thank you to Roger Nelson for kindly teaching me how to use and understand the CropSyst program and helping me troubleshoot issues.

I received funding through the United States Department of Agriculture Coordinated Agricultural Project (USDA-CAP) grant entitled “Inland Pacific Northwest Wheat-based Systems: Landscapes in Transition”. This generous support made my research and education possible.

Dedication

To Megan and Evan for lending me their computers.

Table of Contents

List of Tables

List of Figures

Chapter 1: Background and Introduction

Purpose

The Inland Pacific Northwest (IPNW) contains much of Idaho and Washington's 3.4 million acres of wheat (NASS USDA, 2020), and its local economy and many of its people depend on the success of wheat crops. However, changing environmental and economic conditions promote shifts in typical production models. Unfavorable environmental impacts, reduced yield or quality, and diminishing resources motivate farmers to pursue alternate crops and markets to improve farm stability and resilience (Reganold et al., 1990).

Replacing traditional crop rotations with those that include winter peas or cover crops may improve the long-term profitability, nutrient/water cycling outcomes, and environmental impacts of IPNW wheat-based systems. While positive impacts of these alternative crops have established (Chen et al., 2006; Finkelnburg et al., 2019; Kirby et al., 2017; Reganold et al., 1990), they are infrequently employed in large-scale IPNW farm operations due to their limited immediate economic returns and lack of knowledge. This research assesses the long-term viability of alternate rotations, with respect to productivity, resource utilization, and stability.

Introduction

It is challenging to conclusively and comprehensively assess the effects of dryland crop rotations with respect to production, resource utilization, and profitability. While existing field experiments and industry data collection provides valuable insight to current conditions, additional research is needed to investigate and compare large-scale and long-term impacts of agricultural practices.

Traditional crop rotations, which may include fallow or spring crops, present both managerial and environmental concerns. The CropSyst model can be employed to evaluate these traditional rotations as well as novel rotations, which replace fallow or spring crops with cover crops or winter peas. CropSyst is a process-based, multi-crop, multi-year model, frequently employed to study the interactions of crops, soils, weather, and management (Stöckle, 2003). The model allows users to identify important crop-environment relationships.

This research was completed in conjunction with the larger United States Department of Agriculture Coordinated Agricultural Project (USDA-CAP) grant entitled "Inland Pacific Northwest Wheat-based Systems: Landscapes in Transition" (LIT). The project focusses on IPNW dryland wheat-based cropping systems and aims to help farmers adapt to change and increase farm resilience through diversification and optimization. The multi-year project includes extensive data collection and analysis from soil, water, agronomic, entomological, atmospheric, and economic perspectives. This

research complements the effort, assessing the viability and stability of ‘aspirational’ and ‘incremental’ cropping rotations, by extrapolating and forecasting smaller scale, shorter-term data to predict larger-scale, longer-term impacts.

Model Description

CropSyst simulates crop growth based on the availability of resources such as radiation, nutrients, and water, effectively modeling responses to environmental and management conditions (Stöckle et al., 2014). In conjunction with crop production, CropSyst models complete water and nitrogen budgets. The program can simulate a large number of crops, including those assessed in the LIT study, although cover crop modeling efforts are very limited. The model undergoes frequent updates and developments, and the descriptions below reflect the current model options and explanations provided in the current user manual (Stöckle, n.d.).

Multiple evapotranspiration (ET) models are available in CropSyst, with these simulations utilizing the Penman-Monteith method. A crop coefficient adjusts the actual crop ET from the computed potential value, and transpiration is assumed equal to water uptake. However, water uptake is also limited by availability in the soil (i.e., the potential difference between the soil and plant). The Cascade daily or hourly approach estimates water transport in the soil profile (Stöckle et al., 2014), and the Soil Conservation Service (SCS) curve number approximates runoff.

Biomass accumulation is simulated by one of three submodels that determine water use efficiency. Simulations reported in this thesis utilized the transpiration use efficiency regression-based method, which requires inputs for unstressed radiation use efficiency and temperature limitations. Biomass accumulation can also be limited by nitrogen availability. The canopy development relies on a leaf area index model, and phenological events are triggered by thermal time accumulation. Harvest yield is simulated as a function of a specified harvest index. CropSyst can also adjust for the effects of heat and water stress on parameters, such as those associated with phenology, leaf area index, and the harvest index.

CropSyst simulates cycling of nitrogen, including transformations, sorption, mineralization, fixation, and plant uptake. Nitrogen dependent growth and plant uptake follow the approach outlined in Godwin and Jones (1991). Fixation fulfills a fraction of a legume crop’s daily demand, influenced by crop development, temperature, nitrogen present in root zone, and other factors. The rate of mineralization, nitrification, and denitrification are computed using first order kinetics and are assumed to occur between 30 and 50 centimeters below ground surface. Nitrogen transport through the soil is modified utilizing a mass balance method modified from Corwin et al., (1991).

Many studies, such as Bellocchini et al. (2002), Chi et al. (2017), and Ward (2015), support CropSyst's ability to accurately simulate field conditions and crop outcomes. The CropSyst model has also been used to assess the effects of climate and management on agricultural management decisions (Karimi et al., 2017; Stöckle et al., 2018). However, it appears few studies employ datasets as thorough or extensive as the one provided by the LIT project. Additionally, the model's ability to predict the impacts of winter pea and cover crops has not been thoroughly tested.

Region Description

The region of study for this project is the Palouse bioregion. The Palouse covers approximately 9,000 square kilometers (3,500 square miles) within the IPNW and is characterized by rolling hills and deep, fertile soil (Brooks et al., 2012). Geomorphology of the Palouse region has been influenced by flooding of Glacial Lake Missoula upwind during the Pleistocene period (Busacca et al., 1989) and the subsequent deposition of windblown sediment known as loess. In addition to loess, soils in the Palouse have been influenced by volcanic eruptions and distribution of volcanic ash. Soils are generally loamy to silty and overly basalt bedrock, with some granite and sedimentary outcrops (McNab and Avers, 1994). Grassland and meadows, converted to cropland, cover most of the western Palouse, with vegetation transitioning to forests and woodlands in the east (McNab and Avers, 1994).

The Palouse experiences warm, dry summers, with approximately 70% of precipitation received between November and May (Brooks et al., 2012). A steep precipitation gradient exists across the IPNW, with greater annual rainfall observed in the east. Annual precipitation can be divided into three zones: low, less than 300 mm (less than 12 inches); intermediate, 300-450 mm (12-18 inches); and high; greater than 450 mm (over 18 inches) (Schillinger et al., 2003). The LIT project maintained two field studies sites, one in St. John, Washington in the intermediate precipitation zone, and one in Genesee, Idaho in the high precipitation zone. In both areas, dryland agriculture is practiced (i.e., no irrigation inputs), and precipitation, stored in the soil for use during the growing season, heavily influences a crop's success.

Growers generally cultivate wheat-based field crop rotations. The region's high precipitation zone produces world record dryland winter wheat yields, upwards of 135 bushels per acre (bu/ac) (Schillinger et al., 2003). In addition to wheat, other common crops include barley, canola, and legumes (such as lentil or chickpea). In low and intermediate precipitation zones, fallow, the practice of leaving ground unsewn for a growing season, is also common (Schillinger et al., 2003). The heterogeneity of this highly productive agricultural area in management practices, environment, and performance, make the IPNW an ideal location to study dryland crop rotations.

Current Land Use Practices

Agricultural land use in the region can be defined via agroecological classes (AEC), which include annual cropping (AC), annual crop-fallow transition (ACT) (i.e., three-year crop rotation: winter wheat-spring grain-fallow), grain-fallow (GF) (i.e., two-year crop rotation: winter wheat-fallow), and irrigated (Huggins et al., 2014). Dryland wheat farming in low to intermediate rainfall areas of the IPNW often relies on fallow in multi-year crop rotations (ACT or GF) to preserve and replenish soil water. Fallow also serves to reduce overall rotational inputs and maximize soil nutrient availability and production stability during the subsequent growing season (Nielsen and Calderón, 2011). Overall, fallow rotations are considered more profitable and less risky than continuously cultivating a crop in lower precipitation areas (Juergens et al., 2004; Schillinger et al., 2006). Generally, production costs increase with cropping intensity (Zentner, 2002). Reduced time demand also provides growers with the opportunity to cultivate other land, perform other farm activities, and complete custom work (Zentner, 2002).

However, fallow poses many environmental and managerial concerns. This approach often represents lost time and opportunities (reduced production efficiency on a given field), leads to reduced soil health, and leaves ground susceptible to wind and rain erosion. As crop prices rise, the opportunity cost of leaving land fallow rises (Zentner, 2002). Though historically successful, wheat-based fallow rotations can also be risky, as the profitability of the farm is highly sensitive to the price and performance of a single crop.

In higher precipitation regions, AC systems are typically employed. This includes the common winter wheat-spring wheat-spring pulse rotation (i.e., no summer fallow). These crops have established success and markets. Farmers are familiar with their cultivation, which promotes efficiency, operational simplicity, and streamlined use of technology/mechanization. Unfortunately, this approach's inherent lack of diversity and adaptability leave farmers vulnerable to environmental or marketplace change. Spring crop emergence, fertile pod production, seed weight, and, consequently, yield is especially sensitive to environmental conditions, such as soil temperature and moisture, and delayed planting can reduce profitability (Gan et al., 2002; Miller et al., 2006). Research indicates the susceptibility of spring crops to abiotic stress results in highly variable yields and economic instability (Schillinger, 2020). While earlier planting helps avoid late season drought stress, wet early season soil conditions can delay planting (Chen et al., 2006; Gan et al., 2002). This may become an increasing concern in coming years, as climate forecasts project greater winter precipitation and less summer precipitation (Mote and Salathé, 2010).

Across all AECs, most farms continue to follow conventional practices, such as monocultures, synthetic fertilization, and conservation tillage. In an effort to improve profits and reduce inputs, farmers are beginning to turn to less conventional management practices, such as livestock integration, precision seeding and chemical application, and no till to increase soil health, reduce fertilizer use, increase soil water retention and infiltration, and improve drought resistance. Such practices generally support regenerative agriculture, a form of production that enhances and restores resilient, healthy, and functional agricultural ecosystems (Gosnell et al., 2019). Unfortunately, if not carefully orchestrated, transitions to new techniques and crops may not prove immediately successful and could require years of gradual transition (Liebhardt et al., 1989). This reduces attractiveness and serves as a barrier to adoption for many.

Alternative Rotations

Cover crops and winter pea rotations allow farmers to diversify (and intensify, if replacing fallow), while providing potential economic and nutrient and water cycling benefits. Integrating different crops into rotations provides opportunities to mitigate economic risk, expand microbe and insect communities, break pest cycles, and better manage greenhouse gas emissions (Pan et al., 2017). Research indicates possible future opportunities, as forecasted climate may improve yields in diversified rotations, resultant of water availability and demand (Jareki et al., 2018; Stöckle et al., 2018).

Alternative crops can also build soil fertility and promote microbial mineralization, ultimately reducing fertilizer requirements. Additionally, increased groundcover associated with winter crops and cover crops can prevent nitrogen loss through pathways such as erosion, runoff, and leaching. This study will evaluate nitrogen fertilizer requirements, as fertilizer production and use threatens negative environmental impacts, and its application represents a significant time and money investment for farmers. Research, such as that described in Smith et al. (2008), supports the theory that diversity improves nutrient cycling and reduced inputs and enhances overall ecosystem function. Smith et al. (2008) conducted a rotational study in the absence of fertilizer or pesticide and determined that the most diverse three-year rotation (three different crops and three different cover crops) had the highest yields. In comparison to a monoculture rotation, the diverse rotation achieved up to 32% greater soybean yields, up to 53% greater winter wheat, and over 100% greater corn yield (a result very similar to local average yields), despite lack of inputs. Varying degrees of success among species suggest crops respond differently to rotational diversity and its impact on ecosystem function (Smith et al., 2008).

Many speculate that diversified rotations will also improve overall performance, stability, and resiliency. Often, stability is marked by a crop's/rotation's ability to maintain yields and quality under or following stressful conditions, and resiliency describes a crop's/rotation's ability to return to its previous state following a stressor/disturbance (Gaudin et al., 2015). A stable and resilient rotation will yield consistently and will exhibit attenuated responses to extreme conditions. These qualities prove valuable in volatile environmental and market conditions.

There are several examples available of rotational studies that investigate these longer-term considerations. A 31-year study in Ontario, Canada observed that traditional corn-soybean rotations experienced greater variations in yield, reduced cumulative and average yields, higher probabilities of crop failure, and reduced performance under abnormal conditions versus longer rotations that integrated additional crops, particularly legumes (Gaudin et al., 2015). However, the most significant effects occurred during dry/warm weather, with minimal to no rotational impact during cool/wet conditions, implying diversified rotations' ability to better preserve and manage water.

Overall, diverse farms inherently incur less risk, both biologically and economically, than farms which rely on a few, limited crops for income and employ external resources, such as chemical fertilizers, for production (Reganold et al., 1990). The alternative management practices captured in diverse operations promote soil health and reduce inputs, the extent and conditions of which this research seeks to further define and quantify.

Winter Peas

Winter peas, a legume, fix nitrogen and rarely require nitrogen fertilizer applications, which may influence soil nitrogen availability throughout the rotation (Smith et al., 2008). They yield consistently; emerge from deep seeding depths, allowing better access to remaining soil water deep in the profile; survive cold winter temperatures; can be cultivated with the same equipment as wheat; and tolerate certain common herbicides (Schillinger, 2020). While currently considered less economically favorable, CropSyst modeling indicates that under future scenarios winter crops like winter pea may outperform spring crops in the IPNW, especially in high precipitation zones, and partial replacement of winter wheat with winter peas could be feasible in all precipitation zones (Stöckle et al., 2018). Moreover, winter peas reach maturity earlier than spring-planted peas and avoid the heat and water stress that already dramatically reduces yield, particularly in lower precipitation zones (Schillinger, 2020).

The region currently only grows food quality winter peas. Current varieties are used as an ingredient in both human and animal foods but cannot be marketed as whole or split pea (Schillinger, 2020). If

an edible variety becomes available, the crop would likely become far more profitable. Still, a recent study in Ritzville, WA, which compared fallowed rotations with winter wheat versus winter pea, showed that the winter pea rotation generated comparable economic return when considering the entire rotation, as well as used less water, left more soil water in the spring, and required no fertilizer applications (Schillinger, 2017). Similarly, studies in Genesee, ID and Ritzville, WA found winter pea cultivars exhibited higher yields than did spring pea cultivars as a result of mild, wet winters, which promote growth and suppress evaporation but also delay spring planting (Chen et al., 2006).

While winter crops may manage and utilize water better than spring crops, low summer precipitation poses a challenge to winter peas, as planting needs to occur later or in drier seedbeds (Chen et al., 2006). Moreover, winter pea roots do not reach as great a depth as winter wheat, and the crop produces less residue, leaving ground more susceptible to evaporation and erosion (Schillinger, 2017). The presence of many, competing factors and complex relationships highlights the need to consider outcomes on a rotational basis instead of only individual crops. The introduction of winter peas in rotations is identified as an incremental method (INC), as it does not require major changes to existing practices (Janowiak et al., 2016).

Cover Crops

Alternatively, integration of cover crops can increase soil organic matter and nutrients and/or be used for grazing livestock (Finkelnburg et al., 2019). Because this approach requires more dramatic changes or transformations of existing practices, the cover crop rotations are considered "aspirational" (ASP) (Janowiak et al., 2016). Replacing fallow rotations with cover crops may improve water infiltration to the root zone and protect the soil surface, retaining more nutrients on site by reducing runoff and soil export. Additionally, cover crops can effectively disrupt disease and weed cycles (Kirby et al, 2017). Currently, cover crops are limited in the region, as they demand valuable soil moisture, which may reduce the yield of subsequent crops in the rotation (e.g., winter wheat), and farmers must manage and fund their production and harvest, often with no direct economic return.

However, cover crops can be baled for beneficial use or grazed by livestock instead of incorporated back into the soil, as is more traditional, providing some economic gain. This is a particularly attractive strategy to producers who already raise livestock. Further, some proponents, including Gabe Brown, a well-known North Dakota farmer and rancher, consider livestock integration a key contributor to soil health. In addition to redeeming cover crop economics, livestock provide fertilizer, cause soil surface disturbance, and stimulate root growth and microbial activity (White, 2020).

A recent short-term study in South Dakota identified some tradeoffs in grazed versus ungrazed cover crop systems. Tobin et al. (2020) reported soils supporting grazed cover crops experienced increased bulk density, decreased soil organic carbon, and reduced water retention compared to soils managed by ungrazed cover crops. However, the grazed, cover cropped soils still had greater total nitrogen and increased economic return over a fallowed system. No differences in subsequent seasonal yields emerged between grazed and ungrazed cover crop. The value of the livestock feed produced outweighed production expenses and cost of maintaining the cattle in the field (such as water and fencing) (Tobin et al., 2020). Regardless, to avoid potential ill effects, a farmer could elect to bale cover crops for animal consumption elsewhere, although baling forage crops removes carbon and nutrients from the field.

Unlike in areas such as the Midwest United States, climate, particularly seasonal rainfall distribution, influences effectiveness and adoption of cover or forage crop practices, warranting additional investigation in the Palouse region where precipitation is concentrated in winter months. Nonetheless, the practice is gaining more traction locally. Farmers like Drew Leitch of Nez Perce, ID use both spring and fall cover crops to supplement pasture for cattle (Finkelnburg et al., 2019). The cover crops also help address specific soil issues such as compaction. Leitch must carefully manage the cover crops to achieve the greatest soil and agronomic benefits, grazing period, and forage quantity and quality. Leitch attributes cover crops to improved soil health and greater weight gain, and consequently profit, in his cattle. However, Finkelnburg et al. (2019) noted greater labor demands and Leitch's reliance on a government incentive program.

Producers can, to some degree, select cover crop residue quantity and characteristics and water use by choosing specific cover crop species, planting date, and termination timing (Jones et al., 2020). Determining cover crop termination time can pose a challenge due to seasonal precipitation patterns, and, if not carefully considered, cover crops can have detrimental effects. In a recent study conducted during a summer of limited rainfall in Wilke, WA, cover crops withdrew too much moisture and delayed winter wheat seeding (Roberts, 2018). Resulting delayed development and reduced size created challenging management conditions, and, consequently, herbicide damage killed the crop. The research highlighted the inherent risks of cover cropping, especially in regards to soil moisture, and the need to be "flexible and opportunistic" with management decisions (Roberts, 2018). For example, terminating spring cover crops earlier in the season during drier years could preserve soil moisture for the subsequent crop and could provide additional benefits, such as high root mass (Jones et al., 2020). This is likely critical in drier areas, such as St. John, as it is improbable that potential soil benefits will outweigh the effects of water depletion later in the season. This research further

investigates the termination timing which maximizes the advantages and minimizes disadvantages of cover crop cultivation.

It is also important to note that many farmers rely on public agencies for crop management guidance and must conform to the requirements of their insurance policies. In Latah County (Genesee, ID), USDA guidance for cover crop termination recommends growers terminate cover crops "at or before planting the crop", and in Whitman County (St. John, WA), they suggest terminating late spring to fall seeded cover crops "15 days or earlier prior to planting the crop" and early spring seeded cover crops "as soon as practical prior to planting the crop" (USDA, 2019). Also, cover crops are not considered an insurable crop, and cover crop management can impact federal crop insurance coverage (USDA, 2019). However, the USDA allows cover crops to be hayed, grazed, or harvested for silage, unless specifically prohibited by the insurance policy. These are important considerations when investigating and determining optimal management strategies. Regardless, agricultural systems are subject to dynamic environmental conditions, which may influence appropriate termination timing year-to-year.

Research Approach

Agricultural research is inherently complex due to the intricate interactions among environment, weed and disease pressures, and human inputs. It is difficult to isolate variables and clearly identify relationships. However, modeling allows one to eliminate variability across scenarios and evaluate the interaction of multiple factors with few, representative metrics.

LIT data was used to parameterize and calibrate the CropSyst model and evaluate its ability to simulate field conditions and outcomes. Once developed, model scenarios were run over a historic/current period. In addition to the different crop rotations, model simulations incorporated approximately 30 years of detailed climate data obtained from gridMET, high resolution blended data from Parameter-elevation Regressions on Independent Slopes Model and North American Land Data Assimilation System (Abatzoglou, 2011).

This research evaluates metrics intended to capture crop/rotation performance and stability, including yield and water and nitrogen outcomes. Yield is a common measure of productivity and success and affects profit. Water metrics, such as water use efficiency (grain produced per water used), provide insight to crop-climate relations and overall efficiency. Nitrogen cycling influences input requirements, crop quality, and water quality. The CropSyst model is also employed to identify strategies and develop techniques to maximize production and quality, while minimizing risk when

employing these alternate cropping systems. This includes fertilization requirements and cover crop termination timing (where applicable).

Research Objectives

As introduced above, research investigates the performance and stability of winter pea (INC), cover crop (ASP), and business as usual (BAU) crop rotations over time. The main research objectives are to:

1. Parameterize and assess the ability of the CropSyst model to simulate crop production and nitrogen/water cycling at an annual crop and a crop-fallow transition location using replicated rotational strip trial data
2. Evaluate viability of alternate crop rotations under current and historic climate conditions and identify management strategies to optimize/adapt rotation success and stability

This research compliments the greater efforts of the Inland Pacific Northwest Wheat-based Systems: Landscapes in Transition project (LIT), funded under USDA National Institute of Food and Agriculture grant 2017-68002-26819. LIT aims to “guide ongoing land use change in the IPNW towards sustainable, resilient agricultural landscapes and food systems”. This research utilized LIT data to better understand the long-term and large-scale impacts of the environment and management strategies on alternate crop rotations and provides insight as to how best to apply rotations and optimize practices in the years ahead. Researchers and those involved in industry can employ the findings of the LIT project to guide agricultural management decisions, future research, and further model development.

Chapter 2: CropSyst Model Development

Introduction

Process-based models can be valuable research and assessment tools for identifying the net impact of disturbances, management decisions, and climatic changes in complex systems where positive and negative feedbacks are difficult to capture through field experimentation. However, it is often very difficult to parameterize, calibrate, and validate a process-based model due to issues of equifinality, spatial variability, and limited data availability to constrain and reduce uncertainty (Bevan, 1989; Grayson et al., 1992). This chapter relies on a detailed four-year strip trial crop study (Landscapes in Transition, LIT) to parameterize, calibrate, and assess the predictive ability of a complex process-based model, CropSyst (Stöckle, 2003), for alternative cropping situations in the dryland cereal grain production region of the Inland Pacific Northwest (IPNW). A validated model allows users to effectively extend short-term observations to long-term scenarios and simulate the interactions of crops, soils, weather, and management (Stöckle, 2003). It will help isolate variables, identify relationships, and observe responses to varying conditions, supporting the larger goals of understanding the impacts of diverse and intense crop rotations and determining management strategies to optimize their success.

Under the first research objective, two, site-specific CropSyst models were developed using replicated rotational strip trial data from the LIT project, one for the Genesee, annual cropping field site and one for the St. John, crop-fallow transition field site. Unique combinations of weather, soil, management, initialization, and crop input files make up different CropSyst model scenarios. During the calibration phase, each crop file underwent discrete calibration to obtain accurate yield/biomass, soil moisture, and nitrogen simulations. The primary objective of the calibration was to assess the ability of the CropSyst model to simulate crop biomass and yield production, as well as water and nitrogen storage and cycling.

Methodology

Site Description

Available experimental data covers four years (2018-2021) at two trial sites, one corresponding to an annual crop-fallow transition system (ACT) in the intermediate precipitation zone (St. John, Washington) and one corresponding to an annual crop system (AC) in the high precipitation zone (Genesee, Idaho). Field treatments cover three separate, three-year crop rotations: spring wheat-fallow-winter wheat (BAU), spring wheat-winter pea-winter wheat (INC), and spring wheat-spring cover crop-winter wheat (ASP) in the intermediate precipitation zone and spring wheat-chick pea-winter wheat (BAU), spring wheat-winter pea-winter wheat (INC), and winter cover crop-chick pea-

winter wheat (ASP) in the high precipitation zone. Cover crops were five-to-nine-way crop mixes; see Appendix A. In total, each site contains 45, approximately 10-meter-wide by 23-meter-long plots and a larger, field-scale study. As an example, Figure 1 shows the 2018-2019 strip trial design at the Genesee site.

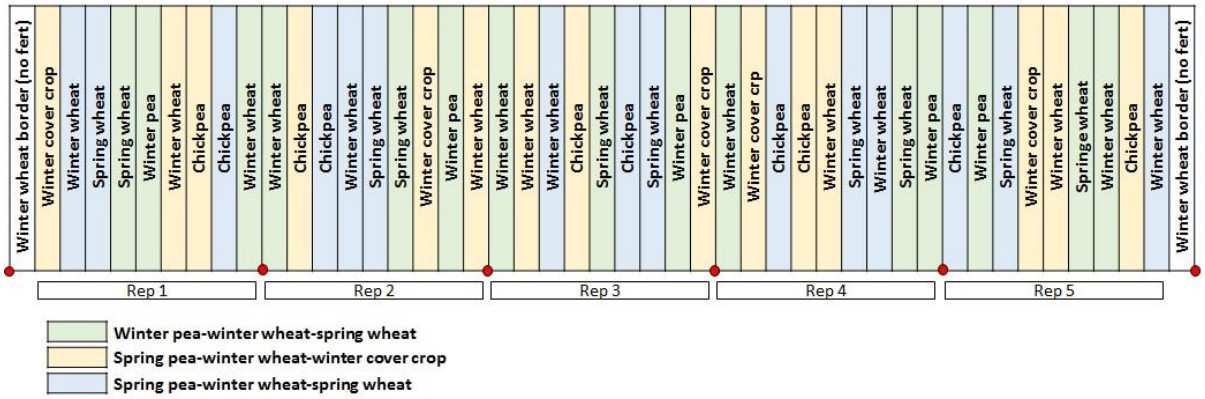

Figure 1: 2018-2019 strip trial design in Genesee, ID.

Field and Laboratory Data

CropSyst parameterization relied heavily on strip trial data collection. Each "treatment" (i.e., crop in a specific rotation) is replicated five times. Management information, such as planting and harvest dates and fertilization amounts, was carefully recorded throughout the field trial. The *Management* section of Model Development details management practices. Game cameras, installed in replicate 5 of Genesee and replicate 3 of St. John during the 2021 season only, provided insight to timing of crop growth stages, particularly flowering. Sentinel-derived NDVI imagery for the entire growing season for the associated field trials and other nearby fields was downloaded from the FluroSense (Regrow Agriculture) crop management tool.

Soil sampling occurred pre-plant each spring (¾-inch diameter manual soil sampling probes) and post-harvest each fall (using a 2.3-centimeter Giddings probe, Giddings Machine Company Inc.™, or with 3-inch diameter soil augers). Samples were taken in every individual "strip" of the strip trial at 30-centimeter (cm) depth increments down to 150 cm below ground surface. For each depth, three individual samples, taken approximately one meter apart in a triangular pattern, contributed to a single composite sample. At the 0-30 cm depth, an additional six samples were taken perpendicular to plant rows to ensure banded fertilizer zones were adequately sampled. Sub-samples of the composites were analyzed for pre-plant and post-harvest soil moisture content, nitrate, and ammonium in the soil profile. Soil nitrate and ammonia concentrations on a weight per weight basis (converted from milligrams per 0.025-liter extract) were determined with a 0.1 molar potassium

chloride (KCl) extraction, analyzed by a Lachat flow injection analyzer (Lachat Instruments™). Gravimetric water content was determined by measuring weight change after drying soil samples at 105°C for 24 hours or more and was converted to volumetric water content using bulk density measurements. Bulk density throughout the soil profile was measured twice, once in fall 2019 and once in fall 2021, from undisturbed 2.3-cm Giddings probe cores (Giddings Machine Company Inc.™). Additional soil health analysis, conducted by Ward Laboratories, Inc. (Kearney, Nebraska), provided metrics including soil organic matter content and soil water-extractable organic C:N ratios. The CropSyst soil input file necessitated additional laboratory tests beyond those discussed above to determine soil-water retention properties and soil texture analysis, described in the *Soil* section. In addition to the manual soil moisture measurements, at each site, continuous soil moisture and temperature sensors (Acclima, Inc.), installed in each strip of a single replicate at each site, recorded values at six-hour increments for much of the trial period (approximately summer 2019 to fall 2021). The sensors were installed at 30-cm increments down to 150 cm below ground surface.

During harvest, (four) one square meter aboveground biomass samples were hand harvested from each strip, dried at 38°C for 48 hours or until no longer losing mass, and weighed. A plot combine also recorded grain weight for each strip. Grain nitrogen content was estimated from measurements of grain protein and moisture made using an Infratec 1241 Grain Analyzer (FOSS™). A TruSpec™ (LECO Corp.) provided nitrogen concentrations of ground crop residue subsamples (0.1-millimeter).

The accompanying field-scale trials (one at each location) split 180-acre and 90-acre fields in Genesee and St. John, respectively, into three smaller areas, each planted to either BAU, ASP, and INC rotations. In addition to providing a valuable reference for soil and crop data, the field trials also contained three weather stations, one in each rotation field. The weather stations (Campbell Scientific, Inc.) provided temperature, wind, solar radiation, and humidity data. At each site, one of the three weather stations also collected precipitation data. Weather data manipulation is described in the *Weather* section of Model Development below.

Model Development

CropSyst requires weather, soil, management, and crop input files. Most input parameters reflected field/laboratory observations and measurements or established values for the region and were not calibrated. This includes weather data, management information, and soil properties. Select crop parameters (refer to Table 4 and Table 6) were updated or calibrated to better match simulated model outputs to observed field data. The following sections detail data collection and input file creation and subsequent calibration and evaluation efforts.

Weather

The CropSyst weather file includes precipitation, solar radiation, wind, minimum and maximum relative humidity, and minimum and maximum temperature on a daily timestep. The weather instrumentation used in this study automatically logged these measurements at five-minute intervals. This data was summarized into daily values using the daily average or daily minimum/maximum observed values, as appropriate. Unfortunately, this solar powered equipment stopped working each winter, due to reduced incidence of sunlight, and during some periods other times of year, as a result mechanical or electrical failures. Gaps in on-site data were filled with nearby weather stations (e.g., Pullman, 53 kilometers to the southeast of St. John field site, or University of Idaho Kambitsh farm, 12 kilometers northwest of the Genesee field site), corrected as necessary to reflect the field sites.

The Genesee site lies in a high precipitation region and St. John in an intermediate precipitation region based on normal average annual precipitation (Schillinger et al., 2003). Table 1 summarizes precipitation observed from our period-of-interest, October 1, 2017 – October 31, 2021. For reference, St. John's average annual precipitation for the years 1963 – 2016 is 17.2 inches, and Moscow, Idaho's (27 kilometers northwest of the Genesee site) average annual precipitation as 23.8 inches for the years 1893 – 2016 (WRCC DRI, 2022). During the majority of the study period, the annual precipitation fell below these normal values, with greater drought conditions experienced in 2020 and 2021.

Table 1: Observed precipitation at each field site with gaps filled with data from nearby weather stations by water year (October 1 – September 30) and calendar year (January 1 – December 31)

	Genesee		**St. John**	
Water year	*mm*	*in*	*mm*	*in*
2017-2018	540.0	21.3	433.8	17.1
2018-2019	474.0	18.7	390.4	15.4
2019-2020	435.5	17.1	354.6	14.0
2020-2021	342.3	13.5	311.2	12.3
Calendar year	*mm*	*in*	*mm*	*in*
2018	444.2	17.5	380.5	15.0
2019	429.5	16.9	342.3	13.5
2020	483.9	19.1	423.1	16.7

Soil

CropSyst soil files require inputs for soil texture, soil-water retention properties, saturated hydraulic conductivity, and bulk density (Table 2). Soil texture was measured based on composite soil samples from 2019. The Genesee strip trial site primarily contains Thatuna-Naff and Naff-Palouse soils (silt loams), and the St. John strip trial is mapped as Mondavi (silt loam) (Soil Survey Staff, n.d.). NRCS soil survey maps indicate little variability throughout the field sites, and sampling depth divisions captured dominant soil horizons. Small quantities of soil (5-10 grams) from a strip (strip D) in each replicate were combined to create three composite texture samples from each site: 0-30 cm, 30-90 cm, and 90-150 cm. Analysis was run on a Meter PARIO (METER Group, Inc.). The PARIO conducts soil particle analysis using the integral suspension method, based on Stoke's Law. Appendix B includes particle size distributions, with results summarized in Table 2. Data classifies Genesee soil as silt loam and silty clay loam and St. John as silt loam, consistent with NRCS soil survey.

Soil-water characteristic curves were measured with a Meter HYPROP (METER Group, Inc.) and Meter WP4 equipment (METER Group, Inc.). Soil cores were collected from replicate 5's BAU spring wheat in Genesee and replicate 3's BAU fallow in St. John during June 2021 at depths of six inches and 1.5 feet below ground surface. Strip selection considered biomass present (for ease of sampling) and utilized soil moisture sensor replicates and BAU rotation plots for consistency. Based on the NRCS soil survey maps (Soil Survey Staff, n.d.), little spatial variability among strips or depths existed and was not expected to influence measurements. HYPROP and WP4 measurements provided complete water retention curves, from which values for water content at saturation, water content at permanent wilting point, water content and potential at field capacity, air entry potential, and Campbell pore size distribution index (*b)* were determined.

Saturation, wilting point, and field capacity are soil hydraulic properties, which define soil moisture held under a specific tension. CropSyst defines permanent wilting point potential as -1,500 kilopascal (kpa), and field capacity potential was specified as -33 kpa. To identify saturation, wilting point, and field capacity values, the laboratory-measured water retention curve was fit to the van Genuchten model (van Genuchten, 1980); see Appendix C. Fitting the Campbell model provided the air entry potential and Campbell *b* values (Appendix C). The models fit observed data well, with R^2 statistics greater than 0.9 and root mean square error (RMSE) less than the standard deviation (σ) of observations for both the van Genuchten model and the Campbell model. The difference between field capacity and wilting point represents plant available soil water (Kirkham, 2014). Saturated hydraulic conductivity, the ease at which water passes through the soil, was computed within

CropSyst using pedotransfer functions based on soil texture and other properties (Saxton and Rawls, 2006).

Table 2: CropSyst soil file input values

Site	*Depth (cm)*	*Sand*[1] *(%)*	*Silt*[1] *(%)*	*Clay*[1] *(%)*	*Saturation (%V)*	*Field capacity at 33 kPa* [2] *(%V)*	*Permanent wilting point at 1,500 kPa* [2] *(%V)*	*Saturated hydraulic conductivity*[3] *(m/d)*	*Campbell b*[4]	*Air entry potential*[4] *(J/kg)*	*Bulk density (g/cc)*
St. John	0-30	15%	70%	14%	49	28.3	8.9	0.013	3.2	-5.59	1.18
	30-60	17%	74%	9%	50	28.6	9.8	0.019	3.6	-4.32	1.18
	60-90	17%	74%	9%	50	28.6	9.8	0.019	3.6	-4.32	1.09
	90-120	16%	74%	10%	50	28.6	9.8	0.019	3.6	-4.32	0.87
	120-150	16%	74%	10%	50	28.6	9.8	0.019	3.6	-4.32	0.81
Genesee	0-30	7%	65%	28%	45	30.6	14.4	0.035	4.9	-5.40	1.25
	30-60	5%	62%	33%	43	31.1	13.8	0.009	4.8	-6.87	1.39
	60-90	5%	62%	33%	43	31.1	13.8	0.009	4.8	-6.87	1.54
	90-120	7%	71%	22%	43	31.1	13.8	0.047	4.8	-6.87	1.55
	120-150	7%	71%	22%	43	31.1	13.8	0.047	4.8	-6.87	1.52

[1] Based on composite samples of 0-30 cm, 60-90 cm, and 90-120 cm.

[2] 0-30 cm and 30-150 cm samples taken at 0.5-feet (15-cm) and 1.5-feet (45-cm) depths, respectively. Based on van Genuchten model (van Genuchten, 1980); see Appendix C.

[3] Estimated by CropSyst using soil texture values.

[4] Based on Campbell approach (Campbell, 1974); see Appendix C.

CropSyst also requires initialization of soil organic matter (SOM), included directly in a scenario (simulation). The mineralization of SOM serves as an important source of nitrogen. SOM measurements, based on loss by ignition, were taken yearly throughout the strip trials at depths of 0-10 cm and 10-20 cm below ground surface. While loss by ignition is a widely used method for determining SOM, it is worth mentioning the many factors influence its accuracy, including the chemical composition of the SOM, type of furnace used, and test protocol such as size of sample, duration, and temperature of ignition (Hoogsteen et al., 2015). SOM remained fairly consistent over the course of the experiment (2018-2021) and across strips and replicates. Consequently, at each site, these measurements were averaged and assigned to the uppermost soil layer universally (same value for all strips). SOM for deeper layers (to 150 cm below ground surface) were estimated from the NRCS soil survey database (Table 3).

Table 3: Initial soil organic matter in percent, separated by depth below ground surface

Percent SOM		
Depth (cm)	*Genesee*	*St. John*
0-30	4.53	3.90
30-60	2.10	1.34
60-90	1.00	1.13
90-120	1.00	1.13
120-150	1.00	1.13

Management

A unique CropSyst management file was created for each crop for each year, totaling 68 files. CropSyst management file inputs included planting date; fertilizer application form, rate, and date; and harvest date. Fertilization rates were assigned each year based on composite pre-plant fertility tests taken from each treatment. At planting, winter and spring wheat crops were fertilized with urea ammonium nitrate (UAN), ammonium phosphate, and ammonium thiosulfate. CropSyst offers an option to automatically supply nitrogen at deficient requirements, but during model development and calibration, fertilizations were assigned in the model at the rates applied during the strip trials. CropSyst does not simulate phosphorus or sulfur uptake, but management files included the nitrogen introduced as ammonium phosphate and thiosulfate. In select years, wheat was top dressed later in the growing season with urea granules. Winter peas, chickpeas, and cover crops were never fertilized.

In Genesee, winter crops were planted in early October, and spring crops were generally planted at the end of April. In St. John, winter crops were typically planted at the end of September and spring crops in early April. Most harvests occurred via combine in August. In 2020 and 2021, chickpeas were desiccated prior to harvest. However, harvest was still assigned to the true harvest date. Cover crops were harvested via swather in mid-summer, with total biomass measured and analyzed as described in *Field and* Laboratory Data. No tillage, irrigation, or residue/biomatter additions occurred.

Appendix D contains planting dates, harvest dates, and fertilization information.

Initialization/Recalibration

CropSyst simulations were initialized with pre-plant observed soil moisture, nitrate, and ammonium values. For early biomass/yield and soil moisture calibration purposes, CropSyst simulations used observed initial conditions for each growing season. Later, the model was initialized at the start of the crop rotation and allowed to run without further recalibration/initialization to assess the long-term predictive ability of the model.

Crop

Single crop files for each crop type at each site, applicable across all rotations and years, were developed based on default crop files in the model. Calibration efforts focused on replicate 5 in Genesee and replicate 3 in St. John, with each strip simulated separately for a total of nine rotational simulations per site. These replicates were selected, as they included continuous soil moisture sensors and game cameras (2021), and certain soil parameters, discussed above, were only available in these strips.

Calibration followed a sequential manual approach. For every crop, each calibrated parameter was incrementally increased or decreased until the best results were achieved (i.e., minimized error in predicted values). Calibration utilized 2018-2020 data, as it represented a complete cycle of the three-crop rotations, with 2021 data included in validation. Calibration started with the BAU strips and their crops, and then progressed across all strips. Initially, each year was calibrated independently, using the initialization/recalibration files discussed earlier, and then complete rotations were simulated and assessed. Initial yield/biomass and soil moisture calibration efforts occurred with nitrogen modeling off; after yield/biomass calibrations were acceptable, only nitrogen parameters were calibrated with nitrogen modeling enabled. Nitrogen calibration aimed to produce the same yield and biomass outcomes as simulated with the nitrogen submodel disabled, as it was assumed no nitrogen stress affected the field trial crops.

Yield/Biomass and Soil Moisture Calibration

Parameter adjustment and calibration followed a specific stepwise approach. Calibration primarily focused on observed data within a specific strip; however, the overall assessment of predictive ability also considered agreement with replicated averages and 95% confidence intervals for a given "treatment". First, harvest indices were adjusted to better reflect the range of biomass and yield relationships observed in the field. Next, phenology parameters were calibrated to reflect game camera information and achieve agreement between normalized difference vegetation index (NDVI) from satellite imagery and the leaf area index (LAI) simulated by CropSyst. LAI, with units of area per area (e.g., m^2/m^2), defines the leaf area in a canopy, and NDVI quantifies vegetative 'greenness', which has been proven to be strongly linked to above ground crop biomass and chlorophyll content, as a function of reflected light. These two metrics should correlate strongly, as green areas are "selective absorbers of solar radiation" (Chen and Cihlar, 1996). However, because LAI and NDVI assess two different canopy characteristics, structure and color, the parameters are not always directly proportional.

Next, canopy extinction coefficient for solar radiation (*k*) and, finally, radiation use efficiency (RUE) were calibrated for all crop files, both of which strongly influence yield, biomass, soil moisture outcomes. In the CropSyst canopy model, *k* serves as a first-order rate constant in the canopy cover fraction calculation. A low *k* value implies lower efficiency, with much of the radiation reaching the bottom on the canopy (Zhang et al., 2014). The unitless variable varies between zero and one, and a greater value of *k* results in a greater fraction of canopy cover. The specified RUE value is associated with unstressed conditions at very low vapor pressure deficits (high humidity) and factors into the transpiration use efficiency based attainable growth model. It represents biomass produced per light intercepted by the canopy. It generally varies between one and five grams per megajoule (g/MJ).

Cover crop stands included a significant amount of winter wheat, so the winter wheat crop file was used as a starting point for cover crop file development. Although adjusting the phenology, *k*, and RUE values allowed for better simulation of observed cover crop outcomes, the "base" crop file utilized was not reflective of a cover *mix*, so it was determined an additional parameter was needed for cover crop calibration. In the final step of calibration, TUE, another influential parameter in determining biomass simulated by CropSyst (Confalonieri et al., 2006a), was calibrated for cover crops only. CropSyst defines transpiration use efficiency, also known as a biomass transpiration coefficient, as grams of biomass produced per kilogram of water at a vapor pressure deficit of one kilopascal. It serves as the slope of the linear regression model (Kemanian et al., 2005).

Table 4 summarizes the sequence of yield/biomass and soil moisture calibration.

Table 4: Summary of the yield/biomass and soil moisture calibration process applied during model development

Adjusted/calibrated parameter	*Observed metric*
1. Unstressed and stressed harvest indices	Relationship between yield and biomass
2. Phenology (flowering, filling, maturity)	Growth stage timing and agreement between measured NDVI and CropSyst simulated LAI
3. Canopy extinction coefficient for solar radiation, *k*	Yield, biomass, and soil moisture
4. Radiation use efficiency, RUE	Yield, biomass, and soil moisture
5. Transpiration use efficiency, TUE[1]	Yield, biomass, and soil moisture
[1]Calibrated for cover crops only	

Nitrogen Calibration

Similar to the yield/biomass and soil moisture calibration, nitrogen parameter adjustment and calibration followed a manual, stepwise approach. Calibration focused on the strip of interest's replicated average crop nitrogen observed value, while maintaining crop biomass and yield achieved during previous calibration efforts (nitrogen submodel disabled). While CropSyst simulates nitrogen fixation for legume crops, it does not offer input parameters to adjust. It is also worth noting that during yield/biomass and soil moisture calibration efforts, results were computed on a daily timestep. However, CropSyst requires Cascade method simulations (utilized in this work) that include nitrogen use an hourly timestep. Small discrepancies may have resulted from this change. The nitrogen submodel was completely 'calibrated' for Genesee only. Select parameters established for Genesee (maximum apparent soil carbon decomposition for undisturbed soil and critical and maximum nitrogen concentrations of the canopy at emergence) were assigned to the St. John crop files, effectively splitting the dataset and allowing for further verification of calibrated parameters.

CropSyst simulates the complete nitrogen cycle, with processes manipulated through crop nitrogen parameters and organic matter characteristics. Although CropSyst offers the option to simulate organic carbon cycling as three different pools, measurements of each pool were not available to parameterize the model, so a single soil carbon pool was simulated. To begin calibration, the soil organic matter's carbon to nitrogen ratio (C:N) was updated to reflect field observations at both sites. The dimensionless C:N relationship affects the relative amount of carbon and nitrogen converted in

the soil or assimilated by microbes (Janssen, 1996). Laboratory C:N values corresponded to water-extractable organic carbon and nitrogen. Water-extractable organic carbon and nitrogen represent portions of the overall organic carbon and nitrogen fractions, as not all organic carbon and nitrogen will partition into water, but these subsets are critical to the microorganisms that drive the nitrogen cycle (Haney et al., 2012). Water-extractable organic matter is considered most representative of the labile fraction (Zhang et al., 2011). However, total and water-extractable C:N ratios can be very similar (Haney et al., 2012). A limited LIT dataset of total soil organic carbon and total soil nitrogen suggested that, in this case, the total organic C:N ratios may be lower than water-extractable values. However, this dataset was not available at the time of model development, and the C:N ratio did not appear highly influential on model outputs. Parameterizing the C:N value left a single unknown decay rate parameter, the 'maximum apparent soil carbon decomposition for undisturbed soil', which was calibrated in the Genesee model to maintain observed organic matter levels and achieve crop nitrogen uptake as observed during the field trial. Organic matter decomposition follows first order kinetics, with the rate constant in units of 1/day (Stöckle, n.d.).

The maximum aboveground nitrogen concentration at maturity and the maximum concentration of nitrogen in chaff and stubble were adjusted based on observed harvest data at each site. Nitrogen concentrations are related as kilograms nitrogen per kilogram dry matter (kg N/kg DM). Next, critical nitrogen concentration at emergence and, finally, maximum nitrogen concentration of the canopy at emergence values were calibrated for the Genesee site. These parameters feed the nitrogen demand model, which CropSyst computes as a dilution curve based on a critical nitrogen concentration. The nitrogen dilution curve is a negative power function, with nitrogen declining over time ("diluting"). Concentration at emergence values correspond to early, linear growth stage in a plant well-supplied with nitrogen and are measured in units of kg N/kg DM (Stöckle, n.d.). Parameter calibration focused on minimizing the error between simulated and observed total crop nitrogen.

Table 5 summarizes the nitrogen calibration process.

Table 5: Summary of the nitrogen calibration process applied during model development

Adjusted/calibrated parameter	*Observed metric*
1. Carbon to nitrogen ratio, C:N	C:N values, soil organic matter
2. Maximum apparent soil carbon decomposition for undisturbed soil (decay rate)	Soil organic matter
3. Maximum aboveground nitrogen concentration at maturity	Percent nitrogen in grain and biomass
4. Maximum concentration of nitrogen in chaff and stubble	Percent nitrogen in biomass
5. Critical nitrogen concentration of the canopy at emergence	Total nitrogen in crop, occurrence of nitrogen stress
6. Maximum nitrogen concentration of the canopy at emergence	Total nitrogen in crop

Statistical Assessment

Statistical analysis confirmed parameter selection. The coefficient of determination (R^2), equation (1), describes the linearity of the relationship between observed and simulated data. It ranges from 0 to 1 and represents the portion of variance explained by the model. Root mean square error (RMSE), equation (2), serves as an error index. This work considers R^2 values greater than 0.5 (Moriasi et al., 2007) and RMSE values less than one standard deviation (σ) of observations as acceptable. The relative error (RE), equation (3), normalizes the RMSE and quantifies error without dimensions; a value of 1 indicates perfect agreement (Stöckle et al., 2004). Standard deviation (σ), equation (4), relates data variation or spread. Mean difference (MD), equation (5), quantifies the difference between the averages of two datasets, and confidence intervals (CI), described in equation (6), provide interval estimates for a parameter based on observations. Finally, the Willmott index of agreement (d), equation (7), is a standardized metric of model error, varying between 0 (no agreement) and 1 (perfect agreement) (Willmott, 1981). It is frequently used to assess cropping models (Ahmed et al., 2016; Benli et al., 2007; Todorovic et al., 2009).

$$R^2 = \frac{\sum_{i=1}^{n}(y_i^{sim} - y^{mean})^2}{\sum_{i=1}^{n}(y_i^{obs} - y^{mean})^2} \quad (1)$$

Where y_i^{obs} is ith observation of y, y_i^{sim} is the simulated value of y for ith observation, $y^{mean}$is the mean of the observed y values, and n is the sample size.

$$RMSE = \sqrt{\frac{\sum_{i=1}^{n}(y_i^{obs} - y_i^{sim})^2}{n}} \quad (2)$$

Where y_i^{obs} is ith observation of y, y_i^{sim} is the simulated value of y for ith observation, and n is the sample size.

$$RE = \frac{RMSE}{y^{mean}} \quad (3)$$

Where RMSE is the root means square error, and $y^{mean}$is the mean of the observed y values.

$$\sigma = \sqrt{\frac{\sum_{i=1}^{n}(y_i^{obs} - y^{mean})}{\mathrm{n}}} \quad (4)$$

Where y_i^{obs} is ith observation of y, $y^{mean}$is the mean of the observed y values, and n is the observation dataset size.

$$MD = \frac{\sum_{i=1}^{n}(y_i^{obs} - y_i^{sim})^2}{\mathrm{n}} \quad (5)$$

Where y_i^{obs} is ith observation of y, y_i^{sim} is the simulated value of y for ith observation, and n is the sample size.

$$CI = y^{mean} \pm t_{\alpha/2} \times \frac{s}{\sqrt{n}} \quad (6)$$

Where $y^{mean}$is the mean of the values, t is the t-test statistic, α is the confidence level, s is the sample standard deviation, and n is the sample size.

$$d = 1 - \frac{\sum_{i=1}^{n}(y_i^{sim} - y_i^{obs})^2}{\sum_{i=1}^{n}(|y_i^{sim} - y_i^{mean}| + |y_i^{obs} - y_i^{mean}|)^2} \quad (7)$$

Where y_i^{obs} is ith observation of y, y_i^{sim} is the simulated value of y for ith observation, $y^{mean}$is the mean of the observed y values, and n is the sample size.

Results

Yield/Biomass and Soil Moisture Calibration

All results summarized in this section correspond to outcomes achieved during full rotational simulations (i.e., no recalibration or re-initialization of soil properties each cropping year). In general, the stressed harvest index fell 0.1 to 0.2 units below the unstressed index (Table 6). Slightly higher harvest indices were achieved in Genesee than in St. John.

Table 6: Adjusted harvest indices applied to CropSyst crop files

Crop	**Harvest index (unstressed/stressed)**
Genesee	
Winter wheat	0.51/0.35
Spring wheat	0.45/0.34
Chickpea	0.54/0.34
Winter pea	0.50/0.35
Cover crop	-
St. John	
Winter wheat	0.45/0.35
Spring wheat	0.45/0.30
Winter pea	0.40/0.20
Cover crop	-

In all cases, degree days for emergence were left at default values due to insufficient field data and the parameter's limited influence (Table 7). Key phenological growth stage timing for winter wheat and winter pea, the only winter crops common to Genesee and St. John, were identical.

Table 7: Calibrated phenology values in growing degree days applied to CropSyst crop files

Crop	**Phenology, °C-day (emergence/flowering/filling/maturity)**
Genesee	
Winter wheat	50/1,300/1,500/2,100
Spring wheat	50/800/900/1,400
Chickpea	1/500/600/1,100
Winter pea	50/1,300/1,500/2,100
Cover crop	50/1,350/1,500/2,500
St. John	
Winter wheat	50/1,300/1,500/2,100
Spring wheat	50/700/850/1,300
Winter pea	50/1,300/1,500/2,100
Cover crop	50/600/700/2,000

Phenology parameters were established based on agreement between simulated LAI and measured NDVI (example plotted in Figure 2), as well as game camera images from 2021. A strong correlation should exist between the rising arm of the seasonal LAI and NDVI curves.

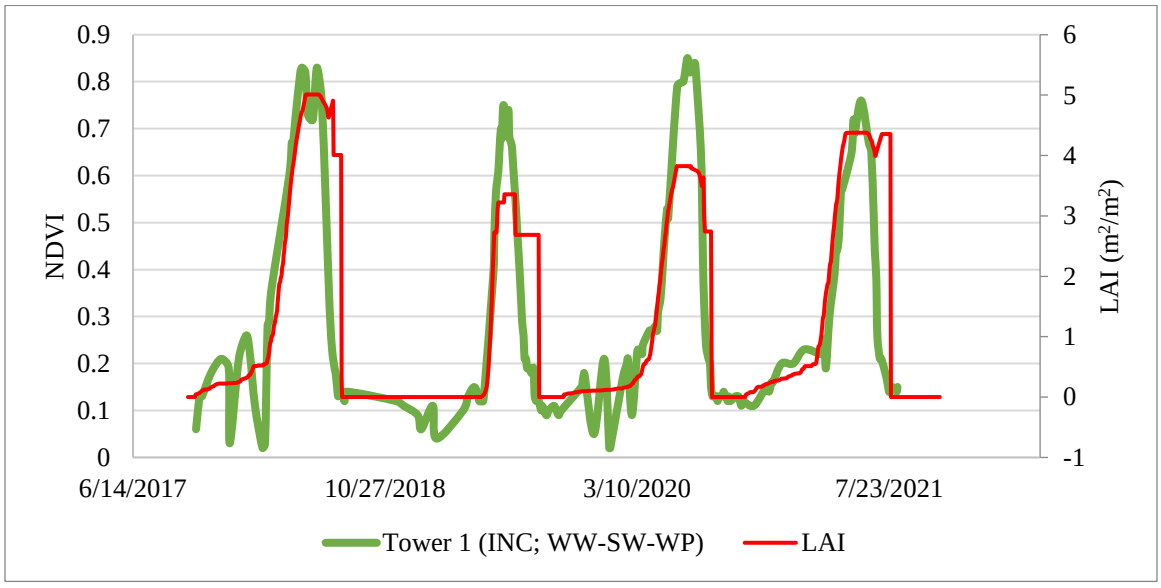

Figure 2: Example graphical comparison of CropSyst simulated leaf area index (LAI) and FluroSense normalized difference vegetation index (NDVI), Strip G in Genesee; INC = Incremental, WW=winter wheat, SW=spring wheat, WP=winter pea

Table 8 and Table 9 list the compared crops, as direct comparisons were not always available. For example, for Genesee strip A in 2020, the CropSyst simulated LAI for spring wheat was compared to a nearby spring barley field's NDVI. Cover crops in the area, beyond those planted in the tower fields, could not be located. The tables only include 2018-2020 crop years, as they represent a complete cycle of the three-year rotations, and 2021 crop type data was not available at the time of analysis. R^2 values reflect the "development stage", the rising arm of the seasonal curve on the graph above. Agreement between simulated LAI and NDVI was good ($R^2 > 0.5$).

Table 8: R^2 between Genesee simulated leaf area index (LAI) and normalized difference vegetation index (NDVI) of nearby fields by strip (labeled A-I); ASP=aspiration, INC=incremental, BAU=business-as-usual, CP=chickpea, SW=spring wheat, WW=winter wheat, WP=winter pea, CC=cover crop, SB=spring barley

		2018	2019	2020
A (BAU)	*LAI (strip)*	CP	WW	SW
	NDVI (nearby field)	CP	WW	SB
	R^2	0.90	0.96	0.94
B (INC)	*LAI (strip)*	WP	WW	SW
	NDVI (nearby field)	WW	WW	SB
	R^2	0.81	0.93	0.93
C (BAU)	*LAI (strip)*	SW	CP	WW
	NDVI (nearby field)	SB	CP	WW
	R^2	0.93	0.96	0.95
D (ASP)	*LAI (strip)*	CC	CP	WW
	NDVI (nearby field)	-[1]	CP	WW
	R^2	-[1]	0.97	0.97
E (INC)	*LAI (strip)*	WW	CC	CP
	NDVI (nearby field)	WW	CC	CP
	R^2	0.77	0.80	0.97
F (INC)	*LAI (strip)*	SW	WP	WW
	NDVI (nearby field)	SB	WW	WW
	R^2	0.91	0.95	0.95
G (INC)	*LAI (strip)*	WW	SW	WP
	NDVI (nearby field)	WW	SW	WP
	R^2	0.90	0.96	0.94
H (ASP)	*LAI (strip)*	CP	WW	CC
	NDVI (nearby field)	CP	WW	-[2]
	R^2	0.90	0.98	-[2]
I (BAU)	*LAI (strip)*	WW	SW	CP
	NDVI (nearby field)	WW	SW	CP
	R^2	0.91	0.94	0.88

[1]No NDVI comparison available

Table 9: R^2 between St. John simulated leaf area index (LAI) and normalized difference vegetation index (NDVI) of nearby fields by strip (labeled A-I); ASP=aspiration, INC=incremental, BAU=business-as-usual, SW=spring wheat, WW=winter wheat, WP=winter pea, CC=cover crop

		2018	**2019**	**2020**
A (INC)	*LAI (strip)*	WP	WW	SW
	NDVI (nearby field)	WW	WW	SW
	R^2	0.94	0.98	0.97
B (BAU)	*LAI (strip)*	F	WW	SW
	NDVI (nearby field)	-	WW	SW
	R^2	-	0.99	0.97
C (ASP)	*LAI (strip)*	SW	CC	WW
	NDVI (nearby field)	SW	CC	WW
	R^2	0.69	0.98	0.90
D (INC)	*LAI (strip)*	WW	SW	WP
	NDVI (nearby field)	WW	SW	WW
	R^2	0.97	0.98	0.99
E (INC)	*LAI (strip)*	SW	WP	WW
	NDVI (nearby field)	SW	WP	WW
	R^2	0.72	0.96	0.90
F (BAU)	*LAI (strip)*	WW	SW	F
	NDVI (nearby field)	WW	SW	-
	R^2	0.93	0.98	-
G (ASP)	*LAI (strip)*	CC	WW	SW
	NDVI (nearby field)	-[1]	WW	SW
	R^2	-[1]	0.91	0.96
H (ASP)	*LAI (strip)*	WW	SW	CC
	NDVI (nearby field)	WW	SW	-[1]
	R^2	0.94	0.98	-[1]
I (BAU)	*LAI (strip)*	SW	F	WW
	NDVI (nearby field)	SW	-	WW
	R^2	0.73	-	0.89

[1]No NDVI comparison available

While somewhat iterative, *k* values were manipulated prior to RUE. In most instances, *k* values were increased from default values. Consequently, calibrated *k* values and relatively high default TUE values resulted in well simulated yield and biomass outcomes without significant changes to default RUE values (Table 10). In many cases, crops common to both sites have the same calibrated parameter values.

Table 10: Calibrated *k* and RUE values applied to CropSyst crop files

Crop	**Canopy extinction coefficient for solar radiation (*k*)**	**Radiation use efficiency (RUE), g/mJ**
Genesee		
Winter wheat	0.60	1.50
Spring wheat	0.80	2.75
Chickpea	0.60	1.10
Winter pea	0.56	1.24
Cover crop	0.40	1.50
St. John		
Winter wheat	0.60	1.50
Spring wheat	0.70	2.75
Winter pea	0.56	1.50
Cover crop	0.50	1.50

As discussed, TUE was only calibrated for cover crops. However, for reference, Table 11 summarizes TUE values for all crops. Cover crop TUE was adjusted downward from the default value provided in the winter wheat file.

Table 11: TUE values applied to CropSyst crop files; TUE calibrated for cover crops only, with all other values corresponding to CropSyst defaults

Crop	**Transpiration use efficiency (TUE), g/kg**
Genesee	
Winter wheat	4.6
Spring wheat	6.6
Chickpea	4.0
Winter pea	3.6
Cover crop	3.25
St. John	
Winter wheat	4.6
Spring wheat	6.6
Winter pea	3.6
Cover crop	3.7

Observed versus simulated biomass and yield center around the dashed diagonal line, which represents a 1:1 relationship (i.e., a "perfect" prediction); refer to Figure 3 – Figure 6. The graphs include a datapoint for each strip for each year. As indicated by the R^2 and RMSE values, simulated biomass and yield outcomes achieve acceptable agreement with observed data, with Genesee predicted with greater accuracy than St. John. Reported d values are also similar to or exceed those reported in similar crop model assessments (Ahmed et al., 2016; Benli et al., 2007; Todorovic et al., 2009). Unlike these similar studies, this work combines multiple crops.

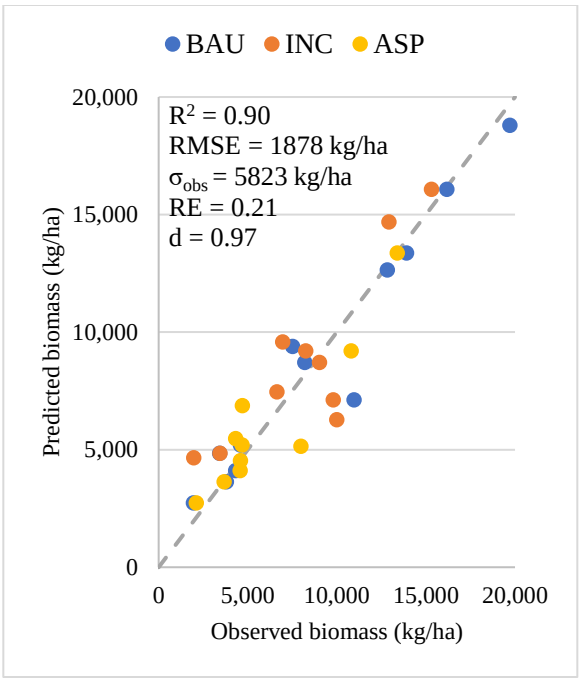

Figure 3: Genesee observed versus simulated biomass; ASP=aspiration, INC=incremental, BAU=business-as-usual, RMSE=root mean square error, σ_{obs}=standard deviation of the observations, RE=relative error, d=index of agreement

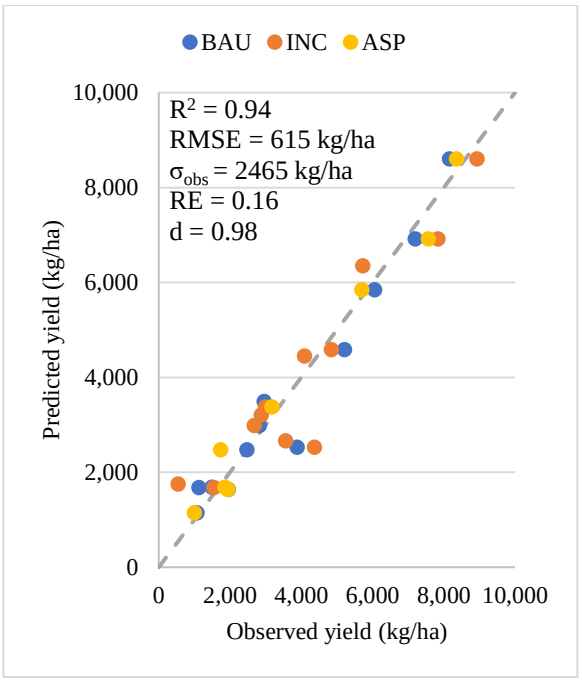

Figure 4: Genesee observed versus simulated yield; ASP=aspiration, INC=incremental, BAU=business-as-usual, RMSE=root mean square error, σ_{obs}=standard deviation of the observations, RE=relative error, d=index of agreement

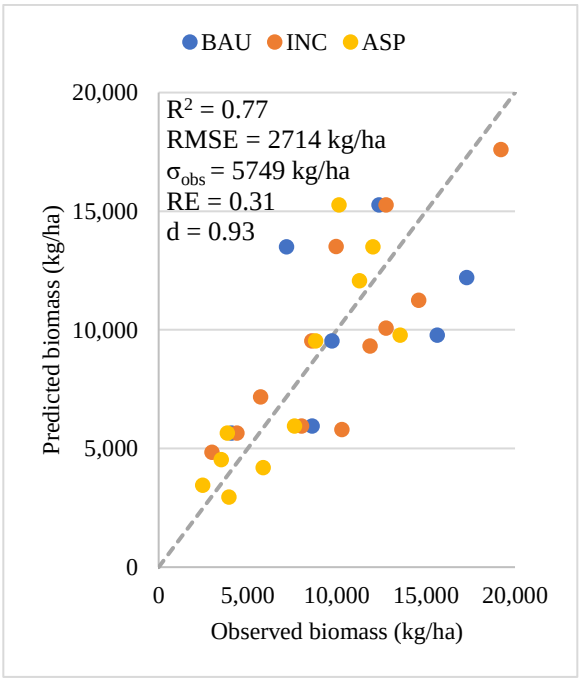

Figure 5: St. John observed versus simulated biomass; ASP=aspiration, INC=incremental, BAU=business-as-usual, RMSE=root mean square error, σ_{obs}=standard deviation of the observations, RE=relative error, d=index of agreement

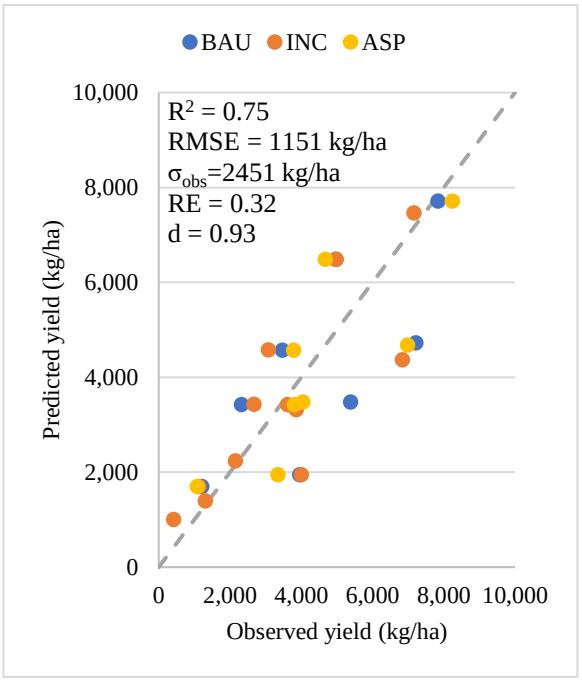

Figure 6: St. John observed versus simulated yield; ASP=aspiration, INC=incremental, BAU=business-as-usual, RMSE=root mean square error, σ_{obs}=standard deviation of the observations, RE=relative error, d=index of agreement

The R^2 and RMSE values for individual rotations also exceed the acceptable criterion; see Table 12. The table also includes a normalized RMSE, RE, and the index of agreement (d), which are approximately equal to or greater than those achieved in CropSyst studies such as Todorovic et al. (2009) and Umair et al. (2017).

Table 12: R^2, root mean square error (RMSE), relative error (RE), and index of agreement (d) between simulations and observations and standard deviation (σ) of the observations, separated by yield and biomass of rotation; ASP=aspiration, INC=incremental, BAU=business-as-usual

	Biomass					**Yield**				
	R^2	*RMSE, kg/ha*	*σ, kg/ha*	*RE*	*d*	R^2	*RMSE, kg/ha*	*σ, kg/ha*	*RE*	*d*
Genesee										
BAU	0.94	1379	5729	0.15	0.98	0.95	526	2416	0.14	0.99
INC	0.84	2088	5393	0.22	0.95	0.89	793	2425	0.19	0.97
ASP	0.94	2095	6711	0.24	0.97	0.98	393	2882	0.10	0.99
St. John										
BAU	0.80	3250	7428	0.41	0.94	0.80	1254	2885	0.41	0.94
INC	0.67	2563	4565	0.25	0.90	0.68	1173	2125	0.34	0.91
ASP	0.80	2229	5155	0.26	0.95	0.67	1238	2215	0.28	0.90

Figure 7 – Figure 10 show yearly simulated and observed biomass and yield, separated by crop type and year, with individual datapoints for each strip.

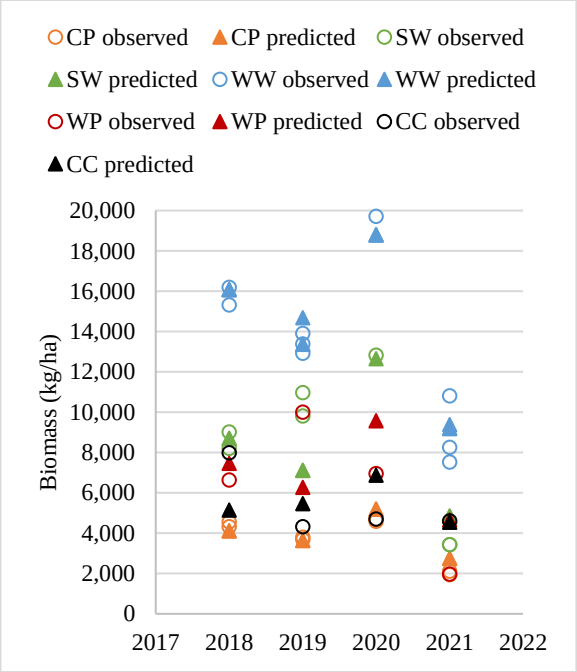

Figure 7: Genesee yearly observed and simulated biomass; CP=chickpea, SW=spring wheat, WW=winter wheat, WP=winter pea, CC=cover crop

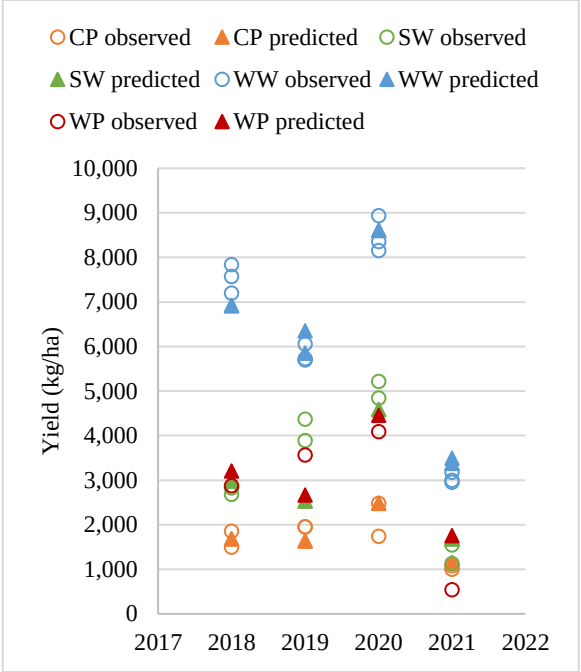

Figure 8: Genesee yearly observed and simulated yield; CP=chickpea, SW=spring wheat, WW=winter wheat, WP=winter pea

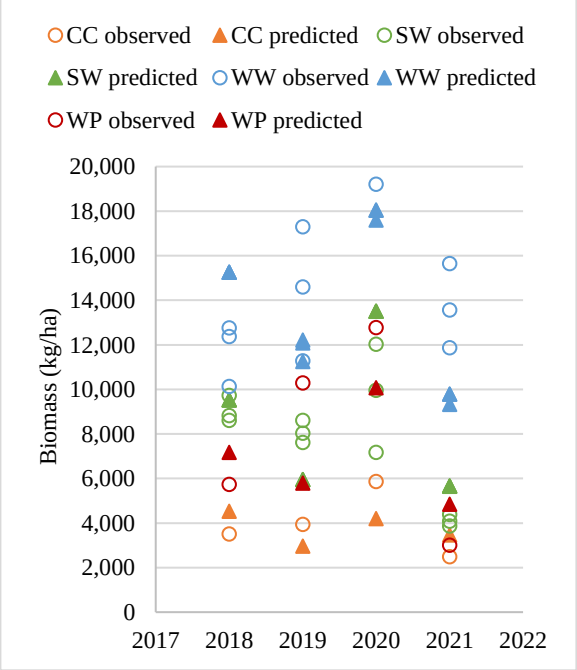

Figure 9: St. John yearly observed and simulated biomass; SW=spring wheat, WW=winter wheat, WP=winter pea, CC=cover crop

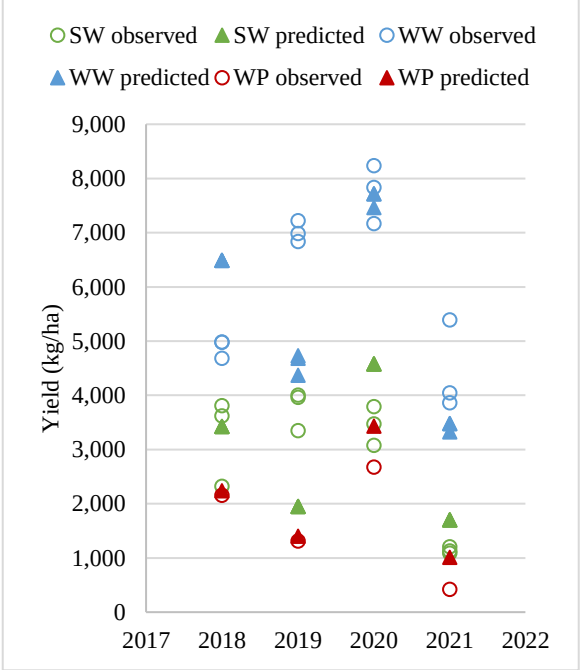

Figure 10: St. John yearly observed and simulated yield; SW=spring wheat, WW=winter wheat, WP=winter pea

Again, the model appears to successfully simulate yield and biomass when separated by year (Table 13). As mentioned, 2021 data was reserved for validation (i.e., was not considered in calibration).

Table 13: R^2, root mean square error (RMSE), relative error (RE), and index of agreement (d) between simulations and observations and standard deviation (σ) of the observations, separated by yearly yield and biomass

	Biomass					**Yield**				
	R^2	*RMSE, kg/ha*	*σ, kg/ha*	*RE*	*d*	*R^2*	*RMSE, kg/ha*	*σ, kg/ha*	*RE*	*d*
Genesee										
2018	0.88	2128	5931	0.20	0.96	0.99	452	2733	0.11	0.99
2019	0.79	1590	4200	0.23	0.93	0.86	435	1632	0.22	0.93
2020	0.98	2126	7643	0.13	0.99	0.97	913	2745	0.08	0.99
2021	0.86	1460	3210	0.30	0.93	0.88	534	1065	0.30	0.93
St. John										
2018	0.93	2247	4177	0.28	0.94	0.90	1577	1734	0.48	0.81
2019	0.87	2850	5202	0.31	0.90	0.95	1927	2689	0.46	0.79
2020	0.80	2980	7126	0.25	0.94	0.95	1347	2912	0.30	0.92
2021	0.87	2723	5591	0.42	0.89	0.90	786	1989	0.37	0.92

Figure 11 – Figure 14 highlight the year-to-year variability, as well as variability across strips and rotations. In particular, 2021 biomass and yield are markedly lower than those measured in previous years. Each average and confidence interval graphed include five data points, one for each replicate of the strip trial.

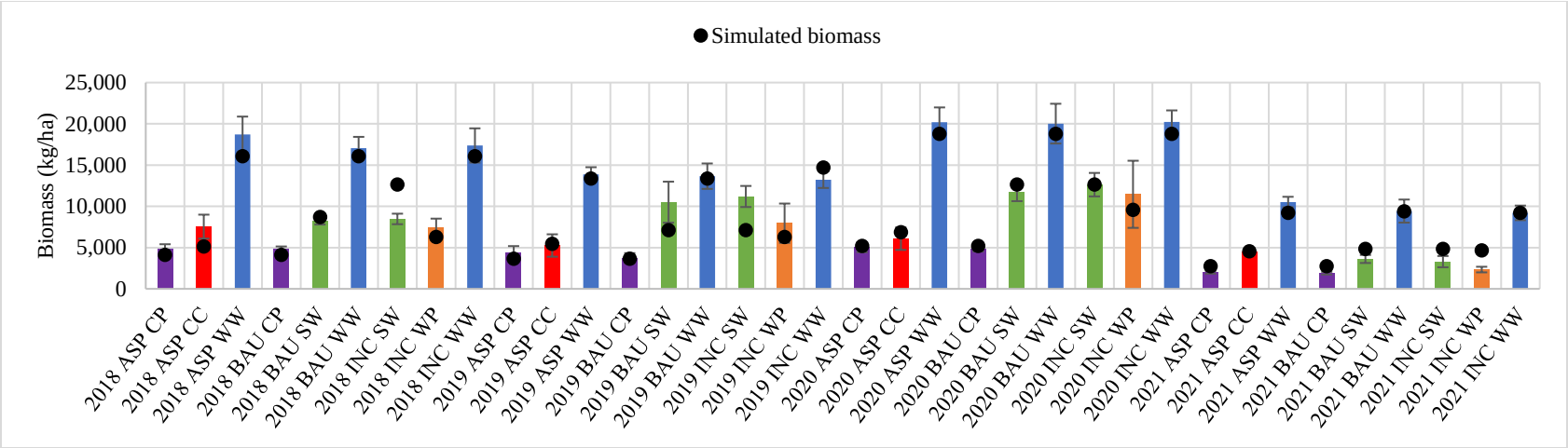

Figure 11: Genesee overall replicate average biomass with 95% confidence interval error bars around observations; ASP=aspiration, INC=incremental, BAU=business-as-usual, CP=chickpea, SW=spring wheat, WW=winter wheat, WP=winter pea, CC=cover crop

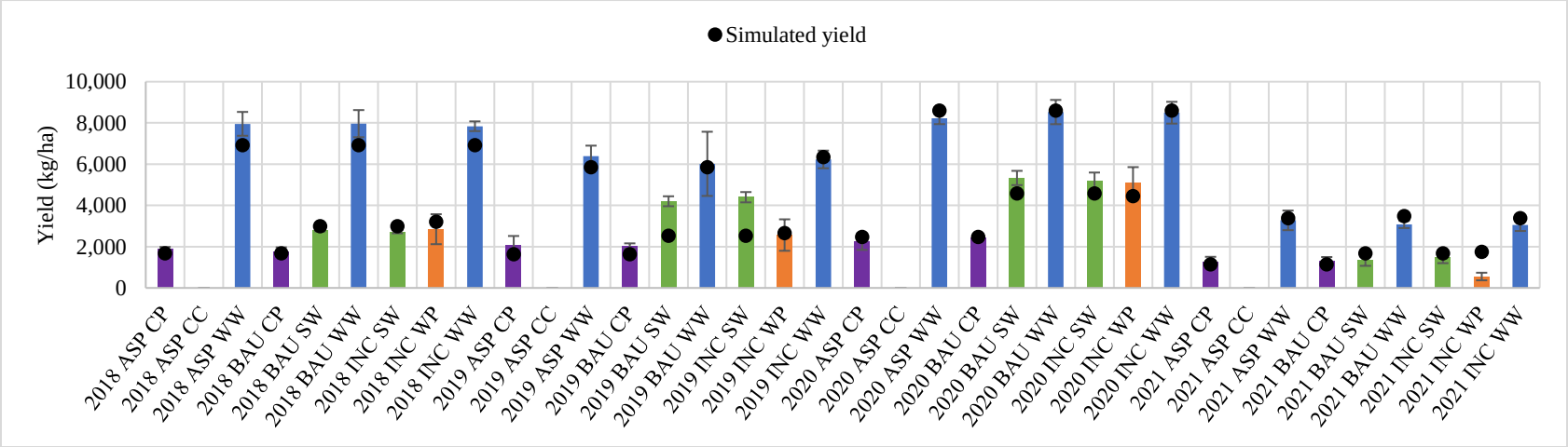

Figure 12: Genesee overall replicate average yield with 95% confidence interval error bars around observations; ASP=aspiration, INC=incremental, BAU=business-as-usual, CP=chickpea, SW=spring wheat, WW=winter wheat, WP=winter pea, CC=cover crop

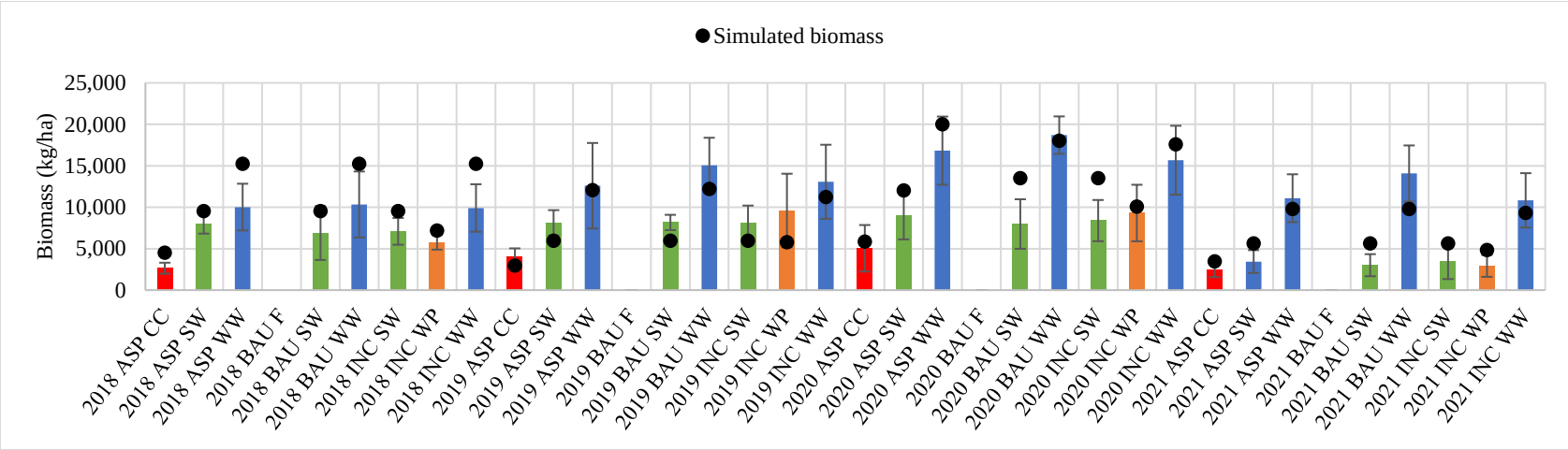

Figure 13: St. John overall replicate average biomass with 95% confidence interval error bars around observations; ASP=aspiration, INC=incremental, BAU=business-as-usual, SW=spring wheat, WW=winter wheat, WP=winter pea, CC=cover crop

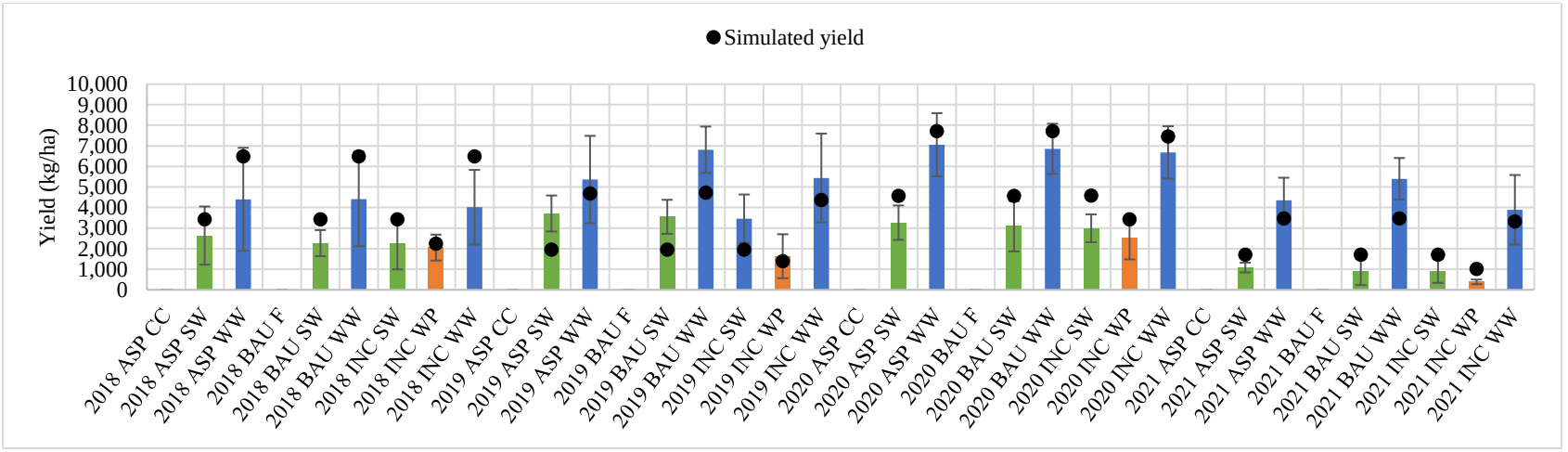

Figure 14: St. John overall replicate average yield with 95% confidence interval error bars around observations; ASP=aspiration, INC=incremental, BAU=business-as-usual, SW=spring wheat, WW=winter wheat, WP=winter pea, CC=cover crop

With the exception of St. John spring wheat, average simulated biomass and yield values fit within the 95% confidence intervals of field observations (Figure 15 – Figure 18). Between 10 and 60 datapoints contributed to each of the averages and confidence intervals, which reflect all years and all rotations.

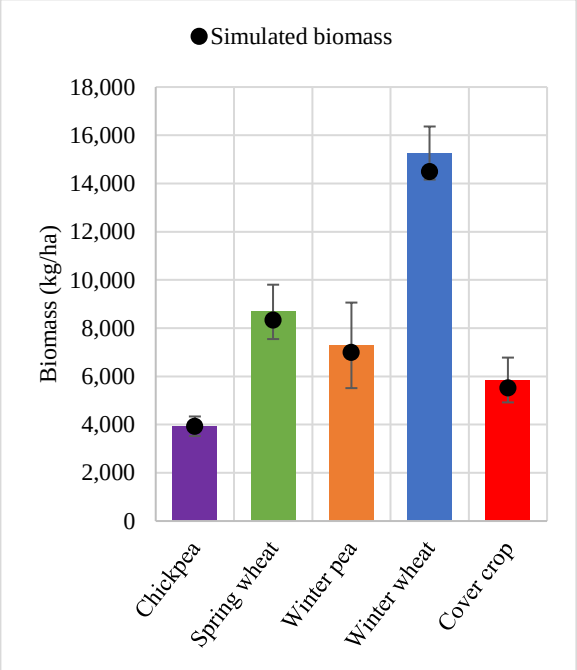

Figure 15: Genesee overall average biomass by crop type with 95% confidence interval error bars around observations

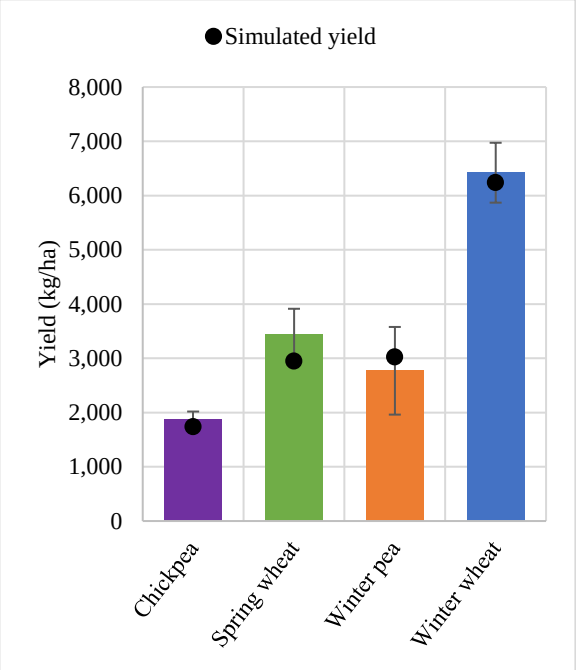

Figure 16: Genesee overall average yield by crop type with 95% confidence interval error bars around observations

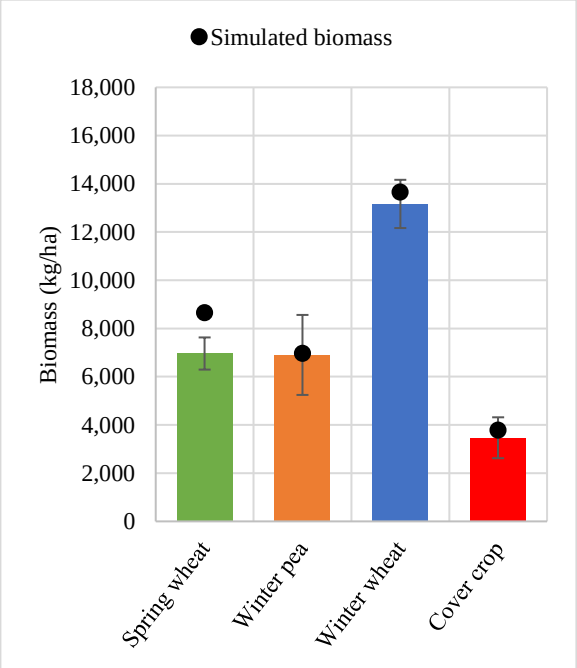

Figure 17: St. John overall average biomass by crop type with 95% confidence interval error bars around observations

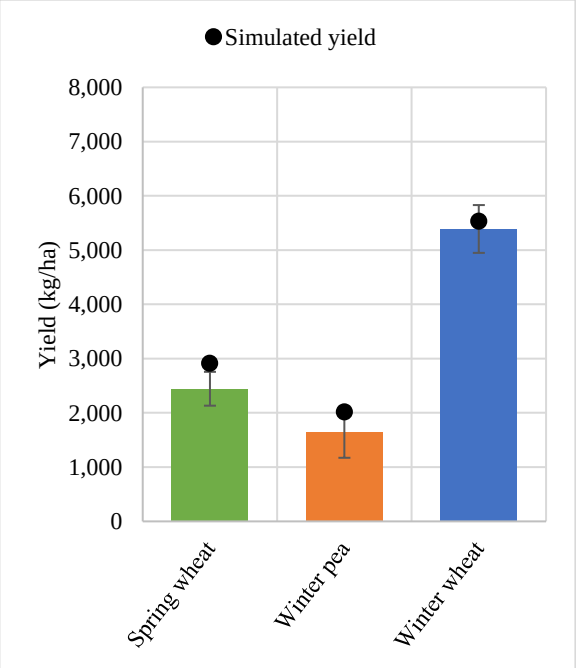

Figure 18: St. John overall average yield by crop type with 95% confidence interval error bars around observations

Appendix E contains biomass and yield statistics by crop, including R^2, MD, and RMSE between the observed biomass/yield and values predicted by CropSyst. R^2 values vary between 0.04 (cover crop biomass) and 0.95 (winter wheat yield) for Genesee and between 0.10 (cover crop biomass) and 0.90 (winter pea yield) for St. John. RMSE falls between 322 and 4,828 kg/ha for Genesee and between 481 and 3,522 kg/ha for St. John. Based on the R^2 and RMSE, model agreement for some individual crops does not meet acceptable criteria. However, since the simulated and observed yield and biomass for each crop (summarized in Table 14 and Table 15) fall in close range, and, over entire crop rotations, biomass and yield results indicate successful agreement, it was concluded that ability to simulate crop biomass and yield was acceptable.

Table 14: Genesee observed and simulated average biomass and yield by crop

	Average biomass (kg/ha)		**Average yield (kg/ha)**	
	Observed	*Simulated*	*Observed*	*Simulated*
Chickpea	3,931	3,920	1,876	1,737
Spring wheat	8,675	8,330	3,432	2,946
Winter pea	7,286	6,990	2,770	3,020
Winter wheat	15,262	14,483	6,421	6,238
Cover crop	5,849	5,506	-	-

Table 15: St. John observed and simulated average biomass and yield by crop

	Average biomass (kg/ha)		**Average yield (kg/ha)**	
	Observed	*Simulated*	*Observed*	*Simulated*
Spring wheat	6,961	8,657	2,444	2,913
Winter pea	6,903	6,969	1,644	2,018
Winter wheat	13,165	13,654	5,390	5,534
Cover crop	3,468	3,785	-	-

As discussed in *Field and* Laboratory Data, LIT data collection included manual soil moisture measurements each spring and fall (see graphic examples in Figure 19 and Figure 20 for 2018 and 2019).

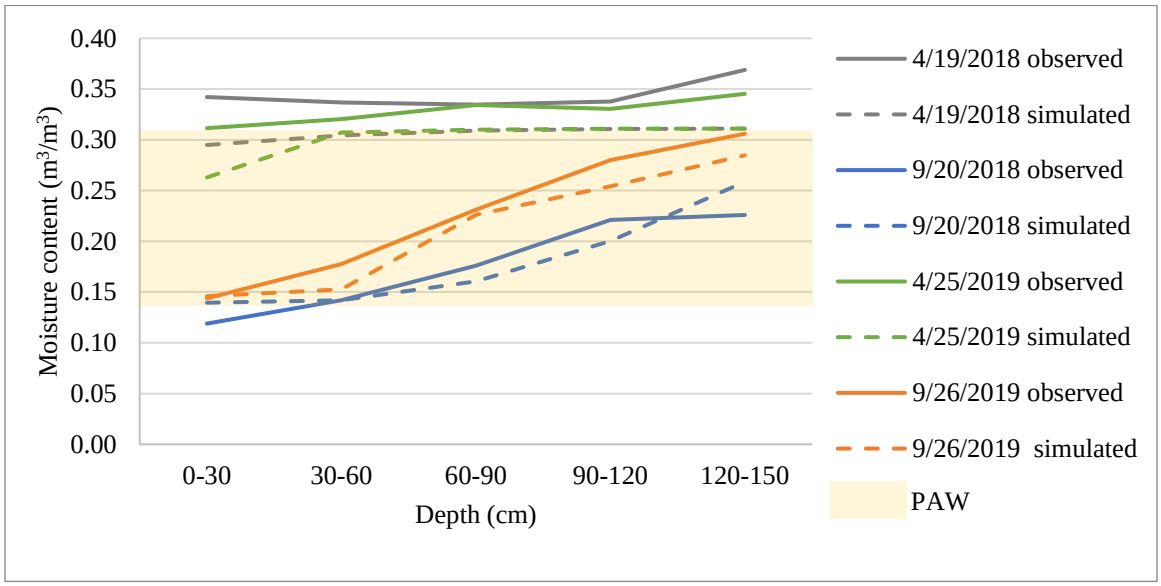

Figure 19: Observed manual and simulated CropSyst soil moisture for 2018-2019 sampling dates, Genesee strip E; PAW = approximate plant available water (soil moisture between field capacity and permanent wilting point)

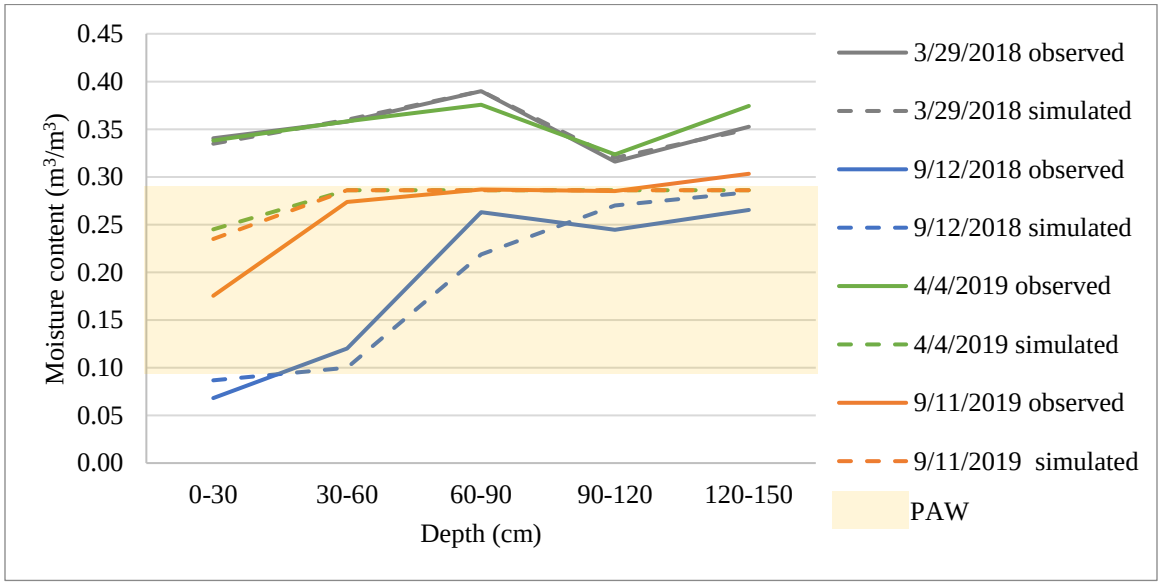

Figure 20: Observed manual and simulated CropSyst soil moisture for 2018-2019 sampling dates, St. John strip I; PAW = approximate plant available water (soil moisture between field capacity and permanent wilting point)

Automated soil moisture sensors were also installed in replicate 5 of Genesee and 3 of St. John. Stored soil water values recorded were compared with CropSyst outputs during calibration; see example profiles in Figure 21 and Figure 22. At times, sensors failed to record, indicated by gaps in the gold “average observed” datapoints.

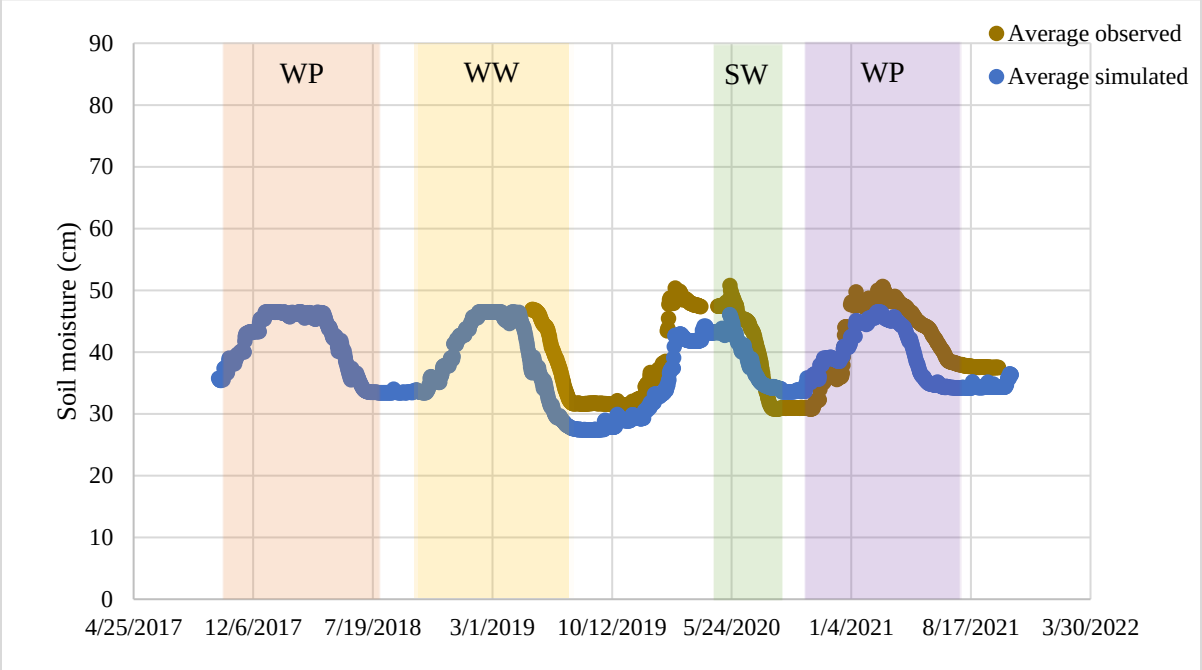

Figure 21: Genesee strip B average sensor observed and CropSyst simulated stored soil water, based on 150-cm profile; WP=winter pea, WW=winter wheat, SW=spring wheat

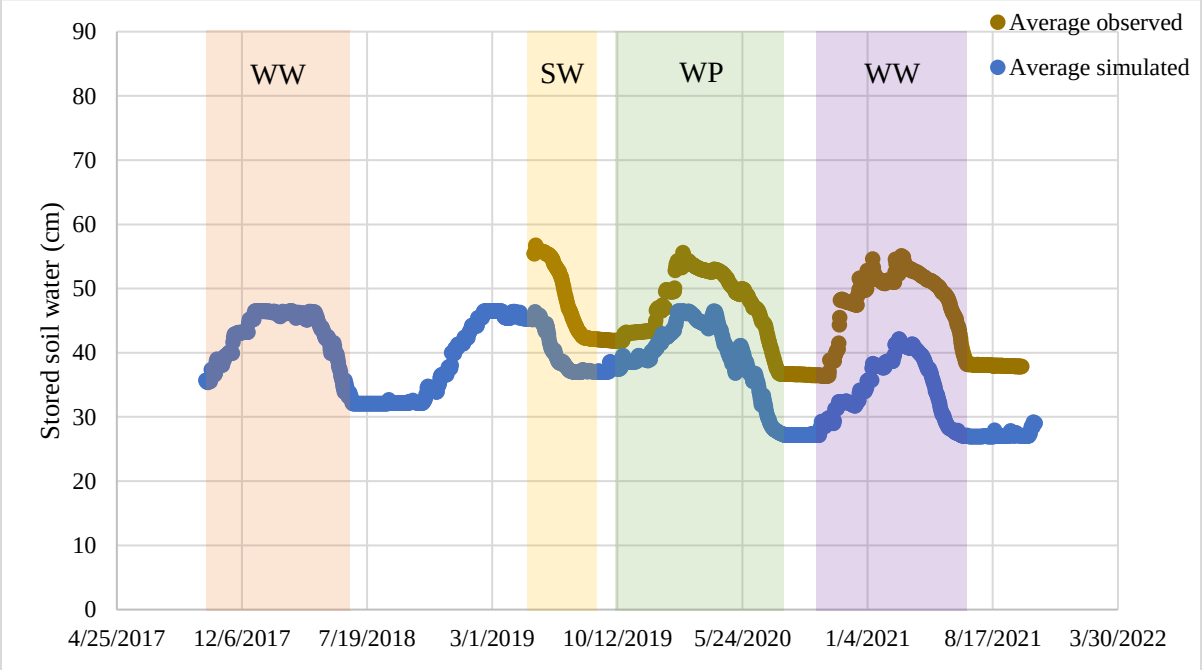

Figure 22: St. John strip D average sensor observed and CropSyst simulated stored soil water, based on 150-cm profile; WW=winter wheat, SW=spring wheat, WP=winter pea

In some instances, limited overlap occurred between the two observed datasets (indicated by low "n" values in Table 16 and Table 17), or dramatic differences between the observed datasets were present. Especially at the St. John site, sensors occasionally malfunctioned or stopped working. To account for these inconsistencies in the observed data, the calibration efforts aimed to achieve simulated soil moisture with as much accuracy as was estimated between the observed datasets, R^2=0.55 and RMSE=0.056 in Genesee and R^2=0.76 and RMSE=0.127 in St. John. Appendix F contains summaries for individual strips.

Table 16: Genesee soil moisture R^2, mean difference (MD), and root mean square error (RMSE) comparisons (replicate 5 average results) by depth (cm)

Observed sensor versus observed manual						
Depth	*Profile Avg.*	*0-30*	*30-60*	*60-90*	*90-120*	*120-150*
R^2	0.549	0.791	0.785	0.655	0.317	0.195
MD	-0.023	0.027	-0.023	-0.031	-0.039	-0.048
RMSE	0.056	0.049	0.044	0.051	0.063	0.074
n		45	38	40	33	44
Observed sensor versus CropSyst simulated						
Depth	*Profile Avg.*	*0-30*	*30-60*	*60-90*	*90-120*	*120-150*
R^2	0.620	0.792	0.494	0.253	0.298	0.271
MD	0.040	-0.009	0.043	0.041	0.039	0.052
RMSE	0.049	0.051	0.070	0.071	0.067	0.063
n		7,350	6,699	6,628	5,818	7,334
Observed manual versus CropSyst simulated						
Depth	*Profile Avg.*	*0-30*	*30-60*	*60-90*	*90-120*	*120-150*
R^2	0.623	0.938	0.889	0.431	0.246	0.277
MD	0.011	0.022	0.019	0.001	0.004	0.011
RMSE	0.051	0.040	0.039	0.060	0.054	0.052
n		72	71	72	72	72

Table 17: St. John soil moisture R^2, mean difference (MD), and root mean square error (RMSE) comparisons (replicate 3 average results) by depth (cm)

Observed sensor versus observed manual						
Depth	*Profile Avg.*	*0-30*	*30-60*	*60-90*	*90-120*	*120-150*
R^2	0.076	0.158	0.080	0.014	0.074	0.055
MD	0.035	0.050	0.023	0.016	0.067	0.017
RMSE	0.127	0.130	0.129	0.110	0.118	0.148
n		20	25	25	27	28
Observed sensor versus simulated						
Depth	*Profile Avg.*	*0-30*	*30-60*	*60-90*	*90-120*	*120-150*
R^2	0.600	0.324	0.423	0.217	0.244	0.249
MD	0.030	0.002	0.007	0.030	-0.017	0.011
RMSE	0.096	0.097	0.094	0.106	0.124	0.132
n		4,331	4,602	4,644	4,847	4,821
Observed manual versus simulated						
Depth	*Profile Avg.*	*0-30*	*30-60*	*60-90*	*90-120*	*120-150*
R^2	0.685	0.877	0.881	0.520	0.267	0.260
MD	0.050	0.043	0.038	0.063	0.061	0.046
RMSE	0.073	0.069	0.054	0.082	0.087	0.061
n		72	71	72	71	72

Nitrogen Calibration

Again, all results summarized in this section correspond to outcomes achieved during full rotational simulations. Table 18 summarizes soil organic matter carbon to nitrogen ratios (SOM C:N), updated for each site, and the calibrated soil carbon decay rate, developed based on Genesee data. Both sites display relatively low organic matter C:N ratios and will decompose faster than materials with higher C:N ratios.

Table 18: Organic matter parameters; water-extractable SOM C:N values measured by Ward Laboratories and soil carbon decay rate calibrated in the CropSyst model

Site	*SOM C:N*	*Soil carbon decay rate (1/day)*
Genesee	15.02	0.0000164
St. John	17.32	

Maximum above ground nitrogen concentration at maturity and maximum aboveground nitrogen concertation of chaff and stubble values (Table 19) were estimated with measured data. Aboveground nitrogen concentration was typically approximately twice as great as maximum nitrogen concentration of the residue due to a higher concentration of nitrogen in the grain. At both sites, legume crops exhibited the greatest nitrogen concentrations.

Table 19: Nitrogen submodel parameters, adjusted based on measured values

Crop	**Maximum aboveground nitrogen concentration at maturity, kg N/kg DM**	**Maximum aboveground nitrogen concentration of chaff and stubble, kg N/kg DM**
Genesee		
Winter wheat	0.015	0.0075
Spring wheat	0.023	0.0090
Chickpea	0.031	0.0100
Winter pea	0.025	0.0150
Cover crop	0.015	0.0075
St. John		
Winter wheat	0.015	0.006
Spring wheat	0.019	0.009
Winter pea	0.027	0.020
Cover crop	0.020	0.009

Table 20 summarizes calibrated crop nitrogen demand values, based on Genesee observations but assigned to both Genesee and St. John crop files.

Table 20: Calibrated nitrogen parameters applied in CropSyst crop files

Crop	*Critical nitrogen concentration of canopy at emergence kg N/kg DM*	*Maximum nitrogen concentration of canopy at emergence, kg N/kg DM*
Winter wheat	0.045	0.055
Spring wheat	0.030	0.055
Chickpea	0.030	0.050
Winter pea	0.042	0.065
Cover crop	0.020	0.050

Observed crop nitrogen values represent the summation of the nitrogen in residue and estimated nitrogen in grain. Simulated values correspond to aboveground nitrogen retained by the plant. Based on the R^2 and RMSE between observed and simulated Genesee crop nitrogen, the model performance was acceptable (Figure 23).

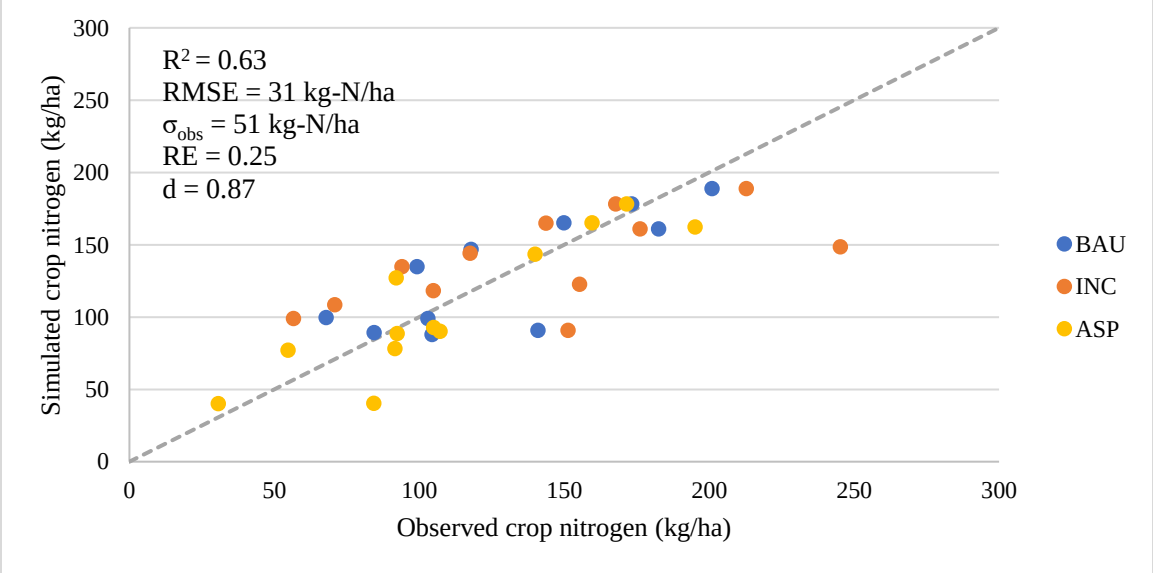

Figure 23: Genesee observed versus simulated crop nitrogen uptake; ASP=aspiration, INC=incremental, BAU=business-as-usual, RMSE=root mean square error, σ_{obs}=standard deviation of the observations, RE=relative error, d=index of agreement

Considering R^2 and RMSE on a rotational basis, all values exceed acceptable criterion established in the *Statistical Assessment* of Methodology, except INC's R^2 (Table 21). Table 21 also includes a normalized RMSE (RE) and d values, which match acceptable ranges presented in other CropSyst modeling studies, such as Benli et al. (2007) and Todorovic et al. (2009).

Table 21: Mean difference (MD), R^2, root mean square error (RMSE), relative error (RE), and index of agreement (d) between simulated and observed crop nitrogen and standard deviation (σ) of the crop nitrogen observations, separated by rotation; ASP=aspiration, INC=incremental, BAU=business-as-usual

	MD, kg-N/ha	*R^2*	*RMSE, kg-N/ha*	*σ, kg-N/ha*	*RE*	*d*
BAU	-3.49	0.70	25	47	0.20	0.91
INC	3.01	0.39	42	56	0.30	0.71
ASP	4.86	0.81	21	48	0.19	0.95

Each observed average and confidence interval shown in Figure 24 includes five data points, one for each replicate of the strip trial. In addition, Appendix E contains R^2, RMSE, and σ statistics on a yearly basis, with all statistics meeting acceptable criterion, except 2019 RMSE.

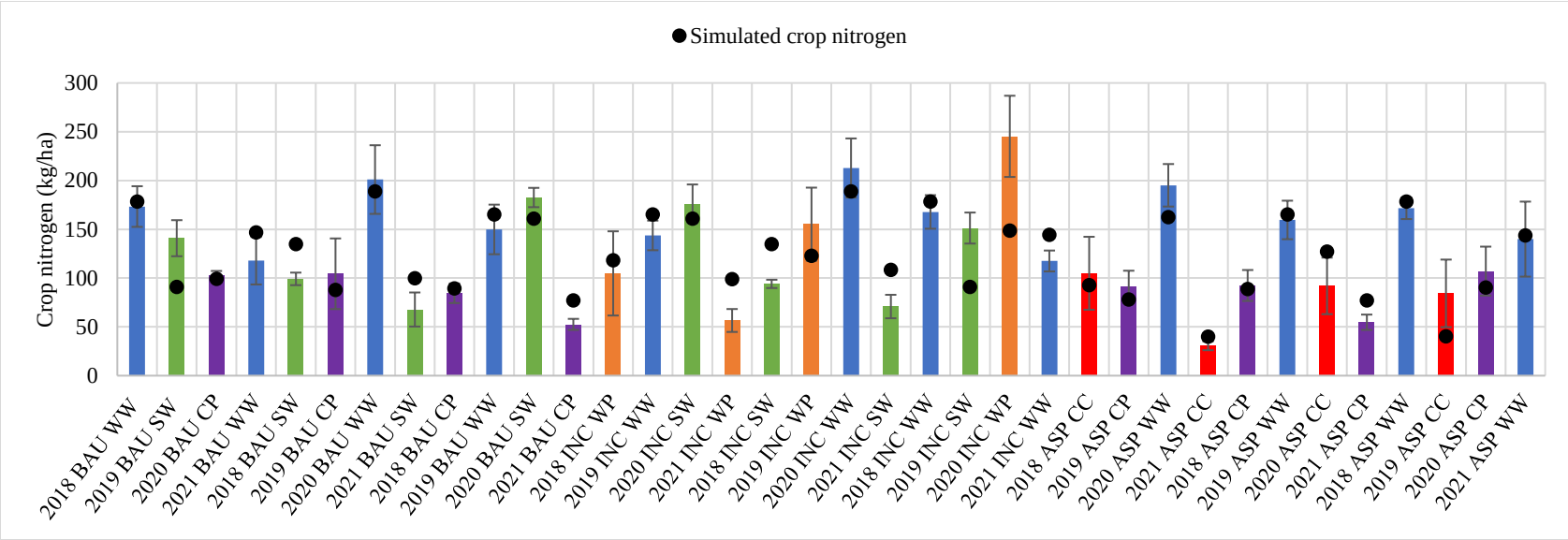

Figure 24: Genesee replicate average crop nitrogen with 95% confidence intervals around observations; ASP=aspiration, INC=incremental, BAU=business-as-usual, CP=chickpea, SW=spring wheat, WW=winter wheat, WP=winter pea, CC=cover crop

Per Figure 25, all average simulated crop nitrogen values fell inside the 95% confidence intervals of the observed values.

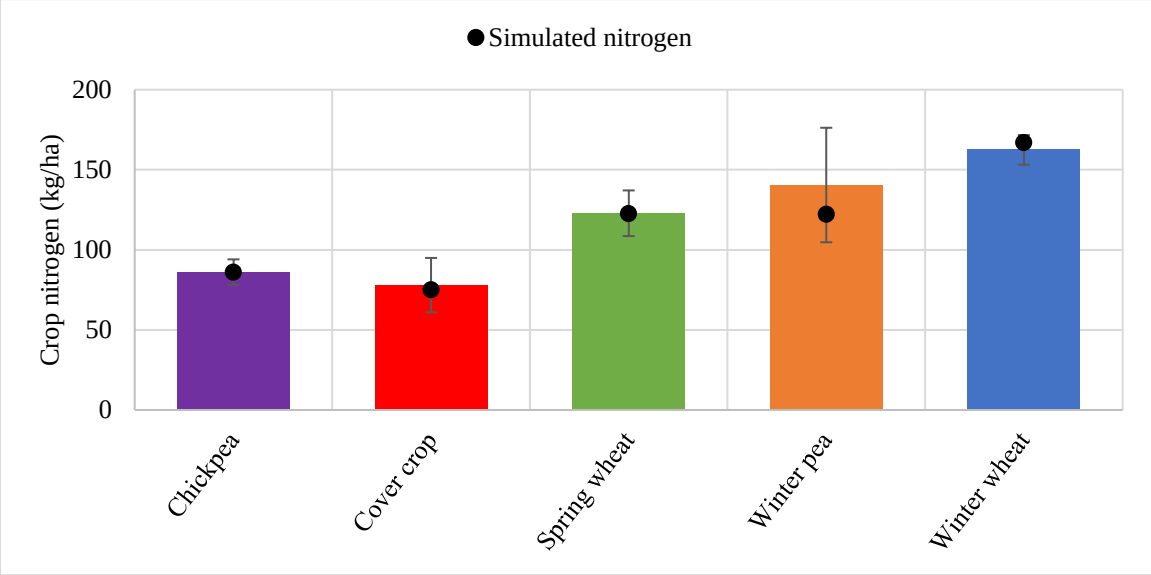

Figure 25: Genesee overall average crop nitrogen by crop type with 95% confidence intervals around observations

Table 22 summarizes average observed and simulated crop nitrogen values, with winter wheat, spring wheat, and chickpea observations and simulations identical. Appendix E contains nitrogen in crop statistics by crop, including the R^2, MD, and RMSE between simulated and observed datasets and the pairs of datapoints that contributed to the metrics. R^2 varies between 0.20 and 0.97 (some values falling below the acceptable 0.5) and RMSE between 15 and 56 kg-N/ha, all less than the standard deviation of observations.

Table 22: Average Genesee observed and simulated nitrogen in crop

Crop nitrogen, kg-N/ha		
Crop	*Observed*	*Simulated*
Winter wheat	163	167
Spring wheat	123	123
Chickpea	86	86
Winter pea	140	122
Cover crop	78	71

CropSyst closely maintained biomass and yield achieved with the nitrogen model disabled (Figure 26 and Figure 27). R^2 and RMSE values displayed meet acceptable criterion.

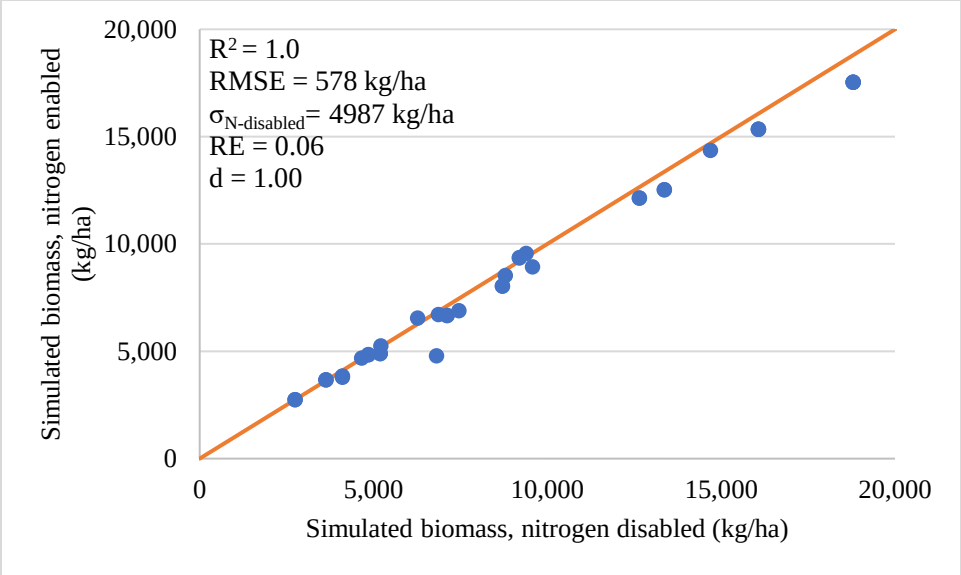

Figure 26: Genesee simulated biomass with and without nitrogen submodel active; RMSE=root mean square error, $\sigma_{N\text{-}disabled}$=standard deviation of the simulations with the nitrogen model disabled, RE=relative error, d=index of agreement

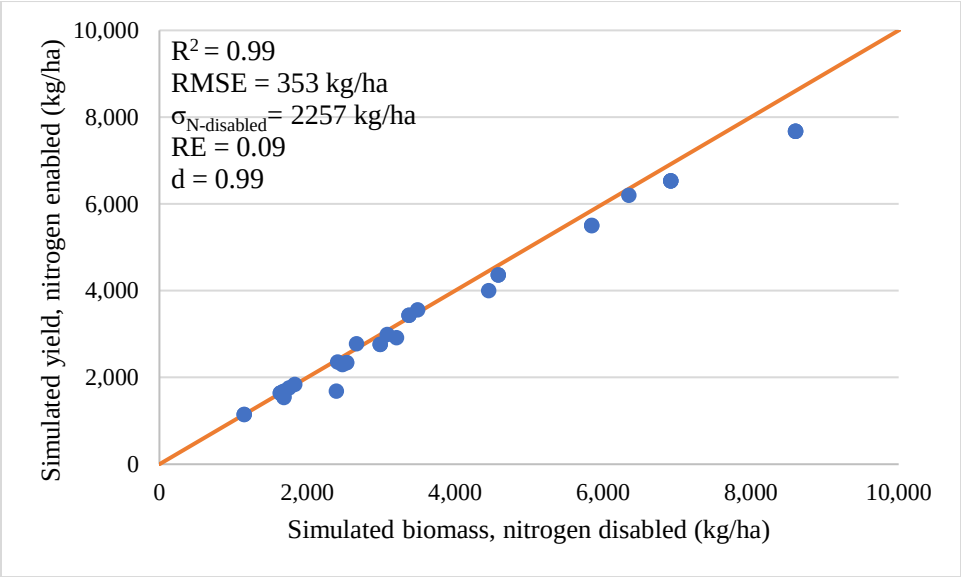

Figure 27: Genesee simulated yield with and without nitrogen submodel active; RMSE=root mean square error, $\sigma_{N\text{-}disabled}$=standard deviation of the simulations with the nitrogen model disabled, RE=relative error, d=index of agreement

Figure 28 shows an example of crop and soil nitrogen outputs, with simulations and observations displaying similar trends but not values. Calibration efforts focused on simulating observed crop nitrogen. In many cases, observed nitrate higher in the soil profile (0-90 cm) did not follow the same trends as CropSyst simulations; however, observed and simulated values fell in a same range. Generally, CropSyst simulated greater nitrate deeper in the soil profile (90-150 cm) than measured. Several ammonium observations were also relatively high, driving elevated levels of total inorganic

nitrogen. For example, in Genesee replicate 5's strip F (Figure 28, below), spring 2020 ammonium measured 214 kg/ha, and in fall 2021, ammonium measured 174 kg/ha, both in excess of measured nitrate. In fact, at four of eight sampling dates (2020 and 2021), measured ammonium exceeded measured nitrate. This was common among simulated strips.

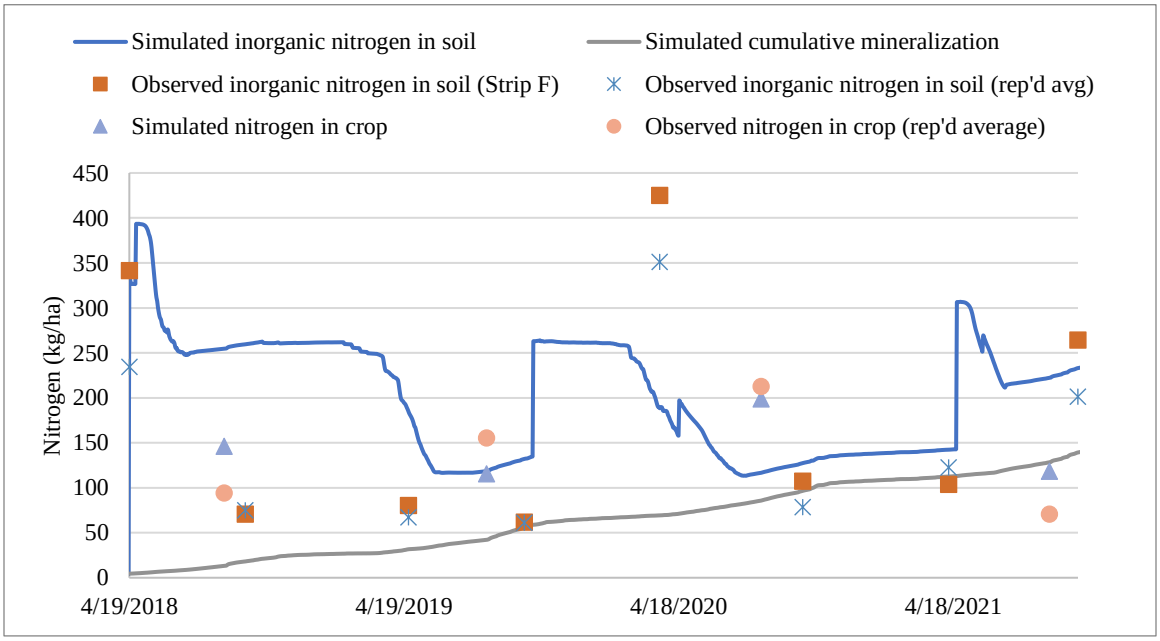

Figure 28: Example of soil and crop nitrogen outputs, replicate 5 Strip F in Genesee (spring wheat-winter pea-winter wheat). Replicated average ("rep'd avg") values represent the average treatment value across all five replicates; simulated values represent replicate 5 Strip F only.

St. John long-term simulations focus on production and water cycling, so an exhaustive nitrogen submodel development was not completed. However, St. John nitrogen simulations further validated selection of nitrogen parameters calibrated for Genesee (refer to Table 18 and Table 20). St. John simulated and observed data achieved an R^2=0.61, but an RMSE value greater than σ (Figure 29).

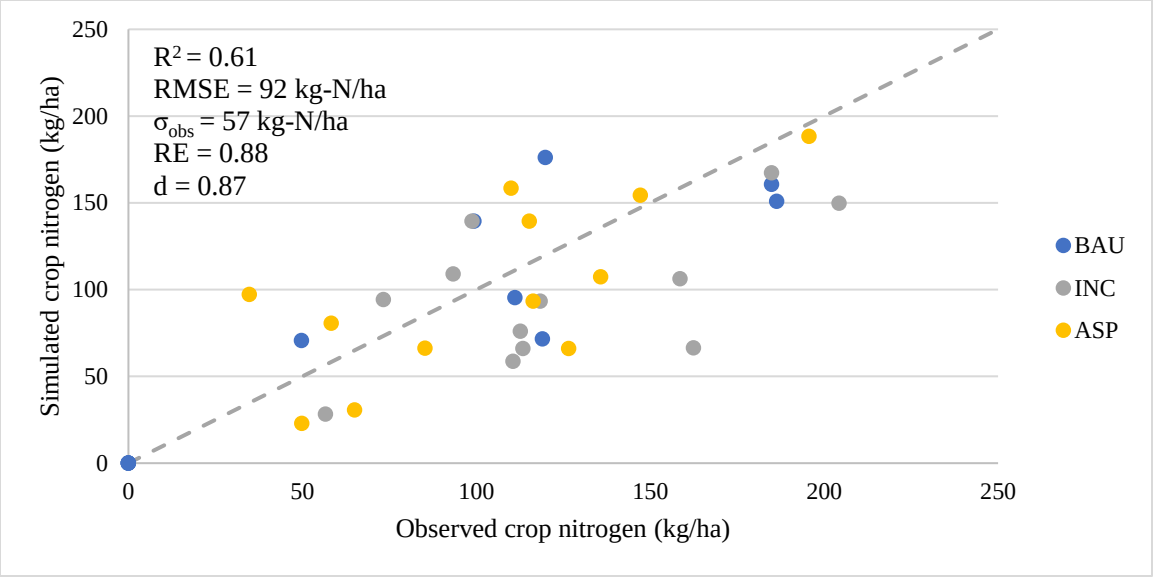

Figure 29: St. John observed versus simulated crop nitrogen uptake; ASP=aspiration, INC=incremental, BAU=business-as-usual, RMSE=root mean square error, σ_{obs}=standard deviation of the observations, RE=relative error, d=index of agreement

Likewise, simulated crop nitrogen fell close to average measured values and well within the 95% confidence interval of observations; see Figure 30.

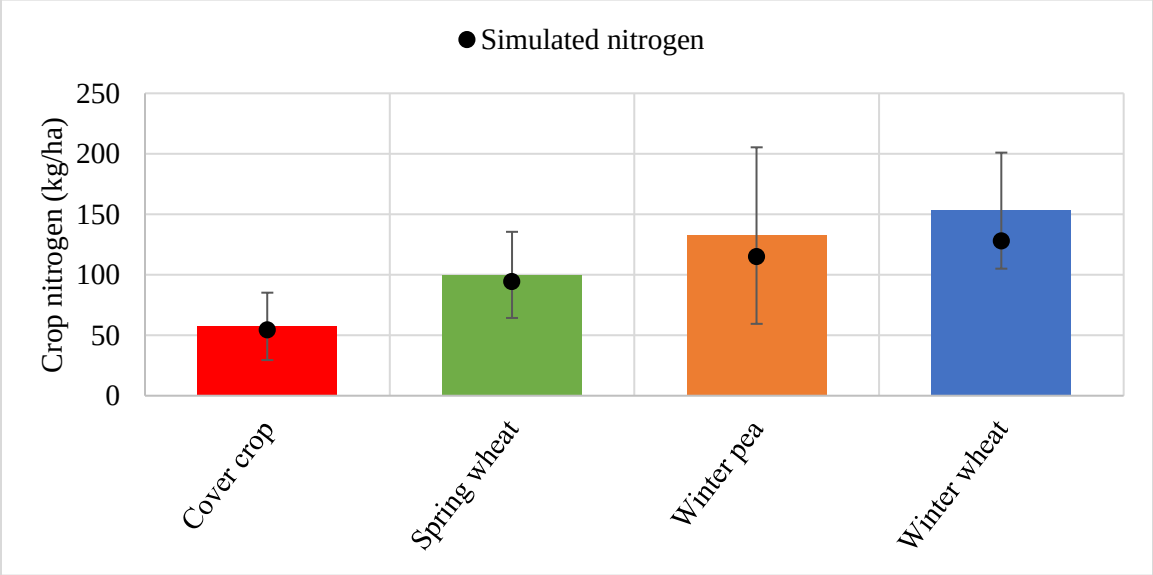

Figure 30: St. John overall average crop nitrogen by crop type with 95% confidence interval

Discussion

Yield/Biomass and Soil Moisture Calibration

Overall, simulated crop growth during the growing season was well represented by CropSyst with only minor adjustments to phenological parameters. Degree days associated with emergence, flowering, filling, and maturity timing were adjusted before calibrating other parameters, as crop phenology drives many important growth processes, varies across crops and cultivars, and significantly impacts model simulations (Archontoulis et al., 2014). All NDVI and simulated crop LAI matched well, with R^2 values exceeding 0.69. Some studies note uncertainty in developed LAI-NDVI relationships, due to spatial variability, complex environments, and error in ground-based measurements (Chen and Cihlar, 1996). However, CropSyst's simulation of LAI effectively eliminates any variability or measurement errors, and this work considered only the correlation between the two indices. In conjunction with the LAI-NDVI relationship, phenology timing also agreed with the growth stages captured by the 2021 game cameras. Although the cameras captured only a single year of photo observations, thermal time targets (growing degree days) and photoperiod algorithms are dynamic and should adapt to environmental conditions observed during other years (Archontoulis et al., 2014; Aslam et al., 2017).

The calibrated canopy extinction radiation coefficient, *k*, fell within expected values. Values for *k* range from 0.40 (Genesee cover crop) to 0.8 (Genesee spring wheat). Zhang et al. (2014) reports *k* for general cropland whole growth season as 0.62 +/- 0.17 based on the results of 35 different studies. *k* can also vary dramatically depending on many factors, including location and time of year. For example, Zhang et al. (2014) summarized wheat *k* values between 0.4 (Argentina; gleaned from Carretero et al., 2010) and 0.93 (Australia; gleaned from O'Connell et al., 2004). After calibrating *k*, only minor adjustments were made to default RUE values. Calibrated RUE also fell within the expected ranges, as identified in studies such as those summarized in Sinclair and Muchow (1999) and Stöckle and Kemanian (2009).

Although only calibrated for cover crops, all TUE values fall within the suggested range presented in the CropSyst documentation and data summarized in publications such as Kemanian et al. (2005) and Mannam (2011). TUE represents a relationship between a plant and a specific environment, and it will increase for a more water-stressed cropped, like a dryland spring wheat (Mannam, 2011). As shown in Table 11, cover crop TUE was adjusted downward from the default wheat values (original base file), which effectively reduced simulated biomass, closer to observed values.

CropSyst appeared to simulate Genesee's observed biomass and yield well (R^2>0.5 and RMSE<σ on overall, rotational, and yearly bases); see Figure 3, Figure 4, Table 12, and Table 13. Although not

considered a criterion for model agreement, d values were also at or above the expected range, as presented in other similar studies such as Ahmed et al. (2016), Benli et al. (2007), and Todorovic et al., (2009). In general, CropSyst simulated Genesee's winter wheat, chickpea, and cover crop more accurately, with greater error in winter pea and spring wheat predictions, especially when considering the replicated averages (Figure 11 and Figure 12). In some instances, CropSyst simulated an individual strip's observed biomass and yield well, but that prediction did not reflect the replicated average well (or vice versa). For example, the 2021 BAU winter wheat biomass prediction was nearly 2,000 kg/ha less than the observed value in the simulated replicate 5 strip, an approximately 25% error, but this simulated value was nearly identical to the replicated average 2021 BAU winter wheat value.

CropSyst generally simulated the St. John cropping system with less accuracy than Genesee cropping system. This may have, in part, resulted from the range of data observations in St. John. For example, in 2019, the winter pea biomass ranged from approximately 4,000 to 14,000 kg/ha across the five replicates in the field, a dramatic 10,000 kg/ha spread with the largest value approximately 3.5 times larger than the smallest. Additionally, while visually unremarkable, lower producing crops, like cover crop, and lower producing years, such as 2021, exhibit higher percentage-based error. Regardless, biomass and yield predictions exceeded $R^2>0.5$ and RMSE<σ on overall, rotational, and yearly basis (Figure 5, Figure 6, Table 12, and Table 13). Note that 2021 data was reserved for model validation and was not considered during calibration. Despite the abnormal weather encountered in 2021(warm and very dry), the model still met established statistical criteria during 2021. Again, d values, while not explicitly considered in model agreement assessment, fell in the expected range (Ahmed et al., 2016; Benli et al., 2007; Todorovic et al., 2009).

When considering the replicated averages, CropSyst appeared to underpredict 2018 and 2019 and overpredict 2020 and 2021 in Genesee (Figure 11 and Figure 12) and underpredict 2019 and 2021 and overpredict 2018 and 2020 in St. John (Figure 13 and Figure 14). This suggesting that the model may not have responded well to specific environmental conditions at the two locations. Likely, both temporal and spatial variability contributed to outcomes. Nonetheless, this dataset included a diversity of conditions, thoroughly testing the model's capability. For example, in addition to the unusual weather experienced in 2021, 2020 weather was also an anomaly. Despite its drought conditions, well-timed precipitation led to exceptional crop yields. It was challenging to develop crop files representative of all years that will predict all individual outcomes well. Nevertheless, considering the crop average biomass and yield outcomes, Figure 15 – Figure 18, it appears CropSyst still performed

very well. These figures highlight the universality of the calibrated crop files, with a single file reflecting all years and rotations.

Simulated soil moisture by CropSyst exhibited similar/greater accuracy than the precision available in the observed soil moisture data. Statistical comparisons of simulated and observed data yielded R^2>0.62 and RMSE<0.051 in Genesee and R^2>0.60 and RMSE<0.096 in St. John versus R^2=0.55 and RMSE=0.056 between observed datasets in Genesee and R^2=0.08 and RMSE=0.127 in St. John; see Table 16 and Table 17. Typically, both observed datasets were higher than CropSyst simulated soil moisture, as indicated by positive MD values. CropSyst generally limits soil moisture to field capacity and simulates rapid drainage of gravitational water, whereas some field observations, particularly at greater depths in the profile, indicated soil moisture above field capacity. However, this likely did not influence crop outcomes markedly, as water held in the soil over field capacity is not considered plant available. CropSyst's soil file was parameterized almost entirely from measured values, with no parameter estimation or calibration; see the *Soil* section of Model Development. In addition to well-calibrated crop files, this was likely crucial to successful soil moisture predictions, as hydraulic properties "directly control the movement of water and water balance partitioning" (Loosvelt et al., 2011).

Overall, CropSyst adequately simulated yield, biomass, and soil moisture outcomes. However, as indicated by graphic and statistic results, particularly Figure 11 – Figure 14 and statistics included in Appendix E, CropSyst did not always accurately simulate individual strips or crops successfully. However, it is important to remember the LIT project provided an extensive and highly variable dataset with wide ranges of field and environmental observations. Considering this, CropSyst proved very powerful and robust. Additionally, many existing studies support the use of CropSyst for simulating crop production and water cycling, including several specific to the region's dryland wheat-based systems (Chi et al., 2017; Karimi et al., 2018; Ward, 2015).

Nitrogen Calibration

There was little difference in observed soil organic matter content over the four-year period, which the model was able to replicate using observed soil water-extractable organic C:N ratios and the calibrated decay rate parameter. The soil C:N ratio in the organic matter submodel was set to the average values observed in the strip trials at both Genesee and St. John. Theoretically, soil microorganisms consume SOM at ratios of 24:1; C:N ratios lower than this ratio (Table 18) leave excess soil nitrogen for plant growth or for microbial decomposition of higher C:N matter (NRCS East National Technology Support Center, 2011). Generally, wheat crops exhibit higher C:N ratios, around 80:1, with legume (17:1) and common cover crop materials (11:1) much lower (NRCS East

National Technology Support Center, 2011). The remaining SOM parameter, the decay rate, was calibrated to match the relatively constant SOM concentration observed throughout the strips and five-year trial period at the Genesee site. The calibrated decay rate value falls within the expected range for a single pool (Jastrow and Six, 2006).

Several crop file nitrogen parameters were also adjusted or calibrated to known values. The measured maximum above ground nitrogen concentration at maturity (between 0.015 and 0.031 kg N/kg DM) and the maximum aboveground concentration of nitrogen in chaff and stubble (between 0.006 and 0.020 kg N/kg DM) reflect measured percent nitrogen in harvest samples and percent protein in grain. Generally, pea crops contained greater nitrogen than did non-legume crops. Critical nitrogen concentration of canopy at emergence and maximum nitrogen concentration of canopy at emergence were calibrated against the observed crop nitrogen values measured at the Genesee site. Reducing the critical nitrogen value also reduced nitrogen stress simulated by CropSyst. Maximum nitrogen concentration at emergence more strongly influenced crop nitrogen values, with a reduction in the concentration parameter effectively reducing the simulated crop nitrogen. CropSyst documentation notes that typical maximum nitrogen concentration of grasses is 0.02 to 0.04, with non-leguminous dicotyledons approximately 10% higher and legumes about 30% higher than grasses (Stöckle, n.d.). The calibrated critical concentration values fall closer to these guidelines, with the maximum concentrations exceeding them (Table 20). However, it appears little published data is available to either support or oppose parameter selection.

Simulated and observed Genesee crop nitrogen were in close agreement following calibration with R^2 values generally exceeding 0.5 and RMSE values lower than σ, the acceptable criteria (Figure 23 and Table 21). High d values also suggested good agreement between observations and simulations. Due to variability across replications, some nitrogen in crop values deviated from the average replicated value and/or 95% confidence interval, as show in Figure 24. Many factors influence crop nitrogen storage, including crop growth and physiology, climate, management practices like fertilization and tillage, and soil conditions (Balasubramanian et al., 2004), contributing to temporal variability in crop nitrogen. CropSyst generally overpredicted Genesee crop nitrogen in 2018 and 2021 and underpredicted 2019 and 2020 (also see Appendix E). Interestingly, this is not consistent with the direction of biomass and yield error, suggesting that different sources of error affected production and nitrogen outcomes. However, when considering results on a per crop basis (Figure 25), CropSyst performed very well, with all simulated values falling within their respective 95% confidence interval.

During the nitrogen submodel development, the accuracy in simulated crop yield and biomass were maintained largely to the same extent as with the simulations with the nitrogen model disabled, as it was assumed no nitrogen stress occurred; see Figure 26 and Figure 27. As mentioned in the Methodology section, the change in computational timestep may have caused the very minor differences observed in yield and biomass outcomes between model simulations with nitrogen enabled versus disabled. Although St. John long-term model simulations focus on production and water cycling outcomes, St. John nitrogen simulations were run to further validate nitrogen submodel calibration. CropSyst simulated St. John crop nitrogen well (Figure 29 and Figure 30), suggesting parameters calibrated at Genesee may be appropriate for both sites, although the RMSE between observations and predictions were greater than the specified acceptable criterion (σ) at St. John. Regardless, long-term simulations of St. John nitrogen outcomes can provide insight to general nitrogen trends and responses to alternative cropping rotations.

CropSyst simulates soil nitrogen cycling and transport, but the calibration available to the user is primarily through the soil C:N ratio and decay parameters in the organic matter submodel or to the crop nitrogen parameters discussed above. The nitrogen calibration of CropSyst focused primarily on minimizing the error between predicted and observed crop nitrogen to better understand and compare rotational nitrogen needs. While changes to calibrated nitrogen parameters successfully drove responses in crop nitrogen, soil nitrogen proved less responsive and more challenging to manipulate. As highlighted in the example shown in Figure 28, CropSyst did not simulate soil nitrogen well. In many cases, a smaller range of soil nitrogen was simulated than measured in the field; field observations generally indicated greater consumption of inorganic soil nitrogen during the growing season. However, because the model still simulates adequate nitrogen removal by the crop, it is possible that competing soil nitrogen processes offset each other in the model. For example, perhaps CropSyst simulated fewer nitrogen losses (such as through leaching, runoff, or during application) and less mineralization than actually occurred during the strip trial, reducing the range of modeled soil nitrogen. Although CropSyst outputs values for each component of the nitrogen cycle, observed data necessary to assess the accuracy of all elements was not collected during the strip trial.

Considering the two inorganic nitrogen components, nitrate and ammonium, independently also provides insight. Accumulation of simulated nitrate deep in the soil profile suggests simulated nitrogen distribution and movement through the soil profile did not reflect observations. It is unlikely the crops withdrew significantly more nitrate deep in the soil profile during the strip trial than was simulated; CropSyst predicted soil moisture well, and both simulated and measured values indicate

little water withdrawal at deeper soil layers. However, belowground biomass nitrogen demand or leaching, neither of which were well assessed, could account for at least some of this discrepancy.

High ammonium levels call into question fertilization rates and nitrogen transformations processes. Elevated ammonium can serve as an indicator of mineralization, the decomposition of organic matter to ammonium. Fertilization was based on fall nitrogen levels, so appreciable over-winter mineralization would result in excess inorganic soil nitrogen. This would account for relatively high overall inorganic nitrogen levels. Additionally, most fertilizer was introduced as ammonium (see the *Management* section of Methodology), although nitrification, the conversion of ammonium to nitrate, typically occurs rapidly (within approximately a week at warmer temperatures) (Faber, 2016). Specific microbes carry out nitrification, and factors such as temperature, moisture, aeration, and salt content affect nitrogen conversion processes in the soil (Sawyer, 2010). Although unusual, high observed ammonium levels could suggest limited nitrification in the strip trials. It is also, of course, possible that inaccuracies in measured values accounted for 'error' between the observations and simulations, or that certain soil samples hit pockets of elevated nitrogen concentrations in the soil, misrepresenting overall levels in the respective strip.

It is also worth noting that these simulations utilized a single organic matter pool, with a single soil C:N value and single decay rate, as only single pool C:N values were measured. Soil C:N values corresponded to water extractable organic carbon and nitrogen. Utilizing total organic carbon and total organic nitrogen or another measure of carbon and nitrogen could change or improve outcomes, although the organic matter decay rate was much more sensitive than the C:N ratio in simulating organic matter processes. CropSyst also offers the option to model multiple organic matter pools (microbial, labile, metastable, and passive), with C:N ratios and decay rates for each. Single pool models treat SOM as a homogenous reservoir, which can be misleading, as turnover of SOM components varies continuously depending on its composition (Jastrow and Six, 2006). Multiple pool models tend to be more representative of true SOM dynamics. Unfortunately, sufficient field data to populate this model was not available, leaving too many unknown variables to reasonably or accurately calibrate. However, if CropSyst was utilized as a decision support tool, in most applications, this single pool carbon cycling model would be selected, as it is difficult to measure these pools.

Assessments of CropSyst's soil nitrogen balance in published literature are limited and generally focus on nitrogen fertilization's influence on biomass and yield outcomes. Both Confalonieri et al., (2006b) and Bellocchi et al., (2002) noted that CropSyst simulation of soil nitrogen seemed acceptable, especially given the wide variability in soil nitrogen and the many factors influence it, but

that further investigation and testing was needed. More locally, Ward (2015) assessed multiple nitrogen outcomes of the three-dimensional version of CropSyst, CropSyst-Microbasin, in the Palouse region. Ward noted several limitations in modeling nitrate transport and nitrogen uptake, including stripping and accumulation of nitrate in a manner not supported by field observations and inaccurate response to excess nitrogen scenarios.

The poor simulation of soil nitrogen is a main deficiency of these modeling efforts. It is unclear whether overfertilization, poorly parameterized variables, inexact model processes, inaccurate measured values, or a combination thereof contributed to the poor simulations. Nevertheless, without successful simulation of critical soil processes, nitrogen cycling cannot be completely assessed during Objective 2. Future work associated with this project could focus on better understanding and developing the soil nitrogen submodels, while maintaining accurate predictions of crop nitrogen. Parameterization of the multiple pool organic matter model may be an appropriate first step in improving this aspect of the model. However, based on previous CropSyst research, additional investigation and possibly development of the model's nitrogen processes may also be necessary.

Limitations

There are several limitations inherent to the CropSyst model and/or the LIT field trials. A select few are discussed here. Firstly, model development can only consider the conditions of the field study. During the LIT field trial period, for example, precipitation generally fell below average levels, so modeling efforts could not explore or assess outcomes achieved during wet years.

CropSyst does not model weeds or insects or changes to soil properties, significant considerations when selecting a crop rotation. For example, winter peas, "provide a means to control grass weeds and soil-borne wheat diseases on fields that have been in monoculture" (Schillinger, 2020), and some cover crops increase soil water holding capacity over time (Jones et al., 2020). These qualities have significant economic and management implications to which CropSyst modeling can provide no insight. Erosion is another significant factor effecting crop/variety selection and management decisions, especially in regions with steep topography (Kirby et al., 2017). Although CropSyst can model erosion, the submodel was disabled during this work, as it was not a main focus of the LIT study, and little information was available to populate or assess the model.

Model inputs also ignored error in field trial management or measurement. Soil moisture comparisons, (see Table 16 and Table 17) highlight error in measured results. It is impossible to judge the accuracy of the simulated outcomes to a degree greater than those detected in the measured values. Another obvious example is fallow strip management. During fallow years, no crop file is

input to CropSyst, and the program does not simulate plant water or nitrogen demand; it assumes the land lies completely barren. Unfortunately, during the 2017-2018 and 2020-2021 growing seasons, weeds overgrew the fallow plots for significant fractions of the growing season, compromising the collected data. As depicted in Figure 31, weed growth outpaced crop growth in 2021 until mid-July when the fallow strips were sprayed. The strips were managed more carefully in 2018-2019 and in 2019-2020. A fallow strip not managed to industry standards will produce results that inherently disfavor the practice, as weeds effectively waste the soil resources that could be used to cultivate a marketable crop.

Figure 31: Fallow strip (left) adjacent to a spring wheat strip (right) in St. John, June 2021

Unfortunately, it is challenging to assess the weeds' impact on resources in CropSyst, as weed growth in fallow plots was not quantified, CropSyst did not simulate soil inorganic nitrogen concentrations well, and observed soil moisture data in fallow strips was limited and incorporated error (refer to Table 17 and Appendix F). However, it appears CropSyst generally simulated lower moisture content deeper in the soil profile (60-150 cm) in fallow strips than was recorded by the sensors or measured manually. This is consistent with results observed in other St. John strips. Conversely, observed data indicated greater fall dry down occurred in upper layers of the soil profile (0-60 cm) than was simulated by CropSyst, possibly suggesting weed transpiration utilized some water higher in the soil profile.

Finally, while CropSyst simulated the strip trials well, there can be challenges extending results to larger fields or regions. Yield and input gaps can exist between plot-scale and field-scale research, as a result of increased variability and greater management challenges encountered in larger areas

(Kravchenkoa et al., 2017). Additionally, conventional crops and management are more resilient to field-scale challenges than are alternative practices or crops (such as the cover crops studied here), which can be more susceptible to biotic stresses or spatial and temporal variability. This leads to uneven outcomes across a landscape and requires more careful and timely management (Kravchenkoa et al., 2017). Additionally, certain parameters, such as soil properties, are heterogeneous across larger landscapes and, hence, are often 'up-scaled' for larger-scale simulations (such as by percentage weighting soil properties across a field). However, a recent crop modelling study found that results were more sensitive to weather scenarios than spatially variable parameters (Fry et al., 2017). Still, these are important considerations when utilizing CropSyst to assess field outcomes or as a decision support tool.

Conclusion

There is a need for accurate cropping models that can assess the impacts of management choices across broad regions. Two site-specific CropSyst models were developed to reflect the LIT project's IPNW strip trial locations: the annual cropping site in Genesee, ID and the annual crop-fallow transition site in St. John, WA. The LIT project provided extensive laboratory and field datasets. Weather, soil, and management files were completely parameterized using measured data or known values. Certain static crop file parameters and organic matter submodel parameters were updated or calibrated to reflect the observed datasets and improve the model's ability to predict yield/biomass, soil moisture, and nitrogen in crop values.

Especially given the replication and range of observed data, the model displayed adequate predictive power of yield, biomass, soil moisture, and nitrogen in crop across the four-year crop rotations and under a variety of conditions. Several calibrated parameters, including many of the calibrated nitrogen parameters, were common to both locations, suggesting the model may be robust and reliable at locations within this region without calibration data. Conclusions are consistent with existing CropSyst research. The developed model will be used under research Objective 2. However, the long-term simulations will not directly consider the soil inorganic nitrogen concentration outcomes. Future research efforts should focus on further developing this aspect of the nitrogen model.

Chapter 3: Long-term Model Simulations

Introduction

Crop models contribute to agricultural advancement by helping us "explore the dynamics between the atmosphere, the crop, and the soil" and assisting in decisions, such as those associated with resource management (Asseng et al., 2014). Robust, validated, process-based models provide a powerful tool for assessing short- and long-term impacts of management, disturbance, and climate. While not intended to be predictive, the CropSyst model provides great insight to crop-environment relationships and the underlying mechanisms that influence outcomes.

In this chapter, the calibrated CropSyst model is utilized to evaluate intensified and diversified rotations under recent climate conditions at each IPNW location: Genesee, the annual cropping site in the high precipitation zone, and St. John, the annual crop-fallow transition site in the intermediate precipitation zone. Crop rotations mirror those of the field experiments, as outlined in the CropSyst Model Development *Methodology* section. Three long-term rotational simulations were run for each site, one each to reflect business-as-usual (BAU; winter wheat-spring wheat-chickpea in Genesee and winter wheat-spring wheat-fallow in St. John), incremental (INC; winter wheat-spring wheat-winter pea), and aspirational (ASP; winter wheat-winter cover crop-chick pea in Genesee and winter wheat-spring wheat-spring cover crop in St. John).

Employing a longer, 30-year period for this baseline captures the effects of extreme or variable weather years. Unlike observed data or short-term model runs, these simulations include multiple rotation iterations (a single rotation repeated continually over simulation period). This provides insight to cumulative effects and also allows one to more easily attribute and explain outcomes. Although a farmer may elect to change crop rotations over time, combining multiple crop rotations in a single model simulation would render it impossible to identify the effects of specific rotations.

Long-term simulated yield/biomass, water use, and nitrogen use are analyzed and compared across different rotations. The analysis of the annual crop-fallow transition site at St. John focuses more on water cycling and availability following summer fallow replacement, as it drives crop production and crop choice in lower precipitation annual crop-fallow transition areas (Kirby et al., 2017), while the analysis of the annual cropping Genesee location will more carefully consider crop nitrogen use. Additionally, the stability of the crop rotation is assessed, focusing on crop performance over time and vulnerability to extreme weather conditions. Specifically, Objective 2 aims to address key management challenges at these locations and explore the impacts of:

1. Diverse/intense rotations on production outcomes and nitrogen requirements
2. Fallow replacement on winter wheat crop yields (St. John)
3. Cover crop termination approach (unharvested, baled, grazed)
4. Cover crop termination date on subsequent winter wheat crop years (St. John)

Methodology

The long-term historic simulations utilized the calibrated crop and soil parameter files developed under Objective 1. All three rotations (BAU, INC, ASP) began with a winter wheat crop, planted in 1980. This approach allows a direct comparison of the impacts of crop management strategies across a 30-year time period on specific crop performance in each climate zone. New weather and management files were developed to represent conditions from 1980-2010.

Weather

High resolution (approximately 4-kilometer) historical daily weather data for 1980-2010 were retrieved from gridMET (Abatzoglou, 2011). Weather metrics included precipitation, temperature, relative humidity, wind, and solar radiation. In comparison to the historic precipitation (Table 23), during the 2018-2021 growing seasons, both sites experienced a lower average precipitation (see Table 1).

Table 23: 1980-2010 average precipitation at Genesee, ID and St. John, WA by water year (October 1 – September 30) and calendar year (January 1 – December 31)

Location	**Water year**		**Calendar year**	
	mm	*in*	*mm*	*in*
Genesee, ID	564	22.2	568	22.4
St. John, WA	445	17.5	448	17.6

Wide variations in annual precipitation were observed over the 30-year period (Figure 32). Precipitation at the two sites followed similar trends, with Genesee receiving greater precipitation each year.

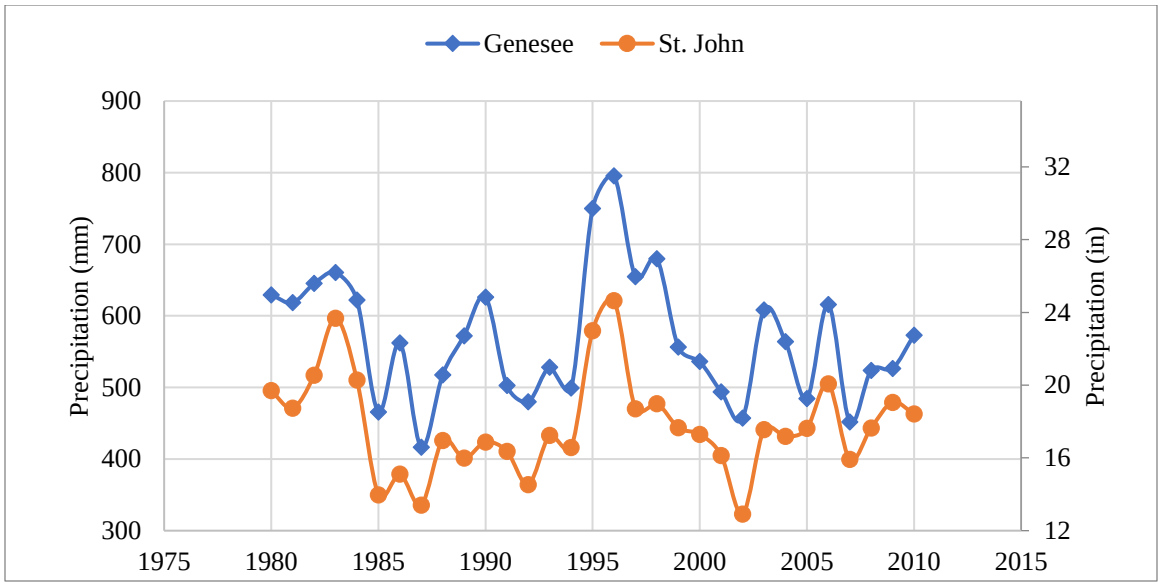

Figure 32: 1980-2010 annual calendar year precipitation

Interestingly, St. John typically experienced lower average temperatures than Genesee; see Figure 33. St. John experienced greater fluctuations in daily temperatures, with higher maximum temperatures and lower minimum temperatures. Large error bars indicate wide variations in observations.

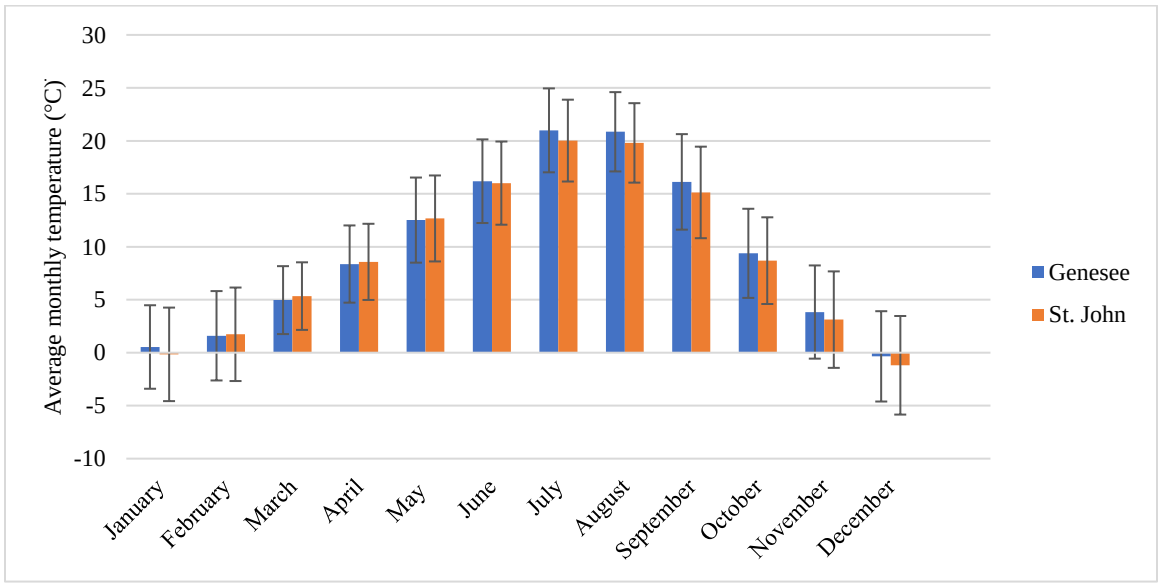

Figure 33: 1980-2010 average monthly temperature with error bars representing one standard deviation of observations

Management

It was assumed the planting dates selected during the field trial (2018-2021) reflected normal practices. Average winter crop plant dates (day of year) for the long-term historic simulations match those established during the strip trial. The historic spring plant dates correspond to the first day the 15-day average temperature consistently exceeded the average temperature experienced during the strip trial spring plant dates. While farmers also consider precipitation when planting, simulated plant dates were not based on rainfall, as CropSyst does not model the ill effects of planting in wet ground (for example, possible seed rot, planting equipment malfunction, or rutting). Table 24 summarizes planting information. See Table 31 and

Table 32 in Appendix D for all 2018-2021 strip trial planting dates.

Table 24: Historic plant dates

	Winter Crops	**Spring Crops**	
Site	*1980-2010 simulated spring planting date*	*Minimum spring planting temperature (°C)*	*1980-2010 average simulated spring planting date*
Genesee	October 5th	9.35	May 2nd
St. John	September 28th	6.25	April 5th

While farmers let crops "dry down" after reaching maturity to reduce grain moisture content and promote successful grain storage (Mrema, 2011), immediately simulating harvest following maturity versus modeling a dry-down waiting period results in very minor differences in CropSyst outputs. Consequently, for consistency, harvest was specified as the day after crops reach phonologic maturity for all crops except cover crops.

During the strip trial, cover crops were harvested with a swather prior to reaching maturity, typically in early July. For most long-term simulations, cover crops were terminated on the average harvest date, but all biomass remained in the field (no harvest) to investigate the long-term effects of a true "cover crop". Additional simulations investigated the effects of removing cover crops (i.e., a forage crop) and varied termination date to help identify trade-offs between production and input requirements.

CropSyst offers an option to automatically supply nitrogen at "deficient requirements, applied directly to plant tissues" to optimize growth. This allows users to model nitrogen cycling and cropping outcomes over long periods, without manually determining and simulating nitrogen fertilizer

applications. During long-term simulations, this option was selected for all crops, including pea and cover crops that were not fertilized during the strip trials. The functionality allows users to easily determine rotational fertilization differences and resultant impact on performance. Additionally, it prevents yield or biomass reduction resultant of nitrogen deficiency from occurring. Note that several nitrogen parameters were developed specifically for the Genesee site, although their selection was validated with St. John nitrogen results.

Statistical Assessment

In addition to average outcomes, the stability of the crops and rotations was assessed. The coefficient of variation, equation (8), helps identify fluctuations in metrics like yield over the simulation periods. It describes the distribution of a dataset (Abdi, 2010). In a dataset of "n" values, c_v will vary between 0 and the square root of (n-1). A higher coefficient of variation implies high variability in the dataset.

$$c_V = \frac{\sigma}{\mu} \qquad (8)$$

Where μ is the mean, and σ is the standard deviation.

Results

Simulated results obtained during the first complete rotation (1980-1983) were removed to prevent the effects of initialization values. Unless noted, graphical results include water year precipitation, as it better captures growing seasons.

Genesee

Limited crop variability exists across rotations, as summarized in Table 25. Generally, winter crops outperformed spring crops.

Table 25: Genesee long-term simulation biomass and yield outcomes by crop for simulations spanning from 1984-2010; WW=winter wheat, SW=spring wheat, CP=chickpea, CC=cover crop, WP=winter pea, ASP=aspiration, INC=incremental, BAU=business-as-usual

		Average biomass, kg/ha	*Average yield, kg/ha*	*Biomass c_v*	*Yield c_v*
WW	*ASP*	15,600	6,668	0.19	0.25
	INC	15,644	6,654	0.18	0.23
	BAU	15,601	6,667	0.19	0.25
SW	*INC*	6,922	2,497	0.21	0.25
	BAU	6,925	2,500	0.21	0.25
CP	*ASP*	4,252	1,966	0.27	0.25
	BAU	4,254	1,967	0.27	0.25
CC	*ASP*	5,637	-	0.13	-
WP	*INC*	7,181	3,042	0.27	0.30

INC produced the greatest biomass and yield and lowest variability on a rotational basis (Table 26). While ASP produced comparable biomass to BAU, it generated markedly less yield, resultant of an unharvested cover crop.

Table 26: Genesee long-term simulation rotational biomass and yield outcomes; ASP=aspiration, INC=incremental, BAU=business-as-usual

	Total biomass, kg/ha	*Total yield, kg/ha*	*Biomass c_v*	*Yield c_v*
ASP	25,490	8,634	0.12	0.21
INC	29,747	12,193	0.10	0.14
BAU	26,780	11,134	0.14	0.18

As displayed in Figure 34, INC biomass outperformed ASP and BAU during each rotation period. In most cases, BAU generated greater biomass than ASP.

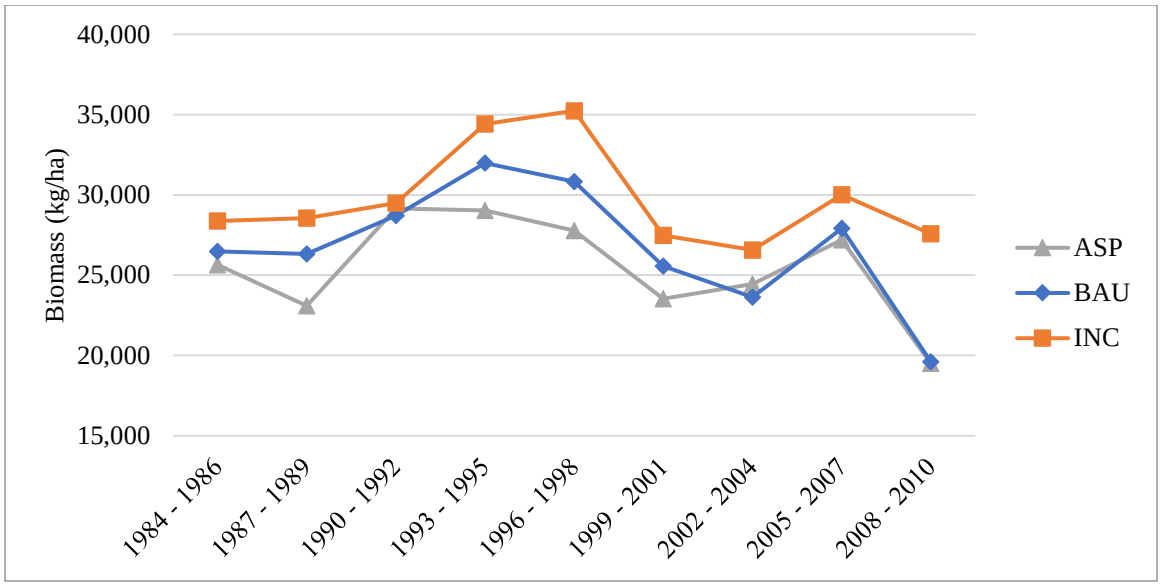

Figure 34: Genesee simulated total rotational crop biomass for each three-year aspirational (ASP), business-as-usual (BAU), and incremental (INC) crop rotation; ASP rotational biomass includes all cover crop biomass (does not account for any removal)

INC produced the greatest yields during most rotation periods but was nearly matched by BAU during select years (Figure 35). Results are included for a harvested cover crop "ASP, harvested CC", which dramatically increases ASP's yield outcomes. This assumes 80% of total aboveground biomass is baled and removed from the field for livestock feed, similar to the strip trials.

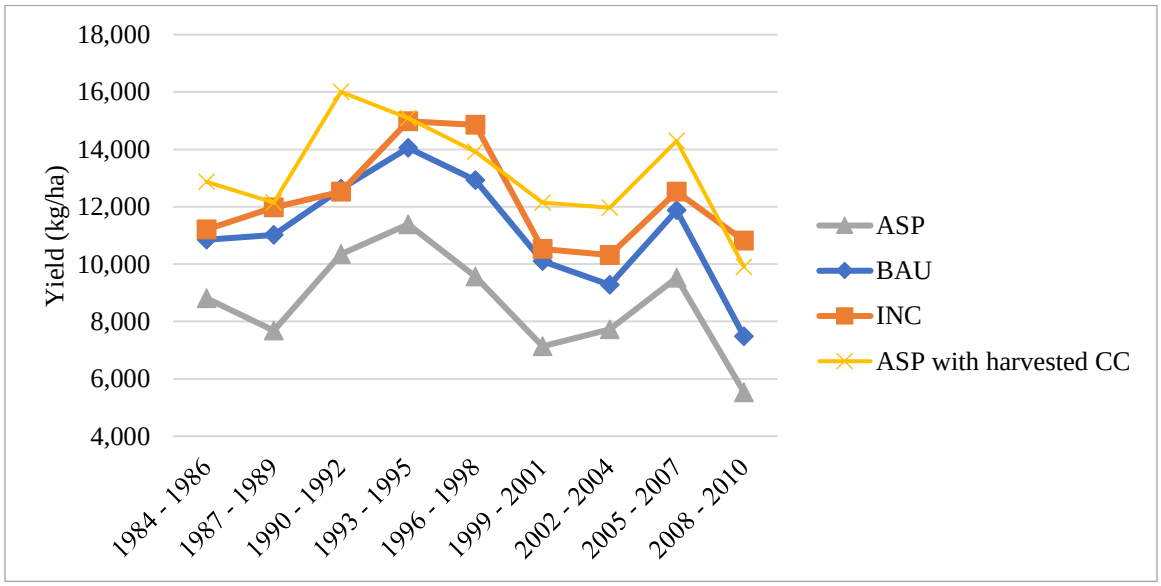

Figure 35:Genesee simulated total rotational crop yield for each three-year aspirational (ASP), business-as-usual (BAU), and incremental (INC) crop rotation; "ASP with harvested CC" assumes 80% of biomass produced contributes to yield

Figure 36 shows total rotational nitrogen fertilization, with BAU demanding the greatest nitrogen followed by INC. The crop file developed for the strip trial's cover crop did not specify nitrogen

fixation. However, as this could be a desirable cover crop trait, the figure includes the ASP rotation with a nitrogen-fixing cover crop ("ASP with CC fixation"), which requires the least nitrogen of any rotation. The figure also includes results for a baled non-fixing cover crop ("ASP with harvested CC"), which increases nitrogen demands over the base ASP scenario.

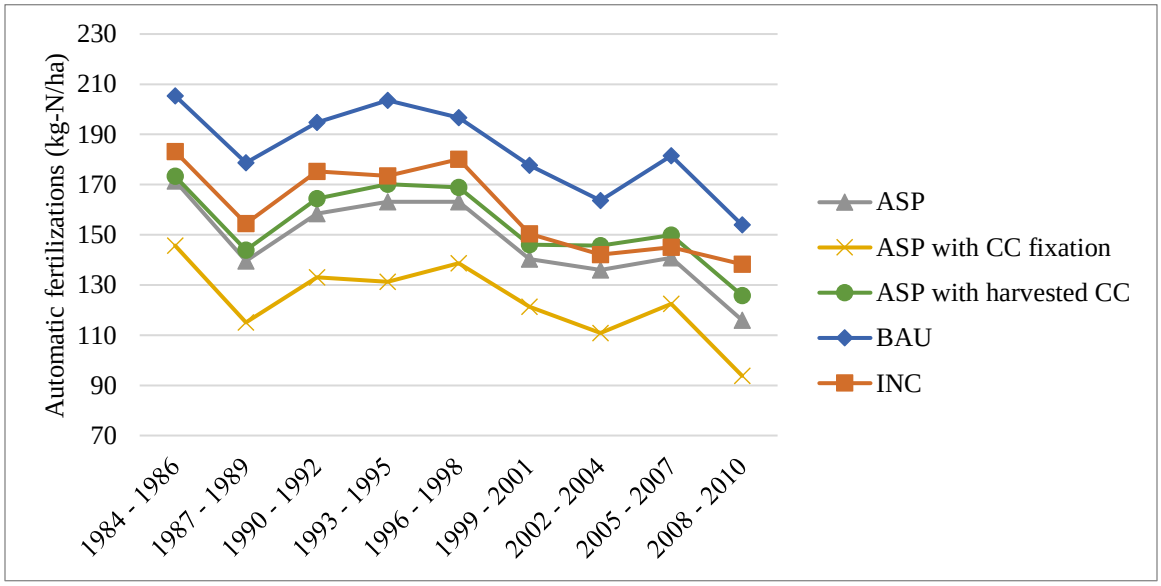

Figure 36: Genesee total rotational automatic nitrogen applications; ASP=aspiration, INC=incremental, BAU=business-as-usual. "ASP with CC fixation" includes a nitrogen-fixing cover crop, and "ASP with harvest CC" assumes a non-fixing cover crop, with 80% of its biomass baled.

Rotational mineralization results, presented in Figure 37, suggest the greatest mineralization occurs in INC, followed by the ASP rotations. In all rotations, mineralization increased throughout time. The figure includes the fixing and harvested cover crops.

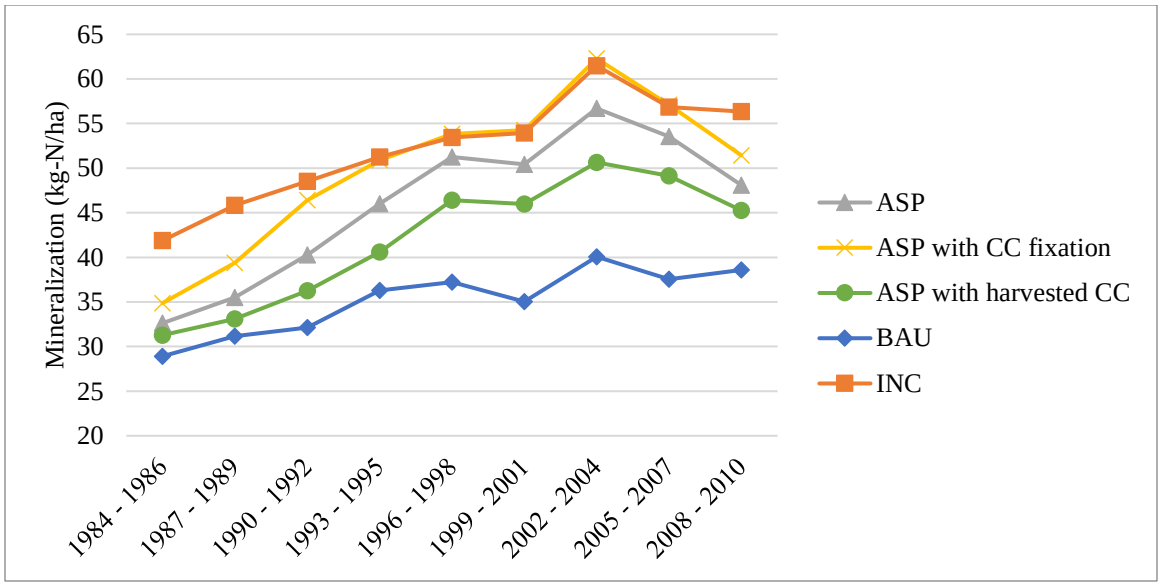

Figure 37: Genesee total rotational mineralization; ASP=aspiration, INC=incremental, BAU=business-as-usual. "ASP with CC fixation" includes a nitrogen-fixing cover crop, and "ASP with harvest CC" assumes a non-fixing cover crop, with 80% of its biomass baled.

Figure 38 shows the greatest rotational water loss (estimated as precipitation received minus evapotranspiration) in BAU. CropSyst simulated an average yearly water loss of 268 mm in BAU, 197 mm in ASP, and 199 in INC.

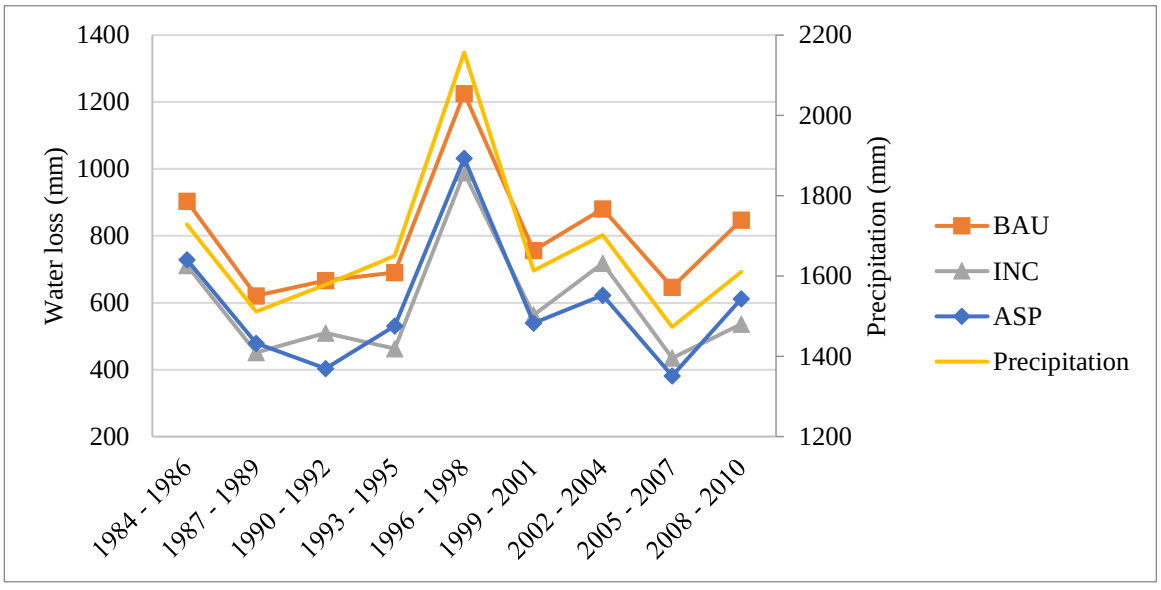

Figure 38: Genesee total rotational water loss, computed as precipitation minus evapotranspiration; ASP=aspiration, INC=incremental, BAU=business-as-usual

St. John

Unlike Genesee, winter wheat and spring wheat outcomes, common to all rotations, differed at St. John (Table 27). Generally, the winter crops exhibited higher c_v values.

Table 27: St. John long-term simulation biomass and yield outcomes by crop; WW=winter wheat, SW=spring wheat, CC=cover crop, WP=winter pea, ASP=aspiration, INC=incremental, BAU=business-as-usual

		Biomass, kg/ha	*Yield, kg/ha*	*Biomass c_v*	*Yield c_v*
WW	*ASP*	12,169	4,734	0.27	0.28
	INC	12,889	5,001	0.24	0.25
	BAU	14,069	5,384	0.17	0.22
SW	*ASP*	7,429	2,362	0.18	0.21
	INC	7,506	2,395	0.19	0.22
	BAU	7,337	2,334	0.17	0.20
CC	*ASP*	4,621	-	0.19	-
WP	*INC*	6,512	1,839	0.16	0.31

As shown in Table 28, INC produced the greatest yield and biomass and lowest variability on a rotational basis.

Table 28: St. John long-term simulation rotational biomass and yield outcomes; ASP=aspiration, INC=incremental, BAU=business-as-usual

	Biomass, kg/ha	*Yield, kg/ha*	*Biomass c_v*	*Yield c_v*
ASP	24,218	7,096	0.15	0.21
INC	26,907	9,236	0.13	0.16
BAU	21,405	7,717	0.14	0.19

Figure 39 shows total rotational biomass by rotation, with INC displaying the greatest biomass during each rotation period. In most instances, ASP outperformed BAU.

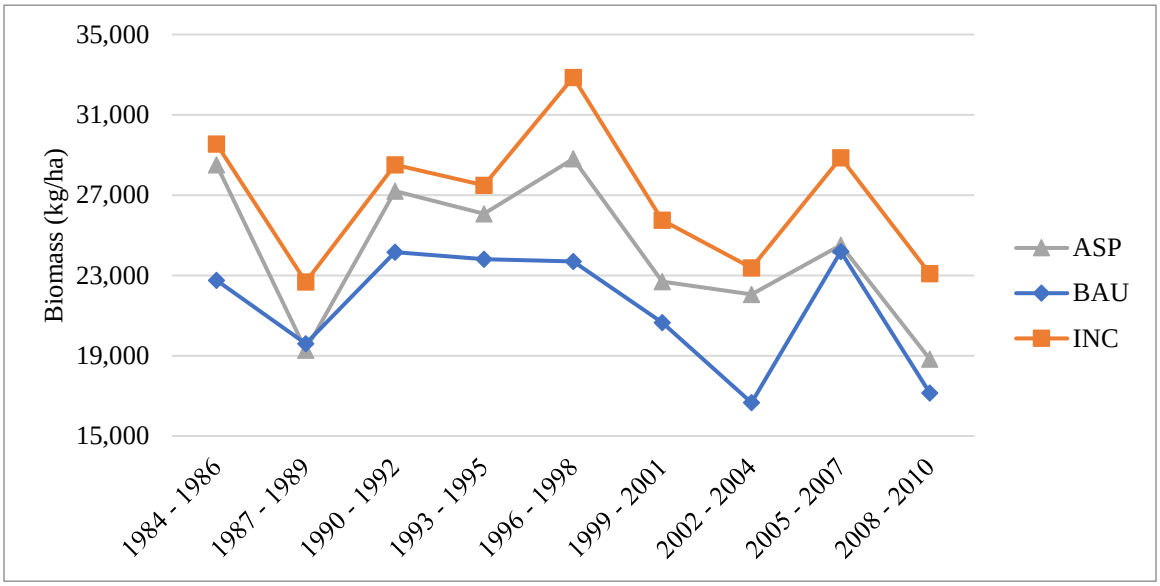

Figure 39: St. John simulated total rotational crop biomass for each three-year aspirational (ASP), business-as-usual (BAU), and incremental (INC) crop rotation; ASP rotational biomass includes all cover crop biomass (does not account for any removal)

A harvested cover crop (assumed 80% of biomass removed from the field) increases ASP rotational yield outcomes over that of INC, second highest, and BAU, typically third highest (Figure 40). In contrast, ASP generates the lowest yield if the cover crop is left unharvested.

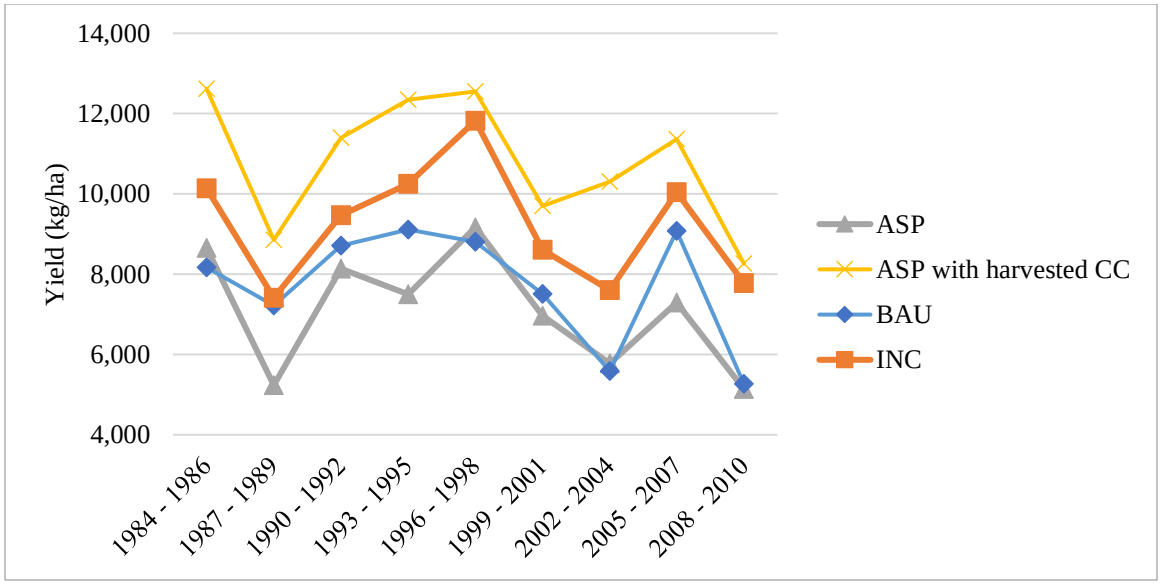

Figure 40: St. John simulated total rotational crop yield for each three-year aspirational (ASP), business-as-usual (BAU), and incremental (INC) crop rotation; "ASP with harvest CC" assumes a non-fixing cover crop, with 80% of its biomass baled.

Figure 41 shows winter wheat yields, which directly follow fallow (in BAU), cover crop (in ASP), and winter pea (in INC). Generally, BAU winter wheat yielded highest, most pronounced during dry periods.

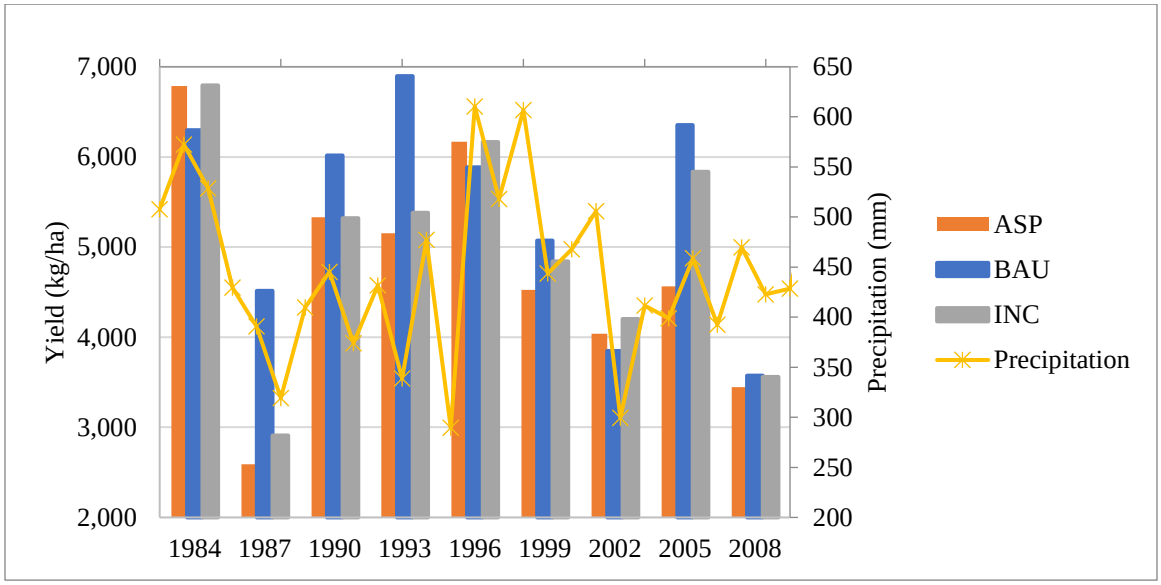

Figure 41: St. John simulated winter wheat yield by rotation; columns represent rotations with ASP=aspiration, INC=incremental, BAU=business-as-usual, and precipitation shown with the yellow line

Schillinger et al., 2008 defines available water as the net increase in soil water from harvest of the previous crop or beginning of the previous fallow period to March 31st plus rainfall received between April 1st and June 30th. The equation displayed on the graph describes the relationship developed by Schillinger et al. (2008) and corresponds to a study conducted in 1993-2005. It suggests each additional centimeter of water increases wheat yield by 154 kg/ha, equivalent to approximately 2.3 bushels per acre per one centimeter of water. In comparison, the CropSyst simulated data yielded a relationship of 186 kg/ha per one centimeter water (2.8 bushels per acre per one centimeter of water) (see Figure 42; $R^2 = 0.96$).

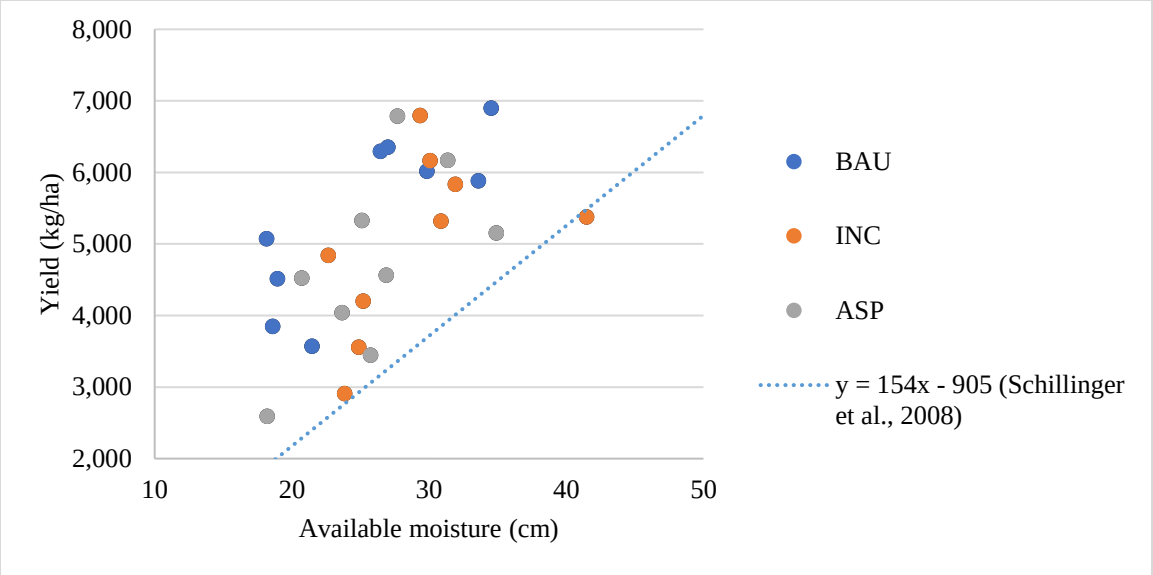

Figure 42: St. John simulated winter wheat available moisture (over winter gain, spring rainfall, and summer fallow water) versus yield; ASP=aspiration, INC=incremental, BAU=business-as-usual

ASP and INC soil water increased over winter during winter wheat years, whereas BAU remained more static; see Figure 43. Fall (solid lines) was assumed October 1 and spring (dashed lines) April 15.

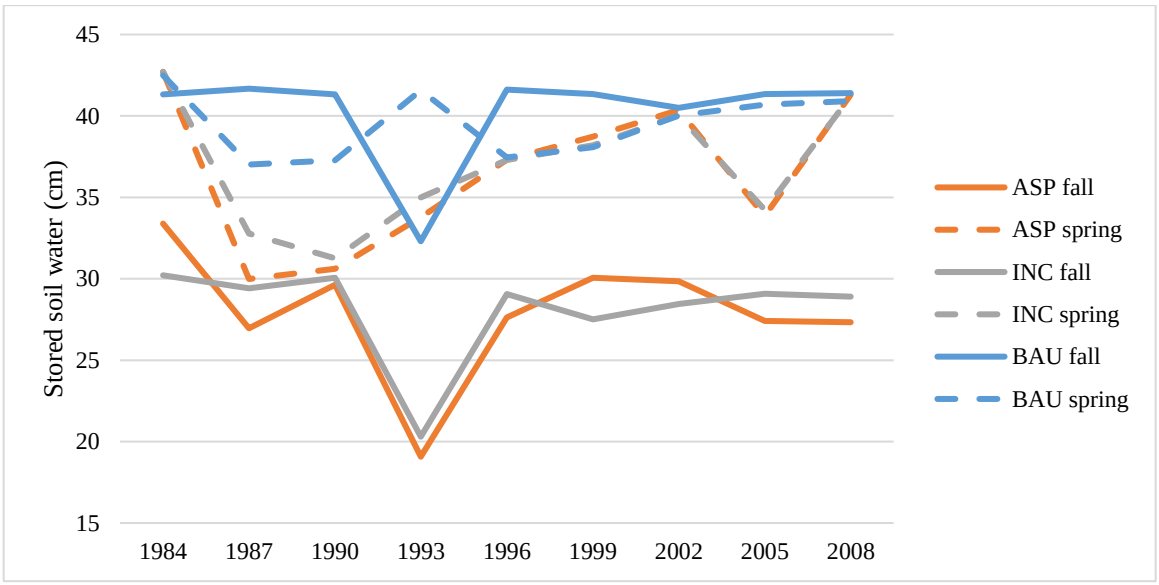

Figure 43: Fall (October 1) and spring (April 15) simulated stored soil moisture for winter wheat crops; ASP=aspiration, INC=incremental, BAU=business-as-usual

Figure 44 shows water loss, assumed as the difference in precipitation and transpiration over the growing season/fallow period, another metric of water use efficiency. In St. John water storage in the soil profile is critical, as water availability governs management decisions and crop success (Kirby et

al., 2017), and loss through leaching or runoff pathways is less likely than in Genesee, which receives greater precipitation. On average, BAU lost 314 mm of water per year, INC lost 248 mm, and ASP lost 265 mm. Note that BAU water loss includes the fallow period (considered from the harvest of the previous spring wheat crop to the plant of the subsequent winter wheat crop) when no transpiration occurs.

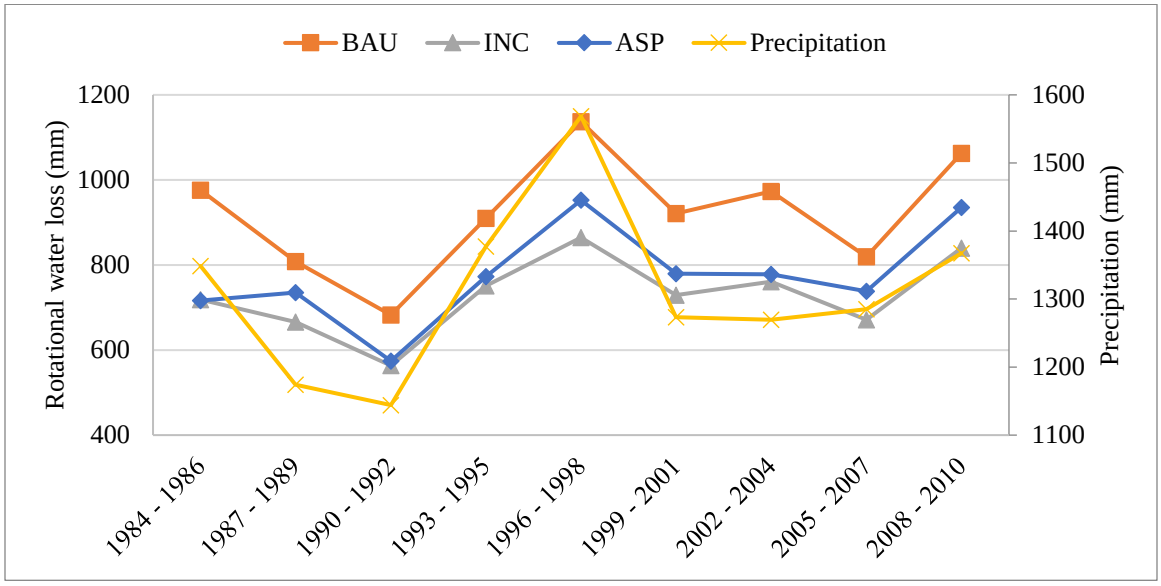

Figure 44: St. John total rotational water loss, computed as precipitation minus crop transpiration; ASP=aspiration, INC=incremental, BAU=business-as-usual

Additional long-term simulations investigated the effects of varying cover crop termination dates. Generally, termination was simulated on the average strip trial termination date and approximately two weeks prior, four weeks prior, and two weeks after than the average strip trial date. As shown in Figure 45, early cover crop termination typically led to an increase in the subsequent wheat yield. Each year BAU winter wheat outperformed ASP winter wheat (following a cover crop with an average termination date) is represented.

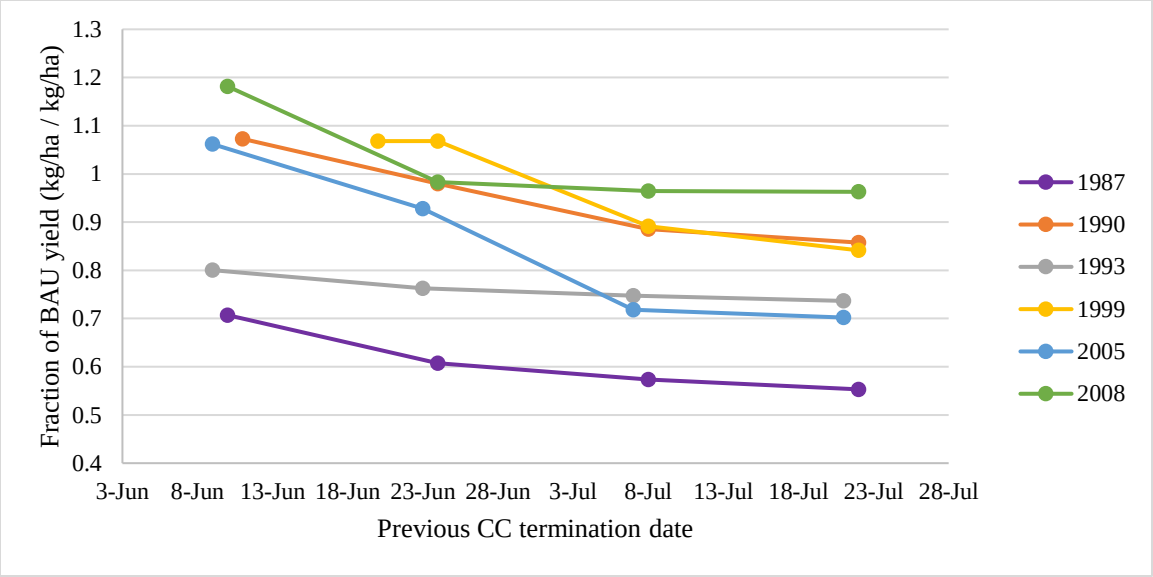

Figure 45: Variable cover crop (CC) termination dates and fraction of business-as-usual (BAU) winter wheat yield achieved for years during which BAU winter wheat outperformed ASP winter wheat (following a cover crop with an average termination date)

CropSyst applied nitrogen directly to tissues at 'deficient requirements', summarized in Figure 46. For reference, the graph also includes results of ASP simulations with a baled cover crop ("ASP with harvested CC") and with a nitrogen-fixing cover crop ("ASP with CC fixation"). INC required the least fertilization, with the non-fixing ASP rotations requiring the most.

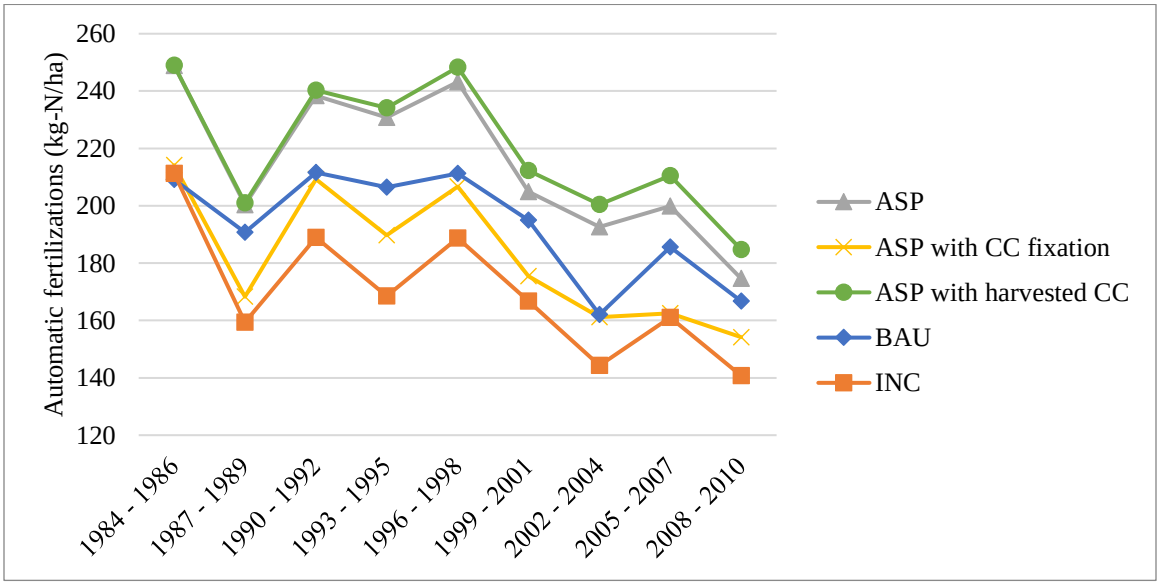

Figure 46: Rotational total automatic nitrogen applications; ASP=aspiration, INC=incremental, BAU=business-as-usual. "ASP with CC fixation" includes a nitrogen-fixing cover crop, and "ASP with harvest CC" assumes a non-fixing cover crop, with 80% of its biomass baled.

Discussion

Genesee

Crop success in the high precipitation zone is generally not limited by water use of the previous crop, and the region supports annual crop cultivation (Kirby et al., 2017). Rotational biomass and yield generally followed annual precipitation trends. As shown in Table 25, differences in simulated total biomass and crop yield were minimal for winter wheat, spring wheat, and chickpea in each rotation. Consequently, variations in Genesee's rotational biomass and yield result primarily from the type of crop in each rotation. However, field-based studies show that diversifying rotations can lead to benefits for staple crops/crops common across rotations, such as improved yield, reduced risk of failure, and protection against abnormal weather (Bowles et al., 2020; Gaudin et al., 2015). Simulated results may not have supported that conclusion for a variety of reasons; for instance, the model eliminates field variability; does not account for factors like weeds, disease, pests, or erosion, which can compromise production; and does not capture changes in soil properties.

As displayed in Figure 34 and Figure 35, the INC rotation produced the greatest biomass in all instances, followed by BAU. However, BAU generated similar yield to INC. In part, the chickpea included in the BAU rotation exhibited a higher average harvest index (produced more grain per biomass) than the winter pea included in INC, and a greater range of winter pea biomass and yield outcomes were observed throughout time. These results are consistent with those of the strip trial. CropSyst simulated the lowest rotational biomass and yield in the ASP rotation, as it included the two lowest producing crops, chickpea and cover crop. However, during the 1990-1992 and 2002-2004 rotations, both low precipitation periods, ASP produced greater biomass than did BAU, indicating the ASP rotation may be less vulnerable to drought conditions.

If considering forage harvested from the cover crops as a yield outcome, ASP appears advantageous, in part due to a high yield to biomass ratio; CropSyst simulated 80% of aboveground cover crop biomass harvested versus an average harvest index of about 0.42 for the other market crops. However, it is important to distinguish true seed yield versus biomass harvested as yield, as is the case for the forage crops. Nonetheless, based on total crop production, a grower that also raises livestock, can lease land to a rancher, or has access to forage/hay markets could benefit from high yield outcomes associated with harvested cover crops. For example, in 2019, the larger, field-scale ASP tower field was planted to cover crop and grazed in June-July, with calves averaging 107 pounds of weight gain over 46 days, equivalent to 2.3 pounds per day.

Surprisingly, harvesting cover crops (i.e., using as a forage crop) versus leaving all biomass in the field as residue did not affect biomass or yield outcomes of subsequent crops. This may have resulted

from the overall lower biomass production of the cover crops versus the market crops and the considerable residue contribution of the other crops in the rotation. Field research suggests that residue must be carefully managed, as some residue will improve soil and water conservation, but too much will cause unfavorable spring growing conditions (Tao et al., 2017), thereby affecting production outcomes. By comparison, in the CropSyst simulations, differences in harvested cover crop outcomes primarily emerged in nitrogen results.

In addition to production, stability is a highly desired cropping system characteristic, as it implies a cropping system's ability to maintain outcomes, even under stressful conditions (Gaudin et al., 2015). The biomass and yield outcomes, and consequently coefficient of variations (dispersion of data about the mean), of a specific crop did not vary markedly across rotations. However, when considering the overall rotation, INC exhibits greater biomass and yield stability, as indicated by lower c_v values; see Table 26. ASP resulted in the greatest yield c_v, which was strongly influenced by its low mean yield, as it only included two harvestable crops. Despite INC's low rotational variability, winter pea exhibits the highest variation on an individual crop basis, likely due to limited and highly variable observations during the strip trials, which influenced the development of the model's crop file.

Generally, the value of increased production must offset cost of fertilization, so crop nitrogen demands must be carefully considered. Nitrogen demand followed similar trends to production, with a slight decrease over time, likely resultant of increased mineralization. The BAU rotation demanded the greatest nitrogen, followed by INC; see Figure 36. However, because the unharvested cover crop produced no yield, the INC rotation, followed by the BAU rotation, used applied nitrogen more efficiently, producing more grain per fertilizer addition. In general, CropSyst simulated less nitrogen fixation by chickpea than winter pea (chickpea fixation was approximately 58% of winter pea). Winter peas produce more grain nitrogen than spring peas and also exhibited "the ability to overcompensate" for high nitrogen removal through greater fixation (Neugschwandtner et al., 2021).

ASP rotations replace the spring wheat in a BAU or INC rotation with a cover crop, which demands less nitrogen (average yearly automatic nitrogen application of 18 kg-N/ha for cover crop versus 51 kg-N/ha for spring wheat). It is also worth noting that in many instances, legumes would represent a portion of a cover crop mix. Model development and, consequently, outputs only reflect strip trial observations, but selection of a different cover crop mix and changing management practices could potentially increase biomass production, nitrogen fixation, and mineralization (Jones et al, 2020). Simulating ASP with a nitrogen-fixing cover crop further reduced its rotational nitrogen requirements (Figure 36). However, CropSyst utilizes a single crop file to represent a given cover crop, and while

CropSyst allows users to select “nitrogen fixation” for a crop, the submodel is not modifiable (i.e., users cannot specify partial crop fixation).

Cover crop simulations modeled unharvested and baled forage, but producers could elect to graze cover crops directly. This would likely yield nitrogen outcomes between those of unharvested and baled cover crops, as greater biomatter would remain in the field in the form of livestock manure. In addition to providing fertilizer, grazed cover crops are also reported cause soil surface disturbance and stimulate root growth and microbial activity (White, 2020) but can increase bulk density, decrease soil organic carbon, and reduce water retention compared to ungrazed cover crops (Tobin et al., 2020). These tradeoffs must be carefully balanced.

As discussed previously, simulated soil nitrogen does not represent strip trial observations well, so complete nitrogen cycling outcomes cannot be assessed. However, CropSyst mineralization outputs still provide insight to general soil nitrogen trends and relationships. As shown in Figure 37, CropSyst simulated mineralization generally increasing throughout time for all three rotations. Simulations did not consider tillage, which increases organic matter decomposition through increased microbial activity and carbon oxidation (Al-Kaisi and Licht, 2005), and assumed all crop residues remained in the field, which builds organic matter (Tao et al., 2017). Greatest mineralization occurred in INC, followed by ASP. The winter pea and spring wheat in the INC rotation produced greater biomass than the chickpea and cover crop in the ASP rotation, respectively, so more residue was left in the field post-harvest. The harvested cover crop further reduced field residue, consequently decreasing mineralization and increasing nitrogen demands versus the unharvested cover crop.

In addition to high production and improved nitrogen outcomes, winter crops offer environmental advantages over spring crops. Genesee’s BAU rotation includes two spring-seeded crops, spring wheat and chickpea, and a single fall-seeded crop, winter wheat. By comparison, both ASP and INC include two fall-seeded crops. Generally, fall crops better manage and utilize winter precipitation (Kirby et al., 2017), and in the IPNW most precipitation falls during winter months (Brooks et al., 2012). Consistent with this, CropSyst simulated approximately 70 mm greater average yearly water loss (precipitation minus evapotranspiration) in BAU than the other rotations, with ASP and INC approximately equivalent; see Figure 38. In addition to utilization by crops directly, this highlights winter crops’ ability to protect surfaces from evaporative losses by increasing ground cover. Lost water also includes surface runoff and leached water and can carry nitrogen and other valuable nutrients. Additionally, while not simulated, lack of winter surface cover encourages erosion, which can further pollute waterways and reduce farm ground’s production capacity (Schillinger et al., 2010).

Growers aiming to better control water and other resource loss may consider fall-seeded crops for this reason.

St. John

Winter wheat and spring wheat crops were common to all St. John rotations. In contrast to Genesee, differences emerged between winter wheat and spring wheat crops planted in different rotations at St. John (Table 27). However, winter wheat crops preceded all spring wheat crops, effectively diminishing the effects of the third year in the rotation (cover crop, winter pea, or fallow) on the spring wheat. As expected, minor differences in spring wheat biomass and yield outcomes suggest water stored during fallow (BAU) or the excess unused water by the cover crop (ASP) had been utilized by the winter wheat crops.

INC rotations produced the greatest average three year total biomass and yield of the three ASP, INC, and BAU rotations considered; see Figure 39 and Figure 40. ASP rotations generally produced greater biomass than did BAU rotations, but the cover crop contributed no yield, so BAU yields were typically higher. During 1987-1990, a low precipitation period, rotational BAU biomass nearly matched ASP, and yield outcomes approached INC, suggesting that BAU's fallow period reduces vulnerability to drought conditions. In contrast, greater precipitation was received during 1996-1998, and ASP and INC increased during this period, whereas BAU decreased slightly, indicating the intensified ASP and INC rotations could better capture and utilize precipitation. Generally, the water use efficiency of a fallowed system decreases with increasing precipitation, as the crop is not as reliant on the stored water for biomass production (Lauenroth et al., 2000). Like Genesee, a harvested cover crop (forage crop) increases ASP yields over those observed in any other rotation (if considering biomass harvested as yield equivalent to a grain yield produced by the other market crops), an advantage for growers with access to livestock or to forage markets.

Water availability strongly influences crop choice in the intermediate precipitation, annual crop-fallow transition zone, with winter wheat considered the most reliable, profitable, and stable (Kirby et al., 2017; Papendick, 1996; Schillinger et al., 2010). Still, winter wheat yields varied throughout time, especially during the first ten years of the simulation (1984-1993) (Figure 41). BAU winter wheat outperformed the other rotations 67% of the time (6 out of 9 instances) with only 4 of 9 instances resulting in 5% or greater differences in crop yield between BAU and ASP/INC. This was primarily observed during or following lower precipitation years. Winter wheat in the INC rotation exceeded that of the ASP rotation 78% of the time (7 out of 9 instances) and nearly matched yields in the BAU during the latter part of the simulation, although differences between INC and ASP were generally minor.

Interestingly, spring crops exhibited lower variability than did winter crops based on c_v values contained in Table 27. By comparison, Schillinger (2020) and Kirby et al. (2017) note that spring-planted crops showed higher variability and limited viability when compared to winter crops in lower precipitation regions due to greater susceptibility to environmental stressors. The data with which the crop files were developed may not have exhibited typical variability, or it is possible that CropSyst is not entirely capturing the effects of water or heat stress, such as challenges associated with germinating spring crops in poor conditions. Of all crops, winter pea exhibited the lowest biomass variability and highest yield variability, likely a function of the wide range of harvest indices observed during the strip trial. BAU spring wheat and winter wheat crops had slightly lower coefficients of variability than those included in the other rotations, indicating less year-to-year variability. Despite the highly variable winter pea, on a rotational basis, INC exhibited the least variability, in part due to its high production. Compared to Genesee, St. John outcomes were slightly more variable, likely a result of greater environmental stress.

Schillinger et al. (2008) identified a relationship between wheat grain yield and available soil moisture at dryland wheat sites throughout eastern Washington. In a 180-cm soil profile, each additional 1 cm of moisture resulted in a 149-154 kg/ha gain in wheat grain yield. This relationship helps farmers determine grain yield potential, which factors into production decisions and profitability outcomes (Schillinger et al., 2008). CropSyst outputs indicate wheat yields increased 186 kg/ha per centimeter of available water. By comparison to these CropSyst simulations, Schillinger et al.'s assessment included spring wheat, utilized a deeper soil profile, and focused on lower precipitation regions, primarily those receiving 240-350 mm precipitation per year. Schillinger et al. (2008) also noted that water efficiency relationships can improve over time based on use of newer cultivars and improved agronomic practices and timing of field operations. Between rotations, BAU exhibited a higher use efficiency than the other rotations, approximately 209 kg/ha / cm water. However, it is important to note the tradeoff between BAU's improved winter wheat outcomes and the greater overall production of the intensified ASP and INC rotations.

Water cycling results indicated BAU protected winter wheat outcomes during unfavorably dry conditions, but ASP and INC better utilized available precipitation. For example, winter wheat preplant soil moisture differed; see Figure 43. CropSyst simulated an average of 0.19 m^3/m^3 soil moisture in ASP and INC on October 1st, with nearly 0.27 m^3/m^3 present in the BAU rotation. ASP and INC recovered more water over winter but to a lesser degree during low precipitation periods, emphasizing the advantage of fallow during drought conditions. BAU also experienced the greatest water loss during each rotational period, computed as precipitation minus transpiration (Figure 44).

Similar to Genesee, INC, with two winter crops, lost the least water per rotation, again highlighting the advantage of winter crops in preventing surface runoff, leaching, and erosion. Overall, St. John rotations experienced less water loss than Genesee, a function of reduced precipitation.

Cover crops in ASP did provide some protection from water loss during the following winter wheat seasons. For example, during the winter wheat seasons following cover crops with average harvest dates in St. John, ASP experienced approximately 377 mm of soil water drainage over the simulation period (equivalent to 9.6% of precipitation received during winter wheat years) versus 1,182 mm of drainage in BAU (30% of precipitation). This can also be observed rotationally in Figure 44. Figure 45 relates the impact of cover crop termination timing on subsequent yield outcomes. Winter wheat yield decreased with later cover crop harvests, although outcomes appeared to plateau mid-July. Early termination (up to four weeks prior to the average termination date) increased winter wheat yields between 6 and 36% over those observed for later terminated cover crops and, in four of six instances, eliminated any detrimental effects on winter wheat yields, indicated by a fraction of BAU yield greater than one.

Especially in dry conditions, excessive moisture depletion by cover crops can delay planting of the subsequent crop, which can cause germination failure or promote challenging management conditions (Roberts, 2018), effects not captured by CropSyst. For reference, the NRCS's cover crop termination guidelines suggest terminating spring cover crops 15 days prior to planting the next crop but as late as crop planting, depending on cover crop seeding date (USDA, 2019). The average CropSyst simulation cover crop harvest date, July 8th, was separated by 82 days from average winter wheat plant date, September 28th. It is also worth mentioning that, in both Whitman (St. John) and Latah (Genesee) counties, the USDA considers ground with cover crops planted during a fallow year that are hayed, grazed, harvested, or otherwise terminated after June 1 insurable as "continuous cropping practice" acreage (i.e., not fallowed). Terminating cover crops earlier reduces their biomass production and positive soil effects (Jones et al., 2020), so it is important to weigh timing against potential improved winter wheat outcomes. While average cover crop termination date generated 4,621 kg/ha biomass on average and used 145 cm of water for transpiration, the earliest simulated termination date produced only 2,817 kg/ha on average with 86 cm of water directed to transpiration. If it is assumed a cow consumes 15 kg/day for 50 days, the 4,621 kg/ha produced under the average termination date would support approximately 6.4 cows/ha, whereas the 2,817 kg/ha from the earliest termination would support 3.8 cows/ha. Note that cattle feed intake varies dramatically based on feed quality and animal age, size, stage of production, and other factors (Rasby, 2013).

As expected, the INC rotation required the lowest nitrogen fertilization, as it was the only rotation that included a nitrogen-fixing crop (winter pea) (Figure 46). BAU required the second highest amount of nitrogen fertilizer, as it included only two crops over three years. ASP, with three non-fixing crops, required the greatest nitrogen. However, simulating a nitrogen-fixing cover crop can reduce overall rotational requirements markedly. Utilizing a cover crop for forage increased nitrogen requirements, as less organic matter remained in the field postharvest.

Additional Considerations

Although CropSyst is a powerful and valuable tool, crop and management decisions must consider other measured effects and adoption factors not quantified by the model, such as those addressed in the *Limitations* section of the CropSyst Model Development chapter. Crop choices are very individual and situational and will vary based on a farm's existing practices, available resources, and specific environmental or economic needs (Reganold, 1990). Economic constraints serve as one of the biggest adoption barriers for new crops and practices. Crop selection often dictates farm revenue and ecosystem services, and crop diversity serves as a key strategy to mitigate risk and income uncertainties (Lee et al., 2016; Reganold et al., 1990). Besides economics, marketing efforts, equipment requirements, nutrient information, and federal farm programs are among the top factors identified for conversion or adoption of practices (Drost et al., 1996). Accordingly, crop choice and rotation selection require an interdisciplinary assessment of opportunities and limitations.

The 1980-2010 weather data included a wide range of environmental conditions and captured some climatic shifts; for instance, 1998, 2002, 2003, 2005, 2006, 2007, and 2010 were the warmest years on record globally (Hansen, 2011). However, future climate scenarios will likely alter historic and existing crop-environment dynamics. On average, climate models predict up to a 1°F increase in temperature and 2% increase in precipitation per decade over the next century primarily in winter months (Mote, et al., 2010). Many speculate that future climate will improve crop performance and provide opportunities to diversify via incorporation of new crops, particularly winter crops (Jareki et al., 2018; Karimi et al, 2018; Stöckle et al., 2018). Further CropSyst modeling efforts could focus on the effects of future climate scenarios on BAU, ASP, and INC rotational outcomes. Long-term simulations may provide insight as to how best to apply rotations and optimize practices in the years ahead.

Conclusion

Long-term CropSyst modeling provides great insight to interactions between crop and environment and rotational effects over time. Results suggest opportunities exist for adoption of diversified and intensified rotations in both the annual crop and annual crop transition regions of the IPNW.

CropSyst simulated similar winter wheat, spring wheat, and chickpea outcomes across all Genesee rotations. On a rotational basis, INC produced the greatest biomass and yield and displayed the greatest stability, based on its coefficient of variation (c_v). However, considering baled cover crop (forage) as yield increased simulated ASP yield over that of INC, and ASP rotation appeared less vulnerable to drought conditions. BAU demanded the greatest nitrogen, followed by INC.

In St. John, CropSyst simulated differences in biomass and yield between winter wheat and spring wheat crops, common among all three rotations. Like Genesee, INC generated the greatest biomass and yield. BAU appeared less vulnerable to drought conditions, while INC and ASP better utilized available precipitation. Surprisingly, CropSyst simulated greater variability among winter crops than spring crops, but, rotationally, INC appeared the most stable. INC and ASP rotations recovered more soil water over winter but to a lesser degree during drought. INC, with two winter crops, lost the least water. Earlier cover crop termination dates increased subsequent winter wheat yields, in some cases to a greater degree than BAU.

Some differences arose between Genesee and St. John outcomes as a function of water availability. However, at both sites, winter crops' longer grower period reduced reliance on scarce spring precipitation and allowed them to better harness limited resources. When considering nitrogen requirements, production, and water utilization, winter pea appears advantageous over alternative crops like chickpea. Cover crops, especially Genesee's fall planted crop, improved water outcomes over BAU and could provide producers with an additional opportunity to diversify, if baled for forage or grazed by livestock. Variable termination dates, modeled in St. John, emphasize the importance of flexible and opportunistic management strategies. Depending on current environmental or other conditions, growers can elect to employ strategies such as fallowing, altering cover crop mix composition, or delaying planting to spring.

Crop choice or management decisions often result in tradeoffs, such as cost of fertilization versus the value of increased production or cover crop biomass production versus moisture preservation. While this work helps quantify these effects, many factors contribute to cropping outcomes beyond those simulated by the CropSyst model. Further integration of this work with other disciplines, such as agronomy, economics, or policy, would prove valuable. Additional CropSyst model simulations could focus on future climate scenarios and understanding longer-term implications of developing environmental conditions.

Chapter 4: Summary and Future Work

Introduction

Farmers in the Inland Pacific Northwest (IPNW) typically cultivate dryland wheat-based crop rotations, which often include spring crops and, in lower precipitation areas, fallow. However, changing environmental conditions, economics, and emerging research motivates shifts in existing production practices. Many speculate that replacing traditional crop rotations with those that include winter peas or cover crops will allow farmers to diversify (or intensify, if replacing fallow) and may improve production and nutrient/water cycling outcomes. This research utilized a process-based crop model to simulate field conditions and investigate the long-term viability of traditional and novel rotations.

Work was completed as part of the Landscapes in Transition (LIT) project. LIT carried out four-year (2018-2021) strip trials at two sites, one corresponding in an annual crop-fallow transition system (ACT) in the intermediate precipitation zone (St. John, Washington) and one corresponding to an annual crop system (AC) in the high precipitation zone (Genesee, Idaho). Field treatments covered three separate, three-year crop rotations: spring wheat-fallow-winter wheat (business-as-usual, BAU), spring wheat-winter pea-winter wheat (incremental, INC), and spring wheat-spring cover crop-winter wheat (aspirational, ASP) in the intermediate precipitation zone and spring wheat-chick pea-winter wheat (BAU), spring wheat-winter pea-winter wheat (INC), and winter cover crop-chick pea-winter wheat (ASP) in the high precipitation zone.

This work aimed to:

1. Parameterize and assess the ability of the CropSyst model to simulate crop production and nitrogen/water cycling at an annual crop and a crop-fallow transition location using the replicated rotational strip trial data
2. Evaluate viability of alternate crop rotations under current and historic climate conditions and identify management strategies to optimize/adapt rotation success and stability

CropSyst Model Development

Two site-specific CropSyst models were developed to reflect the LIT project's IPNW strip trial locations: the annual cropping site in Genesee, ID and the annual crop-fallow transition site in St. John, WA. CropSyst is a process-based, multi-crop, multi-year model, frequently employed to study the interactions of crops, soils, weather, and management (Stöckle, 2003). The LIT project provided an extensive dataset with which to constrain and calibrate the model. The weather, soil, management, and initialization files were completely populated from known or measured values. During the

calibration phase, certain crop files were calibrated to obtain accurate yield/biomass, soil moisture, and nitrogen outcomes.

CropSyst did not always simulate yield, biomass, and moisture outcomes successfully for *individual* strips or crops, but it predicted observations very well on an overall, rotational, and yearly basis. Considering the variability and extent of the data observed during the LIT trial, it proved powerful and robust. Following biomass/yield and soil moisture calibration, several nitrogen parameters were also calibrated, focusing on the Genesee site. Overall, crop nitrogen was simulated well. However, improvement of inorganic soil nitrogen predictions may be valuable in the future. There are several other limitations inherent to this work, including the exclusion of factors such as weeds, disease, and pests.

The two CropSyst models developed under Objective 1 adequately reflect field conditions and were used for scenario testing under Objective 2. They help identify important crop-environment relationships and provide insight to management impacts.

Long-term Model Simulations

Objective 2 utilized the calibrated CropSyst model to evaluate intensified and diversified rotations under recent climate conditions at each IPNW location. Three (one reflecting each ASP, BAU, INC), 30-year simulations were run to explore the long-term interactions between crop and environment. Scenario testing focused on four main subobjectives:

1. Evaluating impacts of diverse/intense rotations on production outcomes and nitrogen requirements
2. Assessing the effects of fallow replacement on winter wheat crops (St. John)
3. Addressing the implications of cover crop termination approach
4. Exploring the impacts cover crop termination date on subsequent winter wheat crop years (St. John)

At both sites, winter crops' longer grower period reduced reliance on spring precipitation and allowed them to better harness limited resources. However, BAU in St. John appeared less vulnerable to drought conditions, especially with respect to winter wheat outcomes. When considering nitrogen requirements, production, and water utilization, the winter pea in INC appeared advantageous over alternative crops like chickpea. In general, inclusion of legume crops reduced nitrogen fertilization demand.

Considering baled cover crop (forage) as yield increased simulated ASP rotational yield over that of INC or BAU, suggesting opportunities for those interested in using cover crops as livestock forage. Integration of livestock directly on land could have further soil health implications not addressed by this study. Earlier cover crop termination dates in St. John led to increased winter wheat yields in the following year; however, termination timing must be balanced with crop biomass production.

While these results provide valuable insight, crop modeling effectively simplifies field conditions by eliminating variability and key factors such as weeds, disease, or policy or economic considerations. It is, therefore, important to integrate this work with other field-based outcomes from various disciplines. Regardless, CropSyst simulations emphasize key relationships and trade-offs that can contribute to a better overall understanding of these traditional and novel crop rotations.

Conclusions and Future Work

The CropSyst model exhibited good predictive ability of LIT strip trial observations across all crop rotations and years. There are limited examples of CropSyst studies which calibrate the model over multiple years using static parameters and achieve good rotational agreement. However, the CropSyst model did not simulate soil inorganic nitrogen well. This can be improved in future work with better parameterization and calibration of the organic matter model or potentially crop nitrogen parameters. It is also possible that measurement errors or overfertilization occurred or that the nitrogen transport and uptake processes simulated in CropSyst require some improvement.

Long-term simulations of the models indicate opportunities exist for adoption of diversified and intensified rotations in both the annual crop and annual crop-fallow transition regions of the IPNW. Scenario testing also suggested that altering management practices strategically can improve outcomes. This might consist of carefully selecting cover crop mixes, integrating livestock, altering cover crop termination date, and incorporating legumes to reduce fertilizer use.

There are many opportunities for future work utilizing the developed CropSyst models. Further scenario-based testing may include future climate predictions, as changing climate conditions will likely influence cropping systems' success. There are also opportunities to link CropSyst with economic tools such as Oregon State University's AgBiz Logic™ or to use it as an online decision support tool, similar to the Flex Cropping tool developed by Washington State University at their Cook Agronomy Farm Long-term Agroecosystem Research station. Additional CropSyst simulations and integrative tools would greatly enhance the current efforts by expanding applicability and flexibility to different locations or situations.

Works Cited

Abatzoglou, J. T. (2011). Development of gridded surface meteorological data for ecological applications and modelling. *International Journal of Climatology, 33*(1), 121-131. doi:10.1002/joc.3413

Abdi, H. (2010). Coefficient of variation. *Encyclopedia of Research Design, 1*. doi:10.4135/9781412961288.n56

Ahmed, M., Akram, M. N., Asim, M., Aslam, M., Hassan, F. U., Higgins, S., ... & Hoogenboom, G. (2016). Calibration and validation of APSIM-Wheat and CERES-Wheat for spring wheat under rainfed conditions: Models evaluation and application. *Computers and Electronics in Agriculture*, 123, 384-401.

Al-Kaisi, M., & Licht, M. (2005). Tillage and residue management effects on soil organic matter. *Resources Conservation Practices: Manure and Tillage Management*.

Archontoulis, S. V., Miguez, F. E., & Moore, K. J. (2014). A methodology and an optimization tool to calibrate phenology of short-day species included in the APSIM plant model: Application to soybean. *Environmental Modelling & Software*, 62, 465–477. https://doi.org/10.1016/j.envsoft.2014.04.009

Aslam, M. A., Ahmed, M., Stöckle, C. O., Higgins, S. S., Hassan, F., & Hayat, R. (2017). Can growing degree days and photoperiod predict spring wheat phenology? *Frontiers in Environmental Science*, 5. https://doi.org/10.3389/fenvs.2017.00057

Asseng, S., Zhu, Y., Basso, B., Wilson, T., & Cammarano, D. (2014). Simulation modeling: Applications in cropping systems. *Encyclopedia of Agriculture and Food Systems*, 102–112. https://doi.org/10.1016/b978-0-444-52512-3.00233-3

Balasubramanian, V., Alves, B., Aulakh, M., Bekunda, M., Cai, Z., Drinkwater, L., ... & Oenema, O. (2004). Crop, environmental, and management factors affecting nitrogen use efficiency. *Agriculture and the Nitrogen Cycle*, 65, 19-33.

Bellocchini, G., Silvestri, N., Mazzoncini, M., & Menini, S. (2002). Using the CropSyst model in continuous rainfed maize (Zea mais L.) under alternative management options. *Italian Journal of Agronomy*, 6(1), 43–56.

Benli, B., Pala, M., Stockle, C., & Oweis, T. (2007). Assessment of winter wheat production under early sowing with supplemental irrigation in a cold highland environment using CropSyst simulation model. *Agricultural Water Management*, 93(1-2), 45-53.

Beven, K. (1989). Changing ideas in hydrology — the case of physically-based models. *Journal of Hydrology*, 105(1-2), 157–172. https://doi.org/10.1016/0022-1694(89)90101-7

Bowles, T. M., Mooshammer, M., Socolar, Y., Calderón, F., Cavigelli, M. A., Culman, S. W, … & Grandy, A. S. (2020). Long-term evidence shows that crop-rotation diversification increases agricultural resilience to adverse growing conditions in North America. *One Earth*, 2(3), 284–293. https://doi.org/10.1016/j.oneear.2020.02.007

Brooks, E. S., Boll, J., & McDaniel, P. A. (2012). Hydropedology in seasonally dry landscapes: the Palouse region of the Pacific Northwest. *Hydropedology: Synergistic Integration of Soil Science and Hydrology* (pp. 329–350). Academic Press. doi:10.1016/B978-0-12-386941-8.00010-1

Busacca, A. J., Nelstead, K., McDonald, E., & Purser, M. (1992). Correlation of distal tephra layers in loess in the channeled scabland and Palouse of Washington State. *Quaternary Research*, 37, 281–303.

Campbell, G. (1974). A simple method for determining unsaturated conductivity from moisture retention data. *Soil Science*, 117(6), 311–314. https://doi.org/10.1097/00010694-197406000-00001

Carretero R., Serrago R. A., Bancal M. O., Perelló A. E., & Miralles D. J. (2010). Absorbed radiation and radiation use efficiency as affected by foliar diseases in relation to their vertical position into the canopy in wheat. *Field Crops Research*, 116(1–2): 184–195

Chen, C., Miller, P., Muehlbauer, F., Neill, K., Wichman, D., & McPhee, K. (2006). Winter pea and lentil response to seeding date and micro- and macro-environments. *Agronomy Journal, 98*(6), 1655. doi:10.2134/agronj2006.0085

Chen, J. M., & Cihlar, J. (1996). Retrieving leaf area index of boreal conifer forests using Landsat TM images. *Remote Sensing of Environment*, 55(2), 153–162. https://doi.org/10.1016/0034-4257(95)00195-6

Chi, J., Maureira, F., Waldo, S., Pressley, S. N., Stöckle, C. O., O'keeffe, P. T., ... & Lamb, B. K. (2017). Carbon and water budgets in multiple wheat-based cropping systems in the Inland Pacific Northwest US: Comparison of CropSyst simulations with eddy covariance measurements. *Frontiers in Ecology and Evolution,5*. doi:10.3389/fevo.2017.00050

Confalonieri, R., Acutis, M., Bellocchi, G., Cerrani, I., Tarantola, S., Donatelli, M., & Genovese, G. (2006a). Exploratory sensitivity analysis of CropSyst, WARM and WOFOST: A case-study with rice biomass simulations. *Italian Journal of Agrometeorology*, 17–25.

Confalonieri, R., Gusberti, D., Bocchi, S., & Acutis, M. (2006b). The CROPSYST model to simulate the N balance of rice for alternative management. *Agronomy for Sustainable Development*, 26(4), 241–249. https://doi.org/10.1051/agro:2006022

Corwin, D. L., Waggoner, B. L., & Rhoades, J. D. (1991). A functional model of solute transport that accounts for bypass. *Journal of Environmental Quality*, 20:647-658.

Drost, D., Long, G., Wilson, D., Miller, B., & Campbell, W. (1996). Barriers to adopting sustainable agricultural practices. *Journal of the Extension*, 34(6).

Faber, B. (2016). Nitrogen changes in the soil, and it changes fast. *Topics in Subtropics*. Retrieved June 16, 2022, from https://ucanr.edu/blogs/blogcore/postdetail.cfm?postnum=21818

Finkelnburg, D., Yorgey, G., Borrelli, K., & Painter, K. (2019). Grazed cover cropping: Drew Leitch farmer-to-farmer case study series: Increasing resilience among farmers in the Pacific Northwest.

Fry, J., Guber, A. K., Ladoni, M., Munoz, J. D., & Kravchenko, A. N. (2017). The effect of up-scaling soil properties and model parameters on predictive accuracy of DSSAT crop simulation model under variable weather conditions. *Geoderma*, 287, 105-115.

Gan, Y. T., Miller, P. R., Liu, P. H., Stevenson, F. C., & McDonald, C. L. (2002). Seedling emergence, pod development, and seed yields of chickpea and dry pea in a semiarid environment. *Canadian Journal of Plant Science*, 82(3), 531-537. doi:10.4141/p01-192

Gaudin, A. C., Tolhurst, T. N., Ker, A. P., Janovicek, K., Tortora, C., Martin, R. C., & Deen, W. (2015). Increasing crop diversity mitigates weather variations and improves yield stability. *PLOS ONE*, 10(2). https://doi.org/10.1371/journal.pone.0113261

Godwin, D. C., & Jones, A. C. (1991). Nitrogen Dynamics in Soi-Plant Systems. *Modeling plant and soil systems*, 31, 287-321.

Gosnell, H., Gill, N., & Voyer, M. (2019). Transformational adaptation on the farm: Processes of change and persistence in transitions to 'climate-smart' regenerative agriculture. *Global Environmental Change*, 59, 101965. doi:10.1016/j.gloenvcha.2019.101965

Grayson, R. B., Moore, I. D., & McMahon, T. A. (1992). Physically based hydrologic modeling: 2. Is the concept realistic? *Water Resources Research*, 28(10), 2659–2666. https://doi.org/10.1029/92wr01259

Haney, R. L., Franzluebbers, A. J., Jin, V. L., Johnson, M. V., Haney, E. B., White, M. J., & Harmel, R. D. (2012). Soil organic C: N vs. water-extractable organic C: N. *Open Journal of Soil Science*, 2, 269-274. doi: 10.4236/ojss.2012.23032

Hansen, K. (2011). NASA research finds 2010 tied for warmest year on record. *Global Climate Change: Vital Signs of the Planet.* Retrieved June 21, 2022, from https://climate.nasa.gov/news/467/nasa-research-finds-2010-tied-for-warmest-year-on-record/

Hoogsteen, M. J., Lantinga, E. A., Bakker, E. J., Groot, J. C., & Tittonell, P. A. (2015). Estimating soil organic carbon through loss on ignition: effects of ignition conditions and structural water loss. *European Journal of Soil Science*, 66(2), 320-328.

Huggins, D. R., Rupp, R., Kaur, H., & Eigenbrode, S. (2014). "Defining agroecological classes for assessing land use dynamics," in *Regional Approaches to Climate Change for Pacific Northwest Agriculture*, 4–7.

Janowiak, M. K., Dostie, D. N., Wilson, M. A., Kucera, M. J., Skinner, R. H., Hatfield, J. L., ... & Swanston, C. W. (2016). Adaptation resources for agriculture: responding to climate variability and change in the midwest and northeast. USDA Tech. Bull. 1944, Washington, D.C., 70

Janssen, B. H. (1996). Nitrogen mineralization in relation to C:N ratio and decomposability of organic materials. *Progress in Nitrogen Cycling Studies*, 69–75. https://doi.org/10.1007/978-94-011-5450-5_13

Jarecki, M., Grant, B., Smith, W., Deen, B., Drury, C., VanderZaag, A., ... & Wagner-Riddle, C. (2018). Long-term trends in corn yields and soil carbon under diversified crop rotations. *Journal of Environmental Quality*, 47(4), 635-643. doi:10.2134/jeq2017.08.0317

Jastrow, J., & Six, J. (2005). Organic matter turnover. *Encyclopedia of Soil Science*. https://doi.org/10.1201/noe0849338304.ch252

Jones, C., Olson-Rutz, K., Miller, P., & Zabinski, C. (2020). Cover crop management in semi-arid regions: Effect on soil and cash crop. *Crops & Soils*, 53(5), 42-51. doi:10.1002/crso.20065

Juergens, L. A., Young, D. L., Schillinger, W. F., & Hinman, H. R. (2004). Economics of alternative no-till spring crop rotations in Washington's wheat–fallow region. *Agronomy Journal*,*96*(1), 154. doi:10.2134/agronj2004.0154

Karimi, T., Stöckle, C. O., Higgins, S., & Nelson, R. (2018). Climate change and dryland wheat systems in the US pacific northwest. *Agricultural Systems*, 159, 144–156. https://doi.org/10.1016/j.agsy.2017.03.014

Karimi, T., Stöckle, C. O., Higgins, S., Nelson, R. L., & Huggins, D. R. (2017). Projected dryland cropping system shifts in the Pacific Northwest in response to climate change. *Frontiers in Ecology and Evolution*, 5, 20. doi: 10.3389/fevo.2017.00020

Kemanian, A. R., Stöckle, C. O., & Huggins, D. R. (2004). Variability of barley radiation-use efficiency. *Crop Science*, 44(5), 1662–1672. https://doi.org/10.2135/cropsci2004.1662

Kemanian, A.R., Stöckle, C. O., & Huggins, D.R. (2005). Transpiration-use efficiency of barley. *Agricultural and Forest Meteorology*, 130(1-2), 1-11

Kirby, E., Pan, W., Huggins, D.R., Painter, K., Bista, P. (2017). Rotational diversification and intensification. WSU Extension Bulletin "Advances in Dryland Farming in the Inland Pacific Northwest." pp. 163-236.

Kravchenko, A. N., Snapp, S. S., & Robertson, G. P. (2017). Field-scale experiments reveal persistent yield gaps in low-input and organic cropping systems. Proceedings of the National Academy of Sciences, 114(5), 926-931.

Lauenroth, W. K., Burke, I. C., & Paruelo, J. M. (2000). Patterns of production and precipitation-use efficiency of winter wheat and native grasslands in the central Great Plains of the United States. *Ecosystems*, 3(4), 344–351. https://doi.org/10.1007/s100210000031

Lee, H., Bogner, C., Lee, S., & Koellner, T. (2016). Crop selection under price and yield fluctuation: Analysis of agro-economic time series from South Korea. *Agricultural Systems*, 148, 1–11. https://doi.org/10.1016/j.agsy.2016.06.003

Liebhardt, W. C., Andrews, R. W., Culik, M. N., Harwood, R. R., Janke, R. R., Radke, J. K., & Rieger-Schwartz, S. L. (1989). Crop production during conversion from conventional to low-

input methods. *Agronomy Journal, 81*(2), 150-159. doi:10.2134/agronj1989.00021962008100020003x

Loosvelt, L., Pauwels, V. R., Cornelis, W. M., De Lannoy, G. J., & Verhoest, N. E. (2011). Impact of soil hydraulic parameter uncertainty on soil moisture modeling. *Water Resources Research*, 47(3). https://doi.org/10.1029/2010wr009204

Mannam, V. (2011). Transpiration-use efficiency coefficient of seven weed species as affected by fraction of transpirable soil water and growth stage (thesis).

McNab, W. H., & Avers, P. E. (1994). Great Plains-Palouse Dry Steppe. *Ecological subregions of the United States: Section descriptions*. Essay, U.S. Dept. of Agriculture, Forest Service, Watershed and Air Management Staff.

Miller, P. R., Brandt, S. A., McDonald, C. L., & Waddington, J. (2006). Chickpea, lentil and pea response to delayed spring seeding on the Northern Great Plains. *Canadian Journal of Plant Science*, 86(4), 1059-1070. doi:10.4141/p05-243

Moriasi, D. N., Arnold, J. G., Liew, M. W., Bingner, R. L., Harmel, R. D., & Veith, T. L. (2007). Model evaluation guidelines for systematic quantification of accuracy in watershed simulations. *Transactions of the ASABE*, 50(3), 885-900. doi:10.13031/2013.23153

Mote, P. W., & Salathé, E. P. (2010). Future climate in the Pacific Northwest. *Climatic Change,102*(1-2), 29-50. doi:10.1007/s10584-010-9848-z

Mrema, G. C. (2011). Chapter 16: Grain crop drying, handling and storage. *Rural structures in the tropics: Design and development*. essay, Food and Agriculture Organization of the United Nations.

NASS USDA. (2020). Small Grains: 2020 Summary. National Agricultural Statistics Service USDA, Washington, DC.

Neugschwandtner, R. W., Bernhuber, A., Kammlander, S., Wagentristl, H., Klimek-Kopyra, A., Lošák, T., Zholamanov, K. K., & Kaul, H.-P. (2021). Nitrogen yields and biological nitrogen

fixation of winter grain legumes. *Agronomy*, 11(4), 681. https://doi.org/10.3390/agronomy11040681

Nielsen, D. C., & Calderón, F. J. (2011). Fallow effects on soil. *Soil Management: Building a Stable Base for Agriculture*, 287-300. doi:10.2136/2011.soilmanagement.c19

NRCS East National Technology Support Center (2011). Carbon to nitrogen ratios in cropping systems. Greensboro, NC.

O'Connell M. G., O'Leary G. J., Whitfield D. M., Connor D. J. (2004). Interception of photosynthetically active radiation and radiation-use efficiency of wheat, field pea and mustard in a semi-arid environment. *Field Crops Research*, 85(2–3): 111–124

Pan, W. L., Schillinger, W. F., Young, F. L., Kirby, E. M., Yorgey, G. G., Borrelli, K. A., ... & Eigenbrode, S. D. (2017). Integrating historic agronomic and policy lessons with new technologies to drive farmer decisions for farm and climate: The case of Inland Pacific Northwestern U.S. *Frontiers in Environmental Science, 5*. doi:10.3389/fenvs.2017.00076

Papendick, R.I. 1996. Farming systems and conservation needs in the northwest wheat region. *American Journal of Alternative Agriculture*, 11(2-3), 52-57.

Rasby, R. (2013). Determining how much forage a beef cow consumes each day. UNL Beef. Retrieved June 2022, from https://beef.unl.edu/cattleproduction/forageconsumed-day

Reganold, J. P., Papendick, R. I., & Parr, J. F. (1990). Sustainable agriculture. *Scientific American, 262*(6), 112-120. doi:10.1038/scientificamerican0690-112

Roberts, D. (2018). Cover cropping and companion cropping for the Inland Northwest: an initial feasibility study. Washington State University Extension.

Sawyer, J. (2010, May 20). Relationship of nitrogen conversion in soil to N loss. *Integrated Crop Management*. Retrieved June 16, 2022, from

https://crops.extension.iastate.edu/cropnews/2010/05/relationship-nitrogen-conversion-soil-n-loss

Saxton, K. E., & Rawls, W. J. (2006). Soil water characteristic estimates by texture and organic matter for hydrologic solutions. *Soil Science Society of America Journal*, 70(5), 1569–1578. https://doi.org/10.2136/sssaj2005.0117

Schillinger, W. F. (2017). Winter pea: promising new crop for Washington's dryland wheat-fallow region. *Frontiers in Ecology and Evolution, 5*. doi:10.3389/fevo.2017.00043

Schillinger, W. F. (2020). New winter crops and rotations for the Pacific Northwest low-precipitation drylands. *Agronomy Journal*, 112(5), 3335-3349. doi:10.1002/agj2.20354

Schillinger, W. F., Kennedy, A. C., & Young, D. L. (2006). Eight years of annual no-till cropping in Washington's winter wheat-summer fallow region. *Agriculture, Ecosystems & Environment, 120*(2-4), 345-358. doi:10.1016/j.agee.2006.10.017

Schillinger, W. F., Papendick, R. I., Guy, S. O., Rasmussen, P. E., & Van Kessel, C. (2003). Dryland cropping in the Western United States. *Pacific Northwest Conservation Tillage Handbook*. https://doi.org/10.2134/agronmonogr23.2ed.c11

Schillinger, W. F., Papendick, R. I., & McCool, D. K. (2010). Soil and water challenges for Pacific Northwest Agriculture. *Soil and Water Conservation Advances in the United States*, 47–79. https://doi.org/10.2136/sssaspecpub60.c2

Schillinger, W. F., Schofstoll, S. E., & Alldredge, J. R. (2008). Available water and wheat grain yield relations in a Mediterranean climate. *Field Crops Research*, 109(1-3), 45–49. https://doi.org/10.1016/j.fcr.2008.06.008

Sinclair, T. R., & Muchow, R. C. (1999). Radiation use efficiency. *Advances in Agronomy*, 215–265. https://doi.org/10.1016/s0065-2113(08)60914-1

Smith, R. G., Gross, K. L., & Robertson, G. P. (2008). Effects of crop diversity on agroecosystem function: Crop yield response. *Ecosystems*, 11(3), 355-366. doi:10.1007/s10021-008-9124-5

Soil Survey Staff, Natural Resources Conservation Service, United States Department of Agriculture. Web Soil Survey. Retrieved May 26, 2021, from http://websoilsurvey.sc.egov.usda.gov/.

Stöckle, C. O. (n.d.). The CropSyst Model: A brief description. Retrieved October 10, 2020, from http://sites.bsyse.wsu.edu/cs_suite/cropsyst/documentation/articles/description.htm

Stöckle, C. O., Donatelli, M., & Nelson, R. (2003). CropSyst, a cropping systems simulation model. *European Journal of Agronomy*, 18(3-4), 289–307. https://doi.org/10.1016/s1161-0301(02)00109-0

Stöckle, C. O., Higgins, S., Nelson, R., Abatzoglou, J., Huggins, D., Pan, W., ... & Brooks, E. (2018). Evaluating opportunities for an increased role of winter crops as adaptation to climate change in dryland cropping systems of the US Inland Pacific Northwest. *Climatic Change*, 146(1), 247-261.

Stöckle, C. O., & Kemanian, A. R. (2009). Crop radiation capture and use efficiency. *Crop Physiology*, 145–170. https://doi.org/10.1016/b978-0-12-374431-9.00007-4

Stöckle, C. O., Kemanian, A. R., Nelson, R. L., Adam, J. C., Sommer, R., & Carlson, B. (2014). CropSyst model evolution: From field to regional to global scales and from research to decision support systems. *Environmental Modelling & Software*, 62, 361–369. https://doi.org/10.1016/j.envsoft.2014.09.006

Stöckle, C. O., Kjelgaard, J., & Bellocchi, G. (2004). Evaluation of estimated weather data for calculating Penman-Monteith reference crop evapotranspiration. *Irrigation Science*, 23(1), 39-46.

Tao, H., Yorgey, G., Huggins, D., & Wysocki, D. (2017). Crop residue management. WSU Extension Bulletin "Advances in Dryland Farming in the Inland Pacific Northwest." pp. 125-162.

Tobin, C., Singh, S., Kumar, S., Wang, T., & Sexton, P. (2020). Demonstrating short-term impacts of grazing and cover crops on soil health and economic benefits in an integrated crop-livestock system in South Dakota. *Open Journal of Soil Science*, 10(03), 109-136. doi:10.4236/ojss.2020.103006

Todorovic, M., Albrizio, R., Zivotic, L., Saab, M. T. A., Stöckle, C., & Steduto, P. (2009). Assessment of AquaCrop, CropSyst, and WOFOST models in the simulation of sunflower growth under different water regimes. *Agronomy Journal*, 101(3), 509-521.

Umair, M., Shen, Y., Qi, Y., Zhang, Y., Ahmad, A., Pei, H., & Liu, M. (2017). Evaluation of the CropSyst model during wheat-maize rotations on the North China Plain for identifying soil evaporation losses. *Frontiers in Plant Science*, 8, 1667.

United States, Department of Agriculture. (2019). NRCS cover crop termination guidelines. Retrieved May 13, 2021, from https://www.nrcs.usda.gov/wps/PA_NRCSConsumption/download?cid=nrcseprd1466429&ext=pdf

van Genuchten, M. T. (1980). A closed-form equation for predicting the hydraulic conductivity of unsaturated soils. *Soil Science Society of America Journal*, 44(5), 892–898. https://doi.org/10.2136/sssaj1980.03615995004400050002x

Ward, N. K. (2015). Improving agricultural nitrogen use through policy incentivized management strategies: Precision agriculture on the Palouse (thesis).

White, C. (2020). Why regenerative agriculture? *American Journal of Economics and Sociology, 79*(3), 799-812. doi:10.1111/ajes.12334

WRCC DRI. (2022). Western U.S. Climate Historical Summaries. Western Regional Climate Center, Reno, NV.

Zentner, R. P., Wall, D. D., Nagy, C. N., Smith, E. G., Young, D. L., Miller, P. R., . . . & Derksen, D. A. (2002). Economics of crop diversification and soil tillage opportunities in the Canadian prairies. *Agronomy Journal, 94*(2), 216. doi:10.2134/agronj2002.0216

Zhang, M., He, Z., Zhao, A., Zhang, H., Endale, D. M., & Schomberg, H. H. (2011). Water-extractable soil organic carbon and nitrogen affected by tillage and manure application. *Soil Science*, 176(6), 307-312.

Zhang, L., Hu, Z., Fan, J., Zhou, D., Tang, F. (2014). A meta-analysis of the canopy light extinction coefficient in terrestrial ecosystems. *Frontiers of Earth Science*, 8(4), 599–609. https://doi.org/10.1007/s11707-014-0446-7

Appendix A

Genesee, ID

Winter cover crop mixture

2017/2018: winter wheat, winter pea, Sudan grass, proso millet, crimson clover, lentil, turnip, radish, flax

2018/2019 – 2020/2021: winter oat, winter pea, crimson clover, turnip, radish, winter wheat (volunteer, not seeded)

St. John, WA

Spring cover crop mixture

2017/2018 – 2020/2021: spring pea, spring oats, spring barley, turnip, sunflower

Appendix B

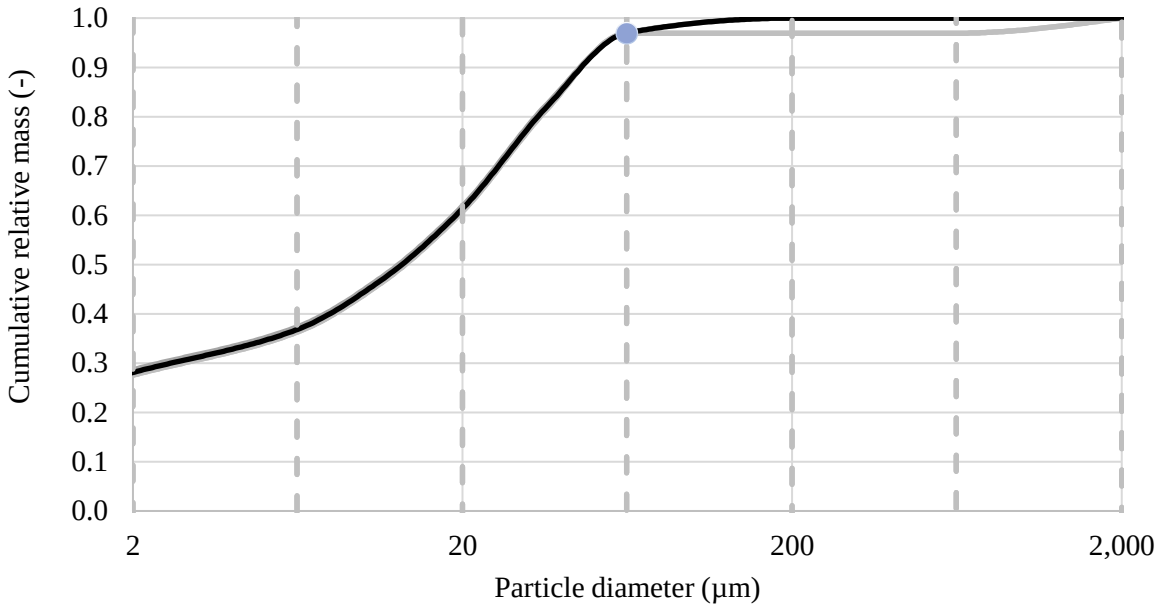

Figure 47: Genesee 0-30 cm cumulative particle size distribution with cumulative mass as a fraction and particle diameter in micrometer (Strip D, rep. 1-5)

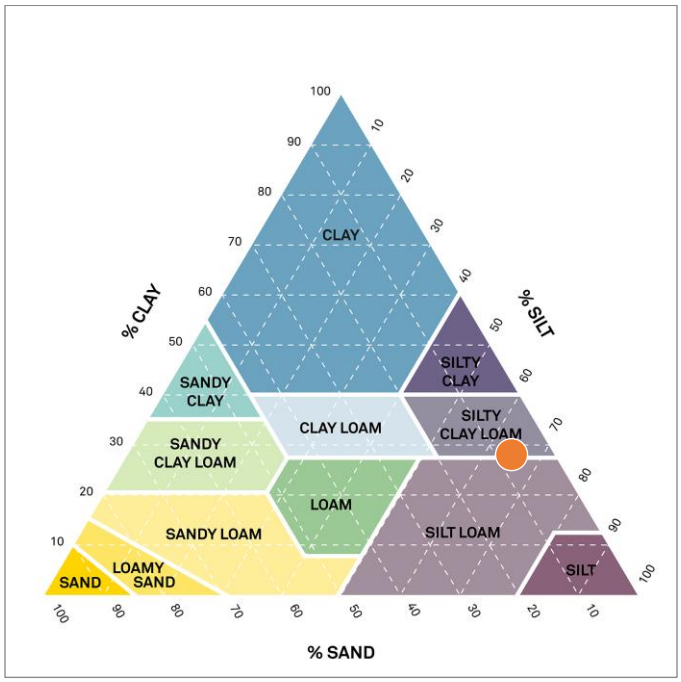

Figure 48: Genesee 0-30 cm soil taxonomy texture triangle (Strip D, rep. 1-5)

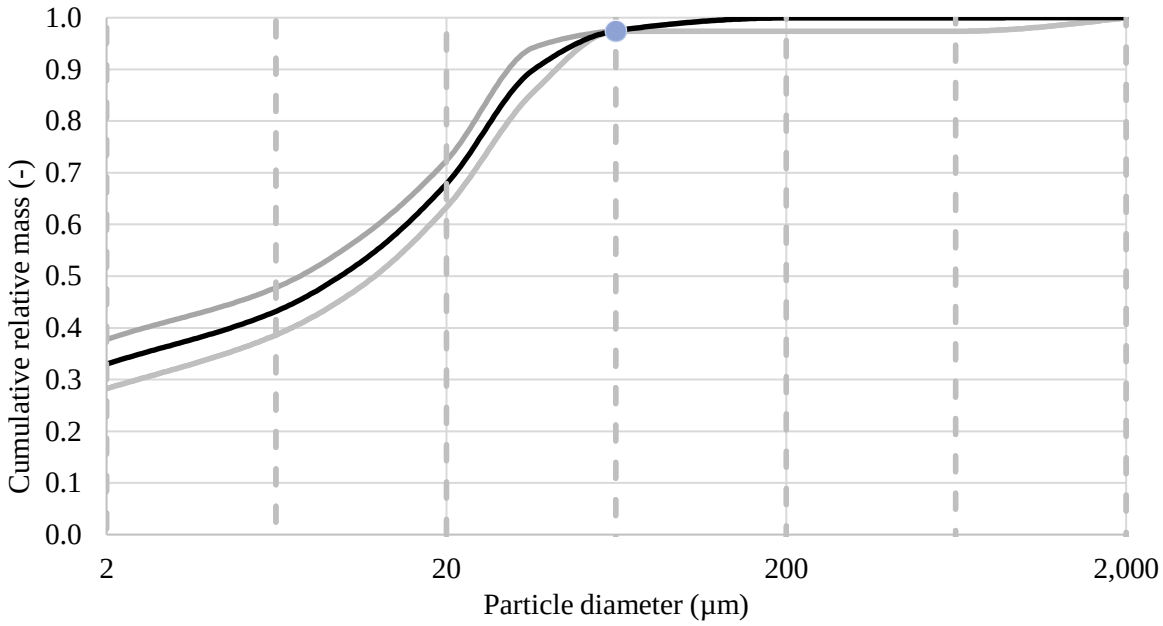

Figure 49: Genesee 30-90 cm cumulative particle size distribution with cumulative mass as a fraction and particle diameter in micrometer (Strip D, rep. 1-5)

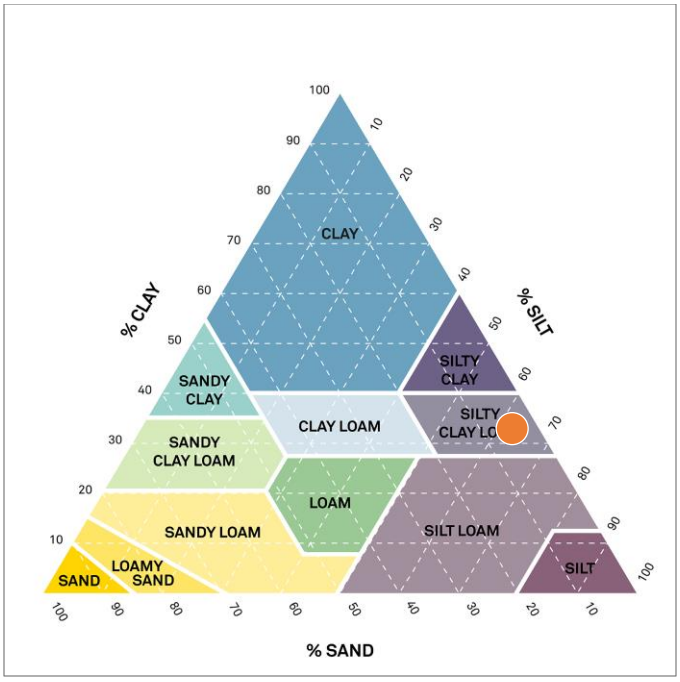

Figure 50: Genesee 30-90 cm soil taxonomy texture triangle (Strip D, rep. 1-5)

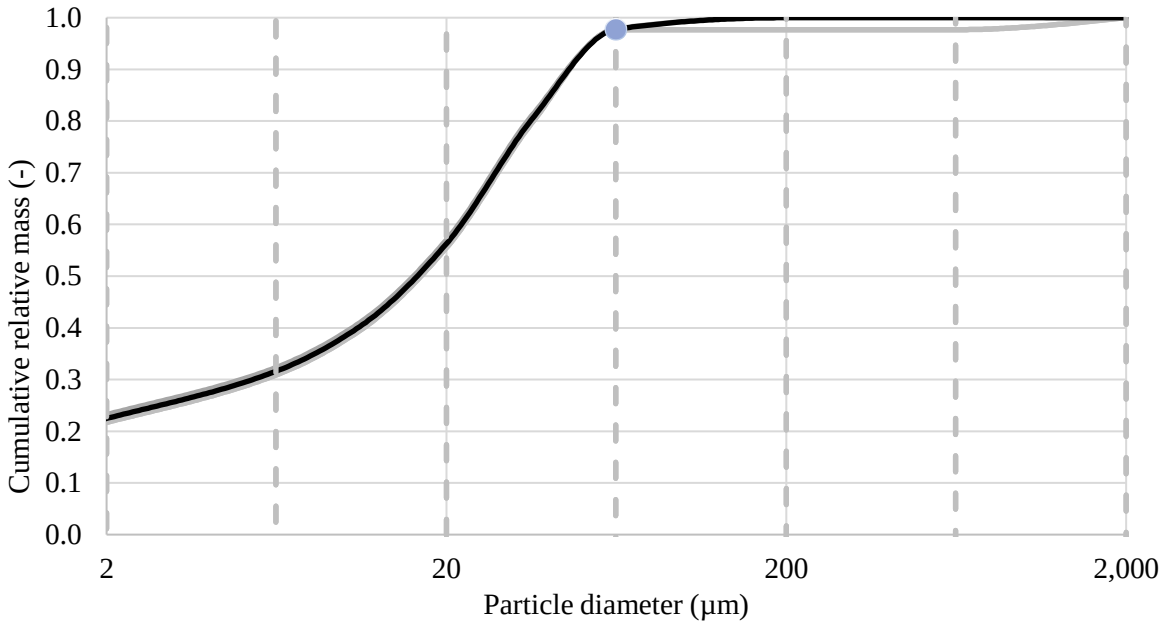

Figure 51: Genesee 90-150 cm cumulative particle size distribution with cumulative mass as a fraction and particle diameter in micrometer (Strip D, rep. 1-5)

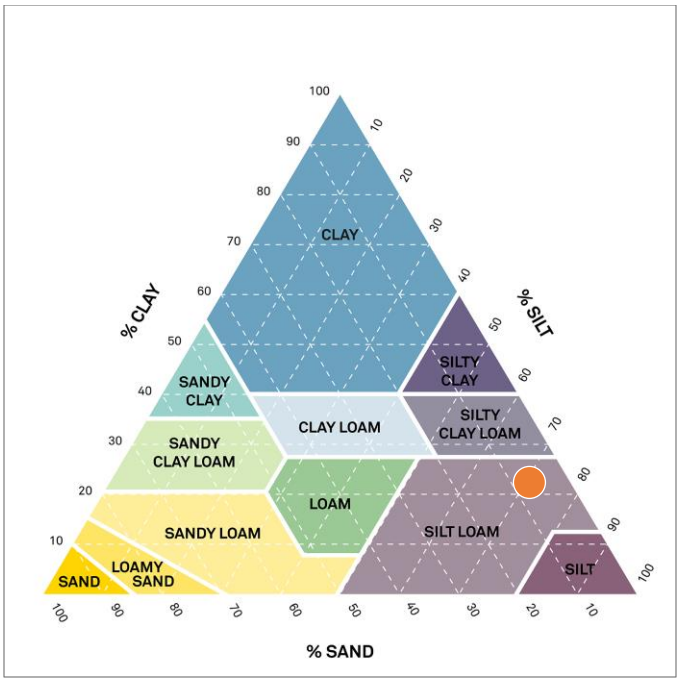

Figure 52: Genesee 90-150 cm soil taxonomy texture triangle (Strip D, rep. 1-5)

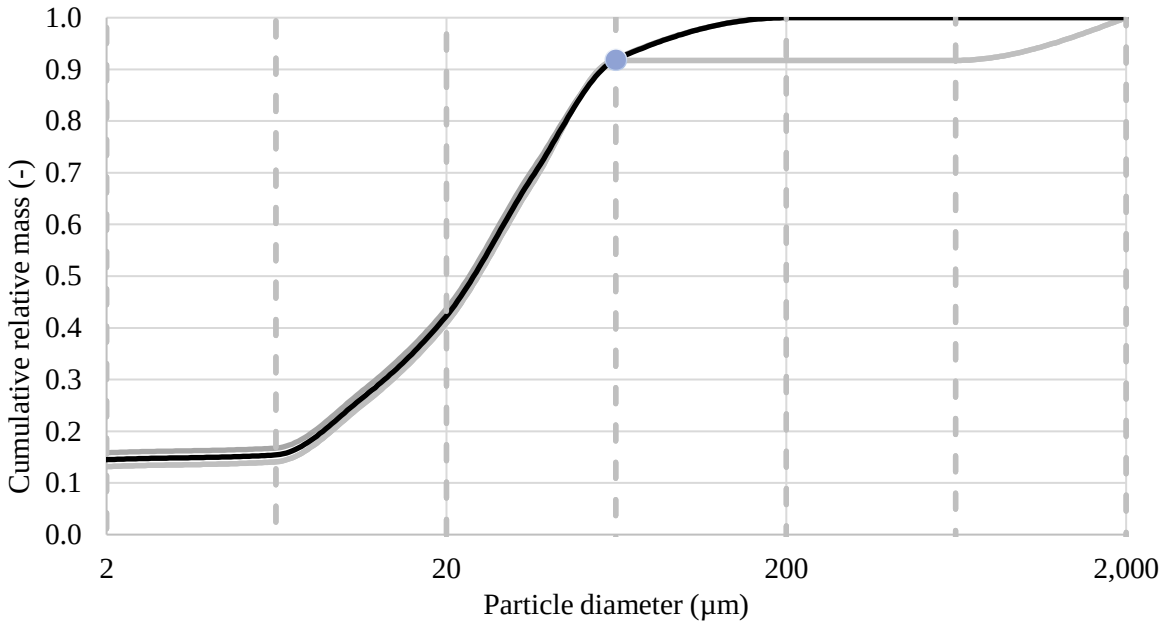

Figure 53: St. John 0-30 cm cumulative particle size distribution with cumulative mass as a fraction and particle diameter in micrometer (Strip D, rep. 1-5)

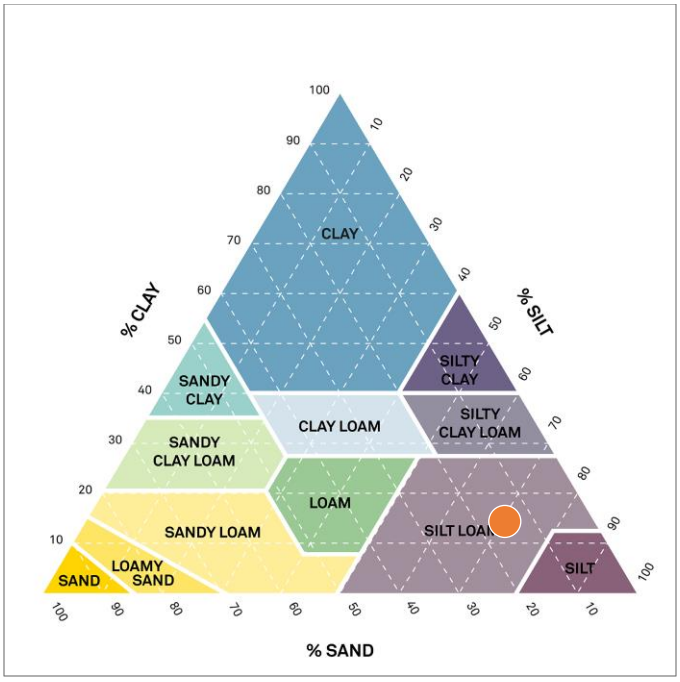

Figure 54: St. John 0-30 cm soil taxonomy texture triangle (Strip D, rep. 1-5)

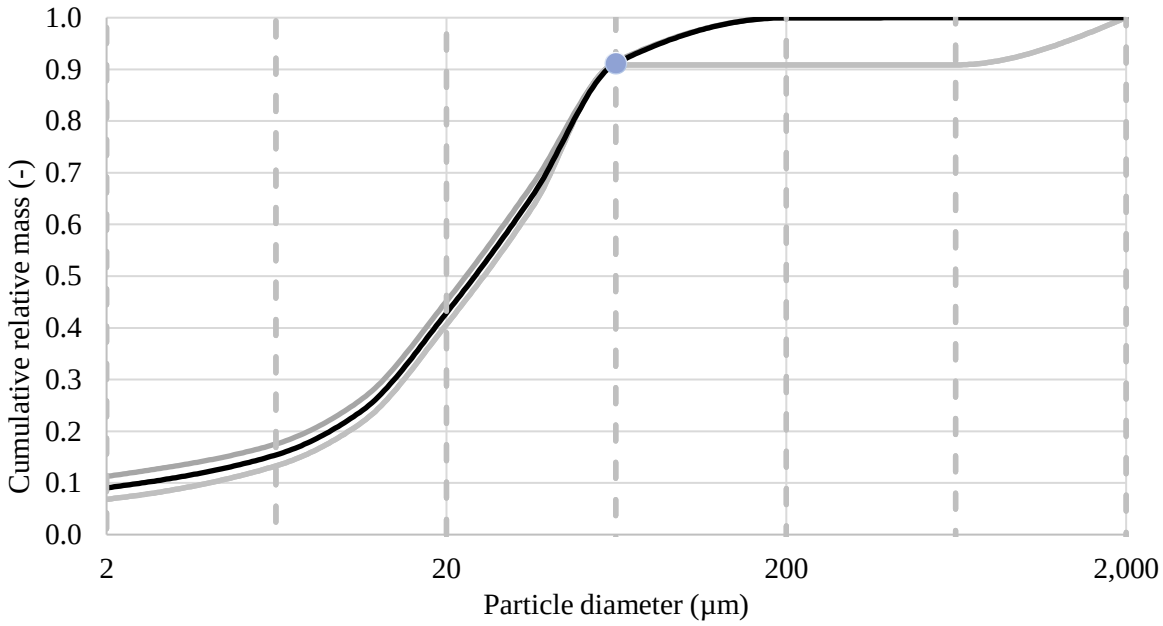

Figure 55: St. John 30-90 cm cumulative particle size distribution with cumulative mass as a fraction and particle diameter in micrometer (Strip D, rep. 1-5)

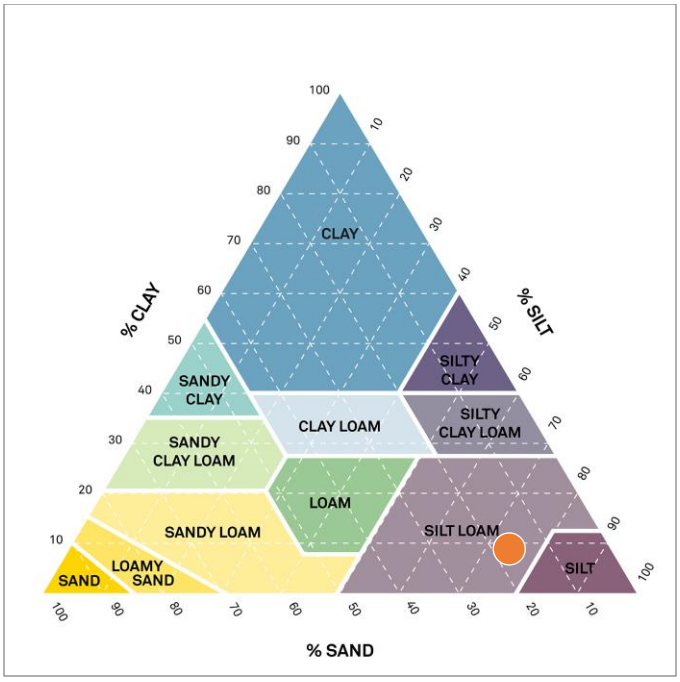

Figure 56: St. John 30-90 cm soil taxonomy texture triangle (Strip D, rep. 1-5)

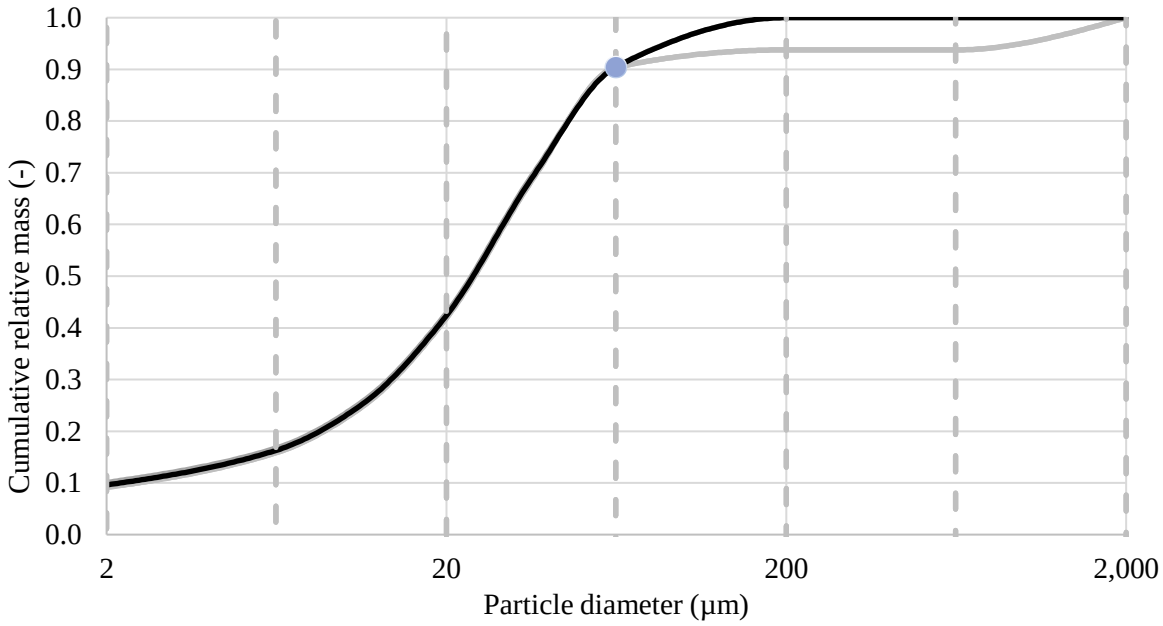

Figure 57: St. John 90-150 cm cumulative particle size distribution with cumulative mass as a fraction and particle diameter in micrometer (Strip D, rep. 1-5)

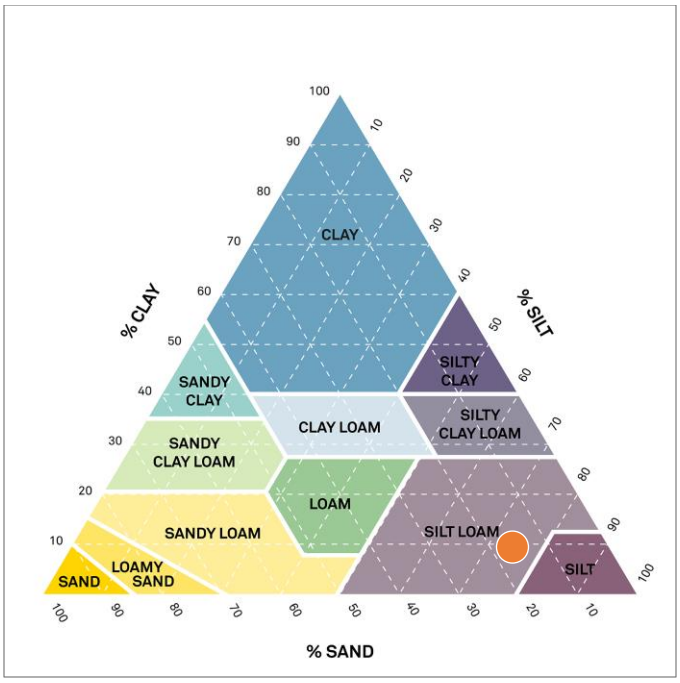

Figure 58: St. John 90-150 cm soil taxonomy texture triangle (Strip D, rep. 1-5)

Appendix C

Table 29: Soil-water retention model statistics by depth; RMSE=root mean square error, σ_{obs}=standard deviation of observations

		van Genuchten			**Campbell**		
Site	*Depth*	*RMSE*	R^2	σ_{obs}	*RMSE*	R^2	σ_{obs}
Genesee	*0-30 cm*	0.68	0.98	9.88	0.41	0.93	1.06
	30-150 cm	1.46	0.98	8.96	0.36	0.93	0.91
St. John	*0-30 cm*	1.40	0.99	10.56	0.41	0.90	0.68
	30-150 cm	1.77	0.98	10.30	0.30	0.95	0.61

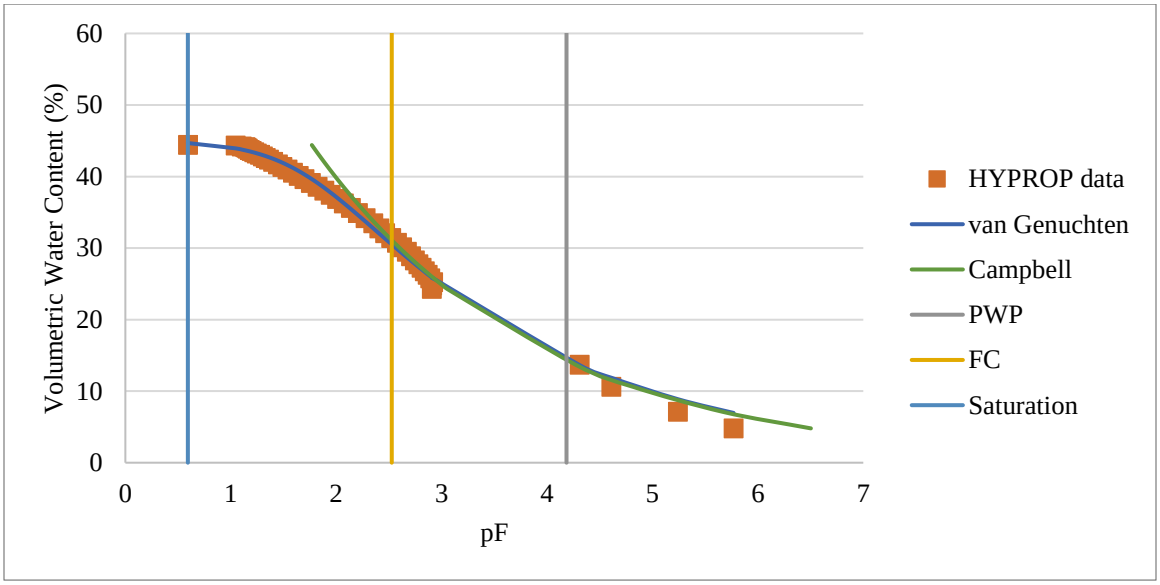

Figure 59: Genesee 0-30 cm soil water retention curve; PWP = permanent wilting point, FC = field capacity

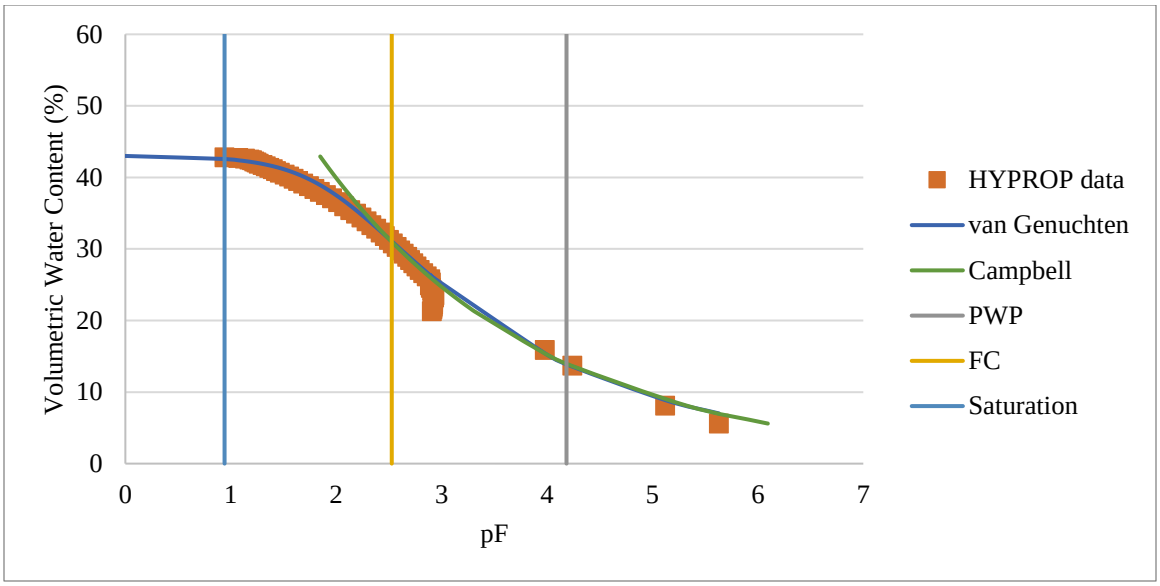

Figure 60: Genesee 30-150 cm soil water retention curve; PWP = permanent wilting point, FC = field capacity

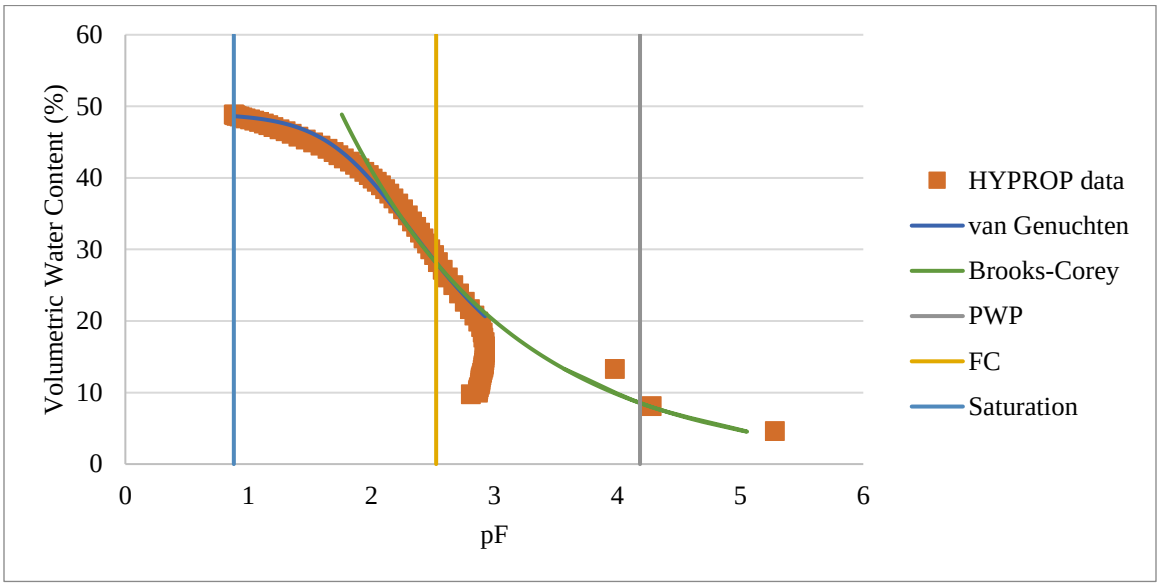

Figure 61: St. John 0-30 cm soil water retention curve; PWP = permanent wilting point, FC = field capacity

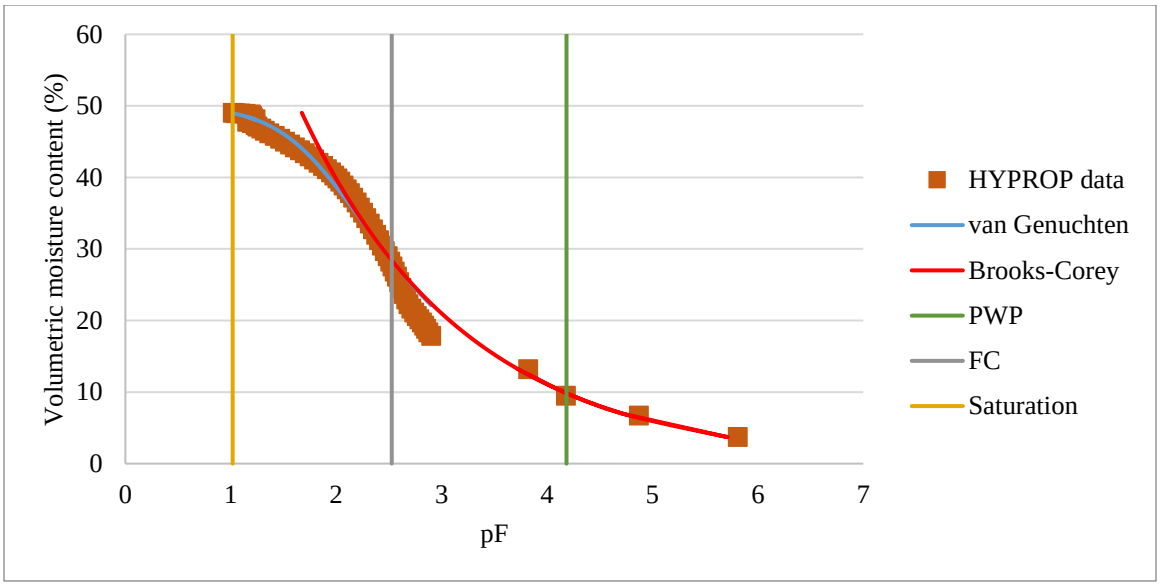

Figure 62: St. John 30-150 cm soil water retention curve; PWP = permanent wilting point, FC = field capacity

Appendix D

Table 30: Nitrogen fertilization by rotation and crop, kg-N/ha; INC=incremental, ASP=aspiration, BAU=business-as-usual, WW=winter wheat, SW=spring wheat

			2017/2018		**2018/2019**		**2019/2020**		**2020/2021**	
			Plant	*Top dress*	*Plant*	*Top dress*	*Plant*	*Top dress*	*Plant*	*Top dress*
Genesee	INC	WW	101	0	101	45	129	45	112	0
	ASP	WW	101	0	123	45	129	45	165	0
	BAU	WW	101	0	123	45	129	45	165	0
	INC	SW	67	0	165	0	165	45	165	24
	BAU	SW	67	0	165	0	165	45	165	24
St. John	INC	WW	101	0	56	0	84	0	34	0
	ASP	WW	101	0	90	0	112	0	112	0
	BAU	WW	101	0	90	0	22	0	34	0
	INC	SW	129	0	129	0	62	0	90	0
	ASP	SW	129	0	129	0	112	0	90	0
	BAU	SW	129	0	129	0	56	0	90	0

Table 31: Genesee site strip trial plant and harvest dates

Planting				
	2017-2018	**2018-2019**	**2019-2020**	**2020-2021**
Winter crops	10/5/2017	10/4/2018	10/7/2019	10/6/2020
Spring crops	4/27/2018	5/2/2019	4/21/2020	4/22/2021
Harvest				
	2017-2018	**2018-2019**	**2019-2020**	**2020-2021**
Cover crop	6/20/2018	7/1/2019	7/7/2020	7/1/2021
Winter wheat	8/2/2018	8/7/2019	8/6/2020	7/27/2021
Winter pea	8/2/2018	8/7/2019	8/6/2020	7/27/2021
Spring wheat	8/23/2018	8/28/2019	8/25/2020	8/24/2021
Chickpea	8/23/2018	9/5/2019	9/10/2020	8/24/2021

Table 32: St. John site strip trial plant and harvest dates

Planting				
	2017-2018	**2018-2019**	**2019-2020**	**2020-2021**
Winter crops	10/3/2017	9/25/2018	9/24/2019	9/30/2020
Spring crops	3/30/2018	4/25/2019	4/9/2020	4/5/2021
Harvest				
	2017-2018	**2018-2019**	**2019-2020**	**2020-2021**
Cover crop	7/2/2018	7/12/2019	7/9/2020	7/8/2021
Winter pea	8/3/2018	8/2/2019	8/7/2020	7/22/2021
Winter wheat	8/21/2018	8/20/2019	8/7/2020	7/22/2021
Spring wheat	8/21/2018	8/27/2019	8/24/2020	8/9/2021

Appendix E

Table 33: Genesee biomass and yield statistics by crop; MD=mean difference, RMSE=root mean square error, n=number of observations

	Biomass				**Yield**			
	R^2	*MD, kg/ha*	*RMSE, kg/ha*	*n*	R^2	*MD, kg/ha*	*RMSE, kg/ha*	*n*
Chickpea	0.81	-208	493	8	0.59	-44	322	8
Spring wheat	0.69	-1118	4,828	7	0.69	366	876	8
Winter pea	0.20	-597	2,673	4	0.71	-252	791	4
Winter wheat	0.86	651	2,088	12	0.95	-17	469	12
Cover crop	0.04	-106	1,880	4				

Table 34: St. John biomass and yield statistics by crop; MD=mean difference, RMSE=root mean square error, n=number of observations

	Biomass				**Yield**			
	R^2	*MD, kg/ha*	*RMSE, kg/ha*	*n*	R^2	*MD, kg/ha*	*RMSE, kg/ha*	*n*
Spring wheat	0.45	-918	2,544	12	0.21	-13	1,179	12
Winter pea	0.55	977	2,872	4	0.90	-379	481	4
Winter wheat	0.27	1317	3,522	12	0.28	483	1,583	12
Cover crop	0.10	162	1,197	4	-	-	-	

Table 35: Genesee crop nitrogen statistics by crop; MD=mean difference, RMSE=root mean square error, n=number of observations, σ=standard deviation of observations

	R^2	*MD, kg-N/ha*	*RMSE, kg-N/ha*	*n*	*σ, kg-N/ha*
Spring wheat	0.20	0.20	39	8	46
Chickpea	0.37	0.86	15	8	22
Winter pea	0.97	18.34	56	4	81
Winter wheat	0.67	-4.25	19	12	31
Cover crop	0.46	6.68	26	4	33

Table 36: Genesee crop nitrogen statistics by year; MD=mean difference, RMSE=root mean square error, n=number of observations, σ=standard deviation of observations

	R^2	*MD, kg-N/ha*	*RMSE, kg-N/ha*	*σ, kg-N/ha*
2018	0.81	-11.16	20	38
2019	0.59	19.52	34	29
2020	0.67	22.52	38	55
2021	0.88	-25.05	28	37

Appendix F

Table 37: Genesee soil moisture comparison by depth (cm) – replicate 5, strip A; MD=mean difference, RMSE=root mean square error, n=number of observations

Observed sensor versus observed manual					
Depth	*0-30*	*30-60*	*60-90*	*90-120*	*120-150*
R^2	0.994	0.880	0.807	0.801	0.545
MD	0.036	-0.022	-0.080	-0.010	0.028
RMSE	0.037	0.050	0.095	0.026	0.044
n	5	5	5	5	5
Observed sensor versus simulated					
Depth	*0-30*	*30-60*	*60-90*	*90-120*	*120-150*
R^2	0.713	0.446	0.441	0.113	0.058
MD	-0.007	0.051	0.058	0.026	-0.003
RMSE	0.049	0.077	0.073	0.054	0.047
n	828	828	810	828	828
Observed manual versus simulated					
Depth	*0-30*	*30-60*	*60-90*	*90-120*	*120-150*
R^2	0.966	0.826	0.376	0.060	0.208
MD	0.013	0.015	-0.023	0.005	0.029
RMSE	0.037	0.053	0.062	0.054	0.041
n	8	8	8	8	8

Table 38: Genesee soil moisture comparison by depth (cm) – replicate 5, strip B; MD=mean difference, RMSE=root mean square error, n=number of observations

Observed sensor versus observed manual					
Depth	*0-30*	*30-60*	*60-90*	*90-120*	*120-150*
R^2	0.831	0.991	0.868	0.618	0.933
MD	0.040	0.002	-0.013	-0.036	-0.012
RMSE	0.056	0.014	0.030	0.050	0.025
n	6	5	6	5	6
Observed sensor versus simulated					
Depth	*0-30*	*30-60*	*60-90*	*90-120*	*120-150*
R^2	0.820	0.680	0.375	0.169	0.350
MD	-0.032	0.043	0.018	0.019	0.052
RMSE	0.046	0.059	0.053	0.045	0.057
n	849	828	935	828	935
Observed manual versus simulated					
Depth	*0-30*	*30-60*	*60-90*	*90-120*	*120-150*
R^2	0.964	0.963	0.787	0.064	0.215
MD	0.021	0.032	0.001	-0.013	0.042
RMSE	0.034	0.036	0.033	0.060	0.057
n	8	8	8	8	8

Table 39: Genesee soil moisture comparison by depth (cm) – replicate 5, strip C; MD=mean difference, RMSE=root mean square error, n=number of observations

Observed sensor versus observed manual					
Depth	*0-30*	*30-60*	*60-90*	*90-120*	*120-150*
R^2	0.998	0.984	0.884	0.202	0.749
MD	-0.018	-0.053	-0.065	-0.090	-0.039
RMSE	0.020	0.061	0.074	0.108	0.043
n	5	5	5	5	5
Observed sensor versus simulated					
Depth	*0-30*	*30-60*	*60-90*	*90-120*	*120-150*
R^2	0.812	0.397	0.269	0.404	0.435
MD	0.041	0.056	0.067	0.091	0.058
RMSE	0.054	0.075	0.086	0.099	0.065
n	878	878	878	878	878
Observed manual versus simulated					
Depth	*0-30*	*30-60*	*60-90*	*90-120*	*120-150*
R^2	0.925	0.929	0.248	0.155	0.008
MD	0.027	0.017	-0.004	-0.001	0.025
RMSE	0.044	0.030	0.061	0.065	0.055
n	8	8	8	8	8

Table 40: Genesee soil moisture comparison by depth (cm) – replicate 5, strip D; MD=mean difference, RMSE=root mean square error, n=number of observations

Observed sensor versus observed manual					
Depth	*0-30*	*30-60*	*60-90*	*90-120*	*120-150*
R^2	0.993	0.885	0.952	0.541	0.546
MD	0.003	-0.052	-0.035	-0.071	-0.063
RMSE	0.009	0.062	0.047	0.080	0.084
n	5	5	5	5	5
Observed sensor versus simulated					
Depth	*0-30*	*30-60*	*60-90*	*90-120*	*120-150*
R^2	0.800	0.429	0.077	0.357	0.628
MD	0.020	0.069	0.052	0.105	0.057
RMSE	0.042	0.086	0.082	0.114	0.066
n	878	878	878	878	878
Observed manual versus simulated					
Depth	*0-30*	*30-60*	*60-90*	*90-120*	*120-150*
R^2	0.960	0.888	0.519	0.182	0.504
MD	0.027	0.022	0.011	0.036	0.024
RMSE	0.047	0.034	0.050	0.067	0.063
n	8	8	8	8	8

Table 41: Genesee soil moisture comparison by depth (cm) – replicate 5, strip E; MD=mean difference, RMSE=root mean square error, n=number of observations

Observed sensor versus observed manual					
Depth	*0-30*	*30-60*	*60-90*	*90-120*	*120-150*
R^2	0.732	0.986	0.974	0.896	0.956
MD	0.077	-0.001	-0.026	-0.037	-0.021
RMSE	0.085	0.012	0.032	0.040	0.037
n	6	4	6	6	6
Observed sensor versus simulated					
Depth	*0-30*	*30-60*	*60-90*	*90-120*	*120-150*
R^2	0.804	0.518	0.347	0.294	0.175
MD	-0.053	0.003	0.025	0.039	0.025
RMSE	0.062	0.052	0.046	0.049	0.032
n	900	624	874	900	900
Observed manual versus simulated					
Depth	*0-30*	*30-60*	*60-90*	*90-120*	*120-150*
R^2	0.861	0.942	0.683	0.622	0.607
MD	0.031	0.012	0.000	0.004	0.005
RMSE	0.046	0.026	0.038	0.031	0.049
n	8	8	8	8	8

Table 42: Genesee soil moisture comparison by depth (cm) – replicate 5, strip F; MD=mean difference, RMSE=root mean square error, n=number of observations

Observed sensor versus observed manual					
Depth	*0-30*	*30-60*	*60-90*	*90-120*	*120-150*
R^2	0.913	0.956	0.974		0.862
MD	0.022	0.002	-0.001		-0.111
RMSE	0.036	0.027	0.015		0.111
n	6	6	6		6
Observed sensor versus simulated					
Depth	*0-30*	*30-60*	*60-90*	*90-120*	*120-150*
R^2	0.870	0.641	0.339		0.326
MD	-0.018	0.006	-0.033	0.009	0.101
RMSE	0.036	0.054	0.072	0.034	0.107
n	878	878	878	67	878
Observed manual versus simulated					
Depth	*0-30*	*30-60*	*60-90*	*90-120*	*120-150*
R^2	0.975	0.812	0.461	0.073	0.019
MD	0.010	-0.010	-0.033	0.014	0.004
RMSE	0.028	0.058	0.072	0.061	0.048
n	8	7	8	8	8

Table 43: Genesee soil moisture comparison by depth (cm) – replicate 5, strip G; MD=mean difference, RMSE=root mean square error, n=number of observations

Observed sensor versus observed manual					
Depth	*0-30*	*30-60*	*60-90*	*90-120*	*120-150*
R^2	1.000	0.981			0.983
MD	0.001	-0.052			-0.088
RMSE	0.013	0.068			0.096
n	4	4			4
Observed sensor versus simulated					
Depth	*0-30*	*30-60*	*60-90*	*90-120*	*120-150*
R^2	0.792	0.437	0.112	0.777	0.032
MD	0.016	0.096	0.134	0.043	0.042
RMSE	0.040	0.108	0.137	0.061	0.049
n	716	716	54	140	716
Observed manual versus simulated					
Depth	*0-30*	*30-60*	*60-90*	*90-120*	*120-150*
R^2	0.933	0.945	0.001	0.438	0.301
MD	0.029	0.039	0.055	-0.005	-0.017
RMSE	0.051	0.045	0.119	0.050	0.057
n	8	8	8	8	8

Table 44: Genesee soil moisture comparison by depth (cm) – replicate 5, strip H; MD=mean difference, RMSE=root mean square error, n=number of observations

Observed sensor versus observed manual					
Depth	*0-30*	*30-60*	*60-90*	*90-120*	*120-150*
R^2	0.973		1.000	0.986	0.786
MD	0.068		-0.023	-0.028	-0.067
RMSE	0.072		0.023	0.034	0.069
n	4		3	3	3
Observed sensor versus simulated					
Depth	*0-30*	*30-60*	*60-90*	*90-120*	*120-150*
R^2	0.909	0.312	0.003	0.001	0.161
MD	-0.072	0.009	0.030	0.069	0.078
RMSE	0.077	0.059	0.054	0.090	0.083
n	653	276	528	528	528
Observed manual versus simulated					
Depth	*0-30*	*30-60*	*60-90*	*90-120*	*120-150*
R^2	0.927	0.793	0.278	0.115	0.117
MD	0.012	0.019	-0.003	0.002	0.004
RMSE	0.028	0.036	0.053	0.055	0.046
n	8	8	8	8	8

Table 45: Genesee soil moisture comparison by depth (cm) – replicate 5, strip I; MD=mean difference, RMSE=root mean square error, n=number of observations

Observed sensor versus observed manual					
Depth	*0-30*	*30-60*	*60-90*	*90-120*	*120-150*
R^2	0.944	0.993	1.000	0.976	0.010
MD	0.003	-0.020	-0.007	0.025	-0.086
RMSE	0.035	0.028	0.045	0.043	0.111
n	4	4	4	4	4
Observed sensor versus simulated					
Depth	*0-30*	*30-60*	*60-90*	*90-120*	*120-150*
R^2	0.605	0.585	0.317	0.272	0.270
MD	0.024	0.049	0.016	-0.045	0.058
RMSE	0.053	0.064	0.039	0.053	0.059
n	770	793	793	771	793
Observed manual versus simulated					
Depth	*0-30*	*30-60*	*60-90*	*90-120*	*120-150*
R^2	0.933	0.903	0.529	0.507	0.511
MD	0.022	0.026	0.010	-0.007	-0.015
RMSE	0.043	0.035	0.049	0.041	0.057
n	8	8	8	8	8

Table 46: St. John soil moisture comparison by depth (cm) – replicate 3, strip A; MD=mean difference, RMSE=root mean square error, n=number of observations

Observed sensor versus observed manual					
Depth	*0-30*	*30-60*	*60-90*	*90-120*	*120-150*
R^2		0.938	0.874	0.840	0.987
MD		-0.014	-0.040	0.029	-0.060
RMSE		0.028	0.045	0.034	0.064
n		5	5	5	5
Observed sensor versus simulated					
Depth	*0-30*	*30-60*	*60-90*	*90-120*	*120-150*
R^2	0.223	0.613	0.000	0.214	0.220
MD	0.021	0.094	0.166	0.090	0.082
RMSE	0.088	0.110	0.181	0.096	0.096
n	398	801	810	810	810
Observed manual versus simulated					
Depth	*0-30*	*30-60*	*60-90*	*90-120*	*120-150*
R^2	0.994	0.983	0.469	0.060	0.193
MD	0.064	0.062	0.098	0.091	0.030
RMSE	0.077	0.066	0.110	0.103	0.049
n	8	8	8	8	8

Table 47: St. John soil moisture comparison by depth (cm) – replicate 3, strip B; MD=mean difference, RMSE=root mean square error, n=number of observations

Observed sensor versus observed manual					
Depth	*0-30*	*30-60*	*60-90*	*90-120*	*120-150*
R^2	0.943	0.972	0.989	0.995	0.958
MD	0.010	-0.120	-0.095	0.018	-0.042
RMSE	0.048	0.128	0.099	0.019	0.043
n	4	4	4	3	4
Observed sensor versus simulated					
Depth	*0-30*	*30-60*	*60-90*	*90-120*	*120-150*
R^2	0.284	0.392	0.207	0.014	0.007
MD	-0.021	0.046	0.086	0.098	0.087
RMSE	0.087	0.084	0.109	0.103	0.092
n	849	828	935	828	935
Observed manual versus simulated					
Depth	*0-30*	*30-60*	*60-90*	*90-120*	*120-150*
R^2	0.586	0.568	0.357	0.368	0.386
MD	0.018	0.015	0.060	0.101	0.033
RMSE	0.082	0.067	0.089	0.114	0.047
n	8	8	8	8	8

Table 48: St. John soil moisture comparison by depth (cm) – replicate 3, strip C; MD=mean difference, RMSE=root mean square error, n=number of observations

Observed sensor versus observed manual					
Depth	*0-30*	*30-60*	*60-90*	*90-120*	*120-150*
R^2					
MD	0.026		-0.058	-0.002	-0.142
RMSE	0.055		0.061	0.004	0.142
n	2		2	2	2
Observed sensor versus simulated					
Depth	*0-30*	*30-60*	*60-90*	*90-120*	*120-150*
R^2	0.569	0.621	0.128	0.008	0.010
MD	0.012	0.026	0.106	0.084	0.165
RMSE	0.053	0.055	0.121	0.100	0.167
n	568	376	556	568	568
Observed manual versus simulated					
Depth	*0-30*	*30-60*	*60-90*	*90-120*	*120-150*
R^2	0.895	0.970	0.689	0.525	0.387
MD	0.041	0.022	0.031	0.075	0.023
RMSE	0.065	0.033	0.049	0.089	0.043
n	8	7	8	8	8

Table 49: St. John soil moisture comparison by depth (cm) – replicate 3, strip D; MD=mean difference, RMSE=root mean square error, n=number of observations

Observed sensor versus observed manual					
Depth	*0-30*	*30-60*	*60-90*	*90-120*	*120-150*
R^2	0.970	0.988	0.973	0.872	0.882
MD	0.040	0.001	0.019	-0.009	-0.096
RMSE	0.046	0.014	0.056	0.018	0.098
n	3	5	5	5	5
Observed sensor versus simulated					
Depth	*0-30*	*30-60*	*60-90*	*90-120*	*120-150*
R^2	0.653	0.660	0.350	0.039	0.354
MD	0.045	0.029	0.015	0.072	0.142
RMSE	0.070	0.065	0.038	0.079	0.146
n	424	675	675	675	676
Observed manual versus simulated					
Depth	*0-30*	*30-60*	*60-90*	*90-120*	*120-150*
R^2	0.970	0.914	0.574	0.133	0.264
MD	0.061	0.043	0.059	0.073	0.061
RMSE	0.073	0.054	0.080	0.085	0.070
n	8	8	8	8	8

Table 50: St. John soil moisture comparison by depth (cm) – replicate 3, strip E; MD=mean difference, RMSE=root mean square error, n=number of observations

Observed sensor versus observed manual					
Depth	*0-30*	*30-60*	*60-90*	*90-120*	*120-150*
R^2	0.979	0.874	0.928	0.982	
MD	0.041	0.014	-0.010	-0.039	
RMSE	0.050	0.036	0.021	0.042	
n	3	4	5	4	
Observed sensor versus simulated					
Depth	*0-30*	*30-60*	*60-90*	*90-120*	*120-150*
R^2	0.419	0.595	0.001	0.025	0.034
MD	0.059	0.061	0.062	0.103	0.073
RMSE	0.087	0.080	0.083	0.117	0.085
n	429	507	675	675	497
Observed manual versus simulated					
Depth	*0-30*	*30-60*	*60-90*	*90-120*	*120-150*
R^2	0.877	0.871	0.601	0.000	0.403
MD	0.046	0.029	0.044	0.015	0.021
RMSE	0.070	0.045	0.064	0.127	0.042
n	8	8	8	7	8

Table 51: St. John soil moisture comparison by depth (cm) – replicate 3, strip F; MD=mean difference, RMSE=root mean square error, n=number of observations

Observed sensor versus observed manual					
Depth	*0-30*	*30-60*	*60-90*	*90-120*	*120-150*
R^2	0.847	0.982		0.630	0.464
MD	0.146	0.185		0.206	0.245
RMSE	0.223	0.251		0.220	0.254
n	4	3		4	4
Observed sensor versus simulated					
Depth	*0-30*	*30-60*	*60-90*	*90-120*	*120-150*
R^2	0.000	0.000		0.281	0.269
MD	-0.078	-0.100		-0.131	-0.154
RMSE	0.140	0.134		0.135	0.156
n	502	413		452	508
Observed manual versus simulated					
Depth	*0-30*	*30-60*	*60-90*	*90-120*	*120-150*
R^2	0.885	0.940	0.564	0.243	0.129
MD	0.050	0.042	0.072	0.053	0.086
RMSE	0.074	0.053	0.088	0.069	0.098
n	8	8	8	8	8

Table 52: St. John soil moisture comparison by depth (cm) – replicate 3, strip G; MD=mean difference, RMSE=root mean square error, n=number of observations

Observed sensor versus observed manual					
Depth	*0-30*	*30-60*	*60-90*	*90-120*	*120-150*
R^2	0.958	0.986	0.969	0.939	0.950
MD	0.103	0.137	0.210	0.189	0.212
RMSE	0.203	0.211	0.234	0.209	0.227
n	4	4	4	4	4
Observed sensor versus simulated					
Depth	*0-30*	*30-60*	*60-90*	*90-120*	*120-150*
R^2	0.374	0.301	0.375	0.371	0.339
MD	-0.050	-0.064	-0.067	-0.112	-0.163
RMSE	0.157	0.142	0.117	0.132	0.167
n	623	631	631	626	630
Observed manual versus simulated					
Depth	*0-30*	*30-60*	*60-90*	*90-120*	*120-150*
R^2	0.929	0.913	0.175	0.258	0.228
MD	0.033	0.042	0.079	0.061	0.042
RMSE	0.050	0.051	0.109	0.079	0.061
n	8	8	8	8	8

Table 53: St. John soil moisture comparison by depth (cm) – replicate 3, strip H; MD=mean difference, RMSE=root mean square error, n=number of observations

Observed sensor versus simulated					
Depth	*0-30*	*30-60*	*60-90*	*90-120*	*120-150*
R^2	0.331	0.363	0.272	0.298	0.760
MD	0.001	-0.085	-0.134	-0.153	-0.141
RMSE	0.098	0.107	0.137	0.155	0.142
n	340	198	186	197	197
Observed manual versus simulated					
Depth	*0-30*	*30-60*	*60-90*	*90-120*	*120-150*
R^2	0.927	0.862	0.740	0.479	0.116
MD	0.049	0.056	0.075	0.044	0.073
RMSE	0.072	0.067	0.081	0.055	0.081
n	8	8	8	8	8

Table 54: St. John soil moisture comparison by depth (cm) – replicate 3, strip I; MD=mean difference, RMSE=root mean square error, n=number of observations

Observed sensor versus simulated					
Depth	*0-30*	*30-60*	*60-90*	*90-120*	*120-150*
R^2	0.067	0.262	0.402	0.944	
MD	0.034	0.055	0.009	-0.199	
RMSE	0.089	0.069	0.058	0.199	
n	198	173	176	16	
Observed manual versus simulated					
Depth	*0-30*	*30-60*	*60-90*	*90-120*	*120-150*
R^2	0.829	0.906	0.512	0.341	0.232
MD	0.023	0.032	0.052	0.039	0.046
RMSE	0.059	0.045	0.073	0.061	0.063
n	8	8	8	8	8